Artium Technologies, Inc.
150 West Iowa Avenue, Suite 202
Sunnyvale, California 94086
USA

Phone : (408) 737-2364
Fax : (408) 737-2374
e-mail: info@artium.com

PDI-200 MD User Manual

OPERATION OF THE PHASE DOPPLER INTERFEROMETER (PDI) FOR SPRAY DROP SIZE AND VELOCITY MEASUREMENT

Table of Contents

Chapter
1 Preface

Thank you for purchasing the PDI-200 MD. We are confident that this product will serve you well. Any comments you may have concerning this product or your application are encouraged. Please feel free to call, fax or e-mail us at:

Artium Technologies, Inc.

Tel: (408) 737-2364

Fax: (408) 737-2374

E-mail: info@artium.com

Internet: http://www.artium.com

This manual is designed to be comprehensive and easy-to-understand. However, should you be uncertain about how to do certain things, or the consequences of doing something, feel free to contact us at **Artium Technologies, Inc**. We will be happy to answer any questions you may have. Also, if you have any comments on improving this manual, we would appreciate hearing from you.

Chapter
2 Before You Start

Upon receipt of the instrument, inspect the shipping carton for any significant external damage. Unpack the unit and inspect for internal damage. If any damage is found, immediately notify the shipper and Artium Technologies Inc.

Retain the shipping carton and packing material. If the **PDI** instrument ever needs repair, the cartons will ensure safe shipment of the unit to Artium Technologies, Inc.

Chapter 3

Artium Technologies, Inc.

Artium Technologies, Inc. ("Artium") was established in 1998 to develop advanced instrumentation and to engage in various opportunities associated with laser-based diagnostics for particle field and spray characterization. Since its inception, Artium has been actively involved in conducting research and development, design, manufacture, and sales/marketing of laser-based instrumentation for particle field and spray characterization; for both fundamental research and process/quality control applications. Our instruments have been used in various applications including characterization of sprays used in coating medical devices, cloud measurements for aircraft icing research studies, characterizing sprays in spray combustion, and measuring soot emissions from diesel engines. We have also developed systems for characterizing black carbon for quality control purposes in carbon black production.

Throughout the years, our team has established an excellent record worldwide for providing innovative advanced diagnostics that perform reliably under difficult conditions. Our instruments set the standard for performance and for their capability in producing results.

Chapter
4 Warranty

Artium Technologies, Inc. (“Artium”) warrants products of its manufacture against defective materials and workmanship for a period of one (1) year from the date of installation by the purchaser or, if shorter, for a period of 13 months from the date of shipment to the purchaser. The liability of Artium under this warranty is limited, at Artium’s option, solely to repair or replacement with equivalent products, or appropriate credit adjustment not to exceed the sales price to the purchaser, provided that:

1. Artium is notified in writing by the purchaser within the warranty period promptly upon the discovery of defects,
2. The purchaser has obtained a Return Materials Authorization Number (“RMA.”) from Artium, which RMA number Artium agrees to provide to the purchaser promptly upon request,
3. The defective products are returned to Artium, in the original packing material or alternate material approved by Artium, with transportation charges prepaid by the purchaser, and
4. Artium’s examination of such products discloses to its satisfaction that defects were not caused by mishandling of the product, careless operation of the system, negligence, misuse, improper installation, accident, or unauthorized attempts to repair or perform alterations.

The original warranty period of any product which has been repaired or replaced by Artium shall not thereby be extended.

THE FOREGOING WARRANTY IS PROVIDED EXPRESSLY IN LIEU OF AND **ARTIUM** HEREBY DISCLAIMS ALL OTHER WARRANTIES, EXPRESS OR IMPLIED, INCLUDING ANY WARRANTY OF MERCHANTABILITY OR FITNESS FOR A PARTICULAR PURPOSE, AND OF ALL OTHER OBLIGATIONS OR LIABILITIES ON ARTIUM’S PART, AND ARTIUM NEITHER ASSUMES STORE AUTHORIZES ANY OTHER PERSON TO ASSUME FOR ARTIUM ANY OTHER LIABILITIES.

The foregoing warranty is only valid for Artium products sold within the United States and Canada. For products sold outside of United States and Canada, please refer to the local authorized Artium distributor for applicable warranty terms and conditions.

LIMITATION OF LIABILITY

The remedies set forth above constitute the sole and exclusive remedies against Artium for the finishing of nonconforming or defective products. In no event, including if the products are nonconforming, effective, delayed, were not delivered, Shall Artium be liable for any special contingent, indirect, or consequential damages, even if Artium has been advised of the possibility of such damages, whether under a contract, tort, property, or other legal theory. Such damages for which Artium is not responsible include, but are not limited to, personal-injury, property damage, anticipated profits, labor expended, delays, and loss of use.

Chapter
5 About This Manual

The purpose of this manual is to provide step-by-step instructions for the proper setup and operation of the PDI instrument. Before attempting to operate the system, the users should familiarize themselves with all aspects of laser safety and ensure that **laser safety glasses are available** to all individuals present when the instrument is operated.

This manual provides a description of the steps required in setting up the system which includes a transmitter and receiver optics package, a mounting platform and traversing system (optional), a signal processor, and a system computer including the software. Basic electrical and electronic connections for the system are described with diagrams in the manual. A description of how to install the optics packages onto the mounting platform and traverse is outlined. Basic alignment techniques and descriptions of the signal under various alignment conditions are given to help the user recognize when the instrument is properly aligned and when it is not. All optical parameters required for optimal measurements are outlined and the means for selecting these parameters are described. A section on the proper setup of the electronic system is given although the system software is designed to automatically set these parameters reliably. The various calculations for the fringe spacing, sample volume, and the calculations for the various spray droplet sizes are outlined for easy reference.

Chapter
6 Laser Safety

Explanations of Terms

Cautions and Warnings used throughout this manual are explained below. Always read and heed this information. It is basic to the safe and proper operation of the system.

WARNING: Hazardous to persons. An action or circumstance which may potentially cause personal injury or loss of life. Mechanical damage may also result.

CAUTION: Hazardous to persons or equipment. To disregard the caution may cause mechanical damage, however it is not likely to cause serious injury or death**.**

SAFETY SUMMARY

CAUTION: The Solid State Laser Systems (green 532 nm and red 660 nm) used in the PDI-200 MD are Class 3B lasers. The laser output beams are, by definition, a safety and fire hazard. Precautions must be taken to prevent accidental exposure to both direct and reflected beams.

Class 3B lasers are defined by the Federal Register 21 CFR 1040.10 laser safety standard. The standard requires that certain performance features and laser safety labels be provided on the product. Reproductions of the warning labels are shown in this section.

The American National Standards Institute publishes a laser safety standard for users titled “American National Standard for the safe use of lasers” (ANSI Z136.1). Artium Technologies, Inc. recommends that laser users obtain and follow the procedures described in this ANSI user standard. Copies may be obtained from:

American National Standards Institute Inc.

1430 Broadway

New York, NY 10018

OR

Laser Institute of America

12524 research Parkway

Orlando, FL 32826

Please refer to the following publications for additional information on laser safety:

Sources of Laser Safety Standards

1. "Safe Use of Lasers" (Z136.1)
   American National Standards Institute (ANSI)
   11th West 42nd Street
   New York, NY 10036 USA
   Phone: (212) 642-4900

2. "A Guide for Control of Laser Hazards"
   American Conference of Governmental and Industrial Hygienists (ACGIH)
   6500 Glenway Avenue, Bldg. D-7
   Cincinnati, OH 45211 USA
   Phone: (513) 661-7881

3. Occupational Safety and Health Administration
   U.S. Department of Labor
   200 Constitution Avenue N.W.
   Washington, DC 20210 USA
   Phone: (202) 523-8148

4. "Safety of Laser Products" (EN60825-1:1994)
   Global Engineering Documents
   15 Iverness Way East
   Englewood, CO 80112-5704 USA
   Phone: (303) 792-2181

LASER SAFETY LABELS

Laser safety labels can be found on various locations both on the outside and inside of the PDI-200 MD.

WARNING: Exposure to laser radiation can be harmful. All apertures which can emit laser energy in excess of levels which are considered safe, or areas of the instrument to which exposure to laser radiation can occur due to disassembly, are identified with the appropriate label shown in this section. Take extreme care when working in areas where these labels are placed.

WARNING: Instrument users must provide protective eyewear suitable for the lasers emission wavelength. The lasers' emission wavelengths are indicated in nanometers (nm). The red solid state lasers emit radiation at 660 nm and the green laser emits at 532 nm.

WARNING: Use of controls or adjustments or performance of procedures other than those specified herein may result in hazardous radiation exposure.

LASER SAFETY LABELS USED ON THE PDI-200 MD TRANSMITTER

1

2

3

LASER SAFETY LABEL PLACEMENT ON THE PDI-200 MD TRANSMITTER

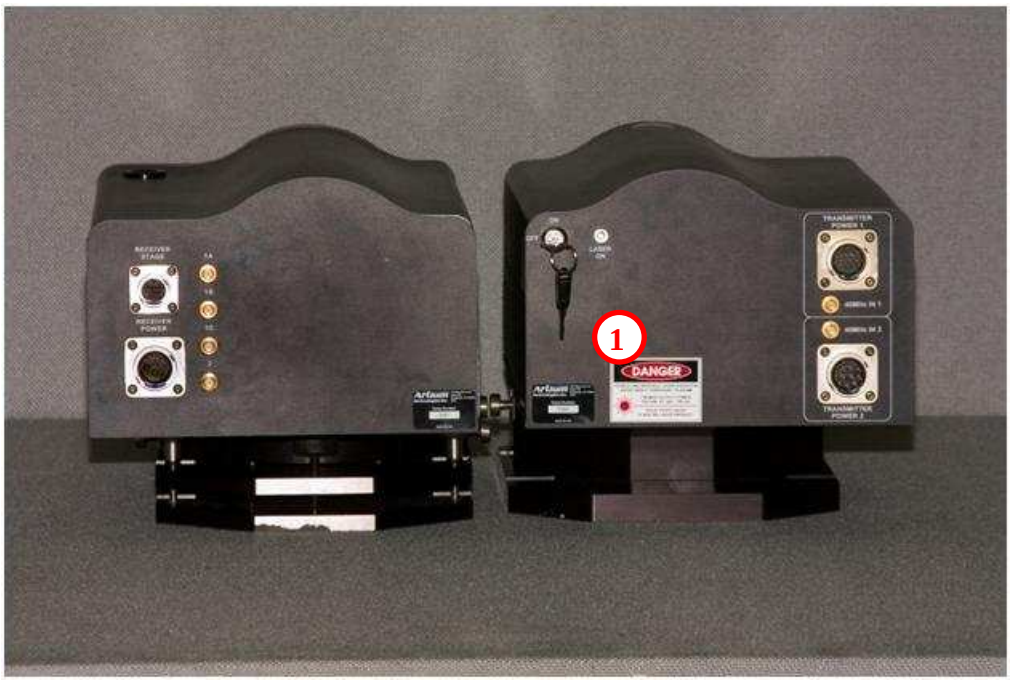

LASER SAFETY LABEL PLACEMENT ON THE LASER

Chapter

7 Hardware Setup/Connection

PDI-200 MD Major Components

1) Power Source

2) PDI Transmitter

3) PDI Receiver

4) ASA Signal Processor – Channel 1

5) ASA Signal Processor – Channel 2

6) Computer

Figure 7.1: The Artium PDI 200 System.

Figure 7.1 shows the components of the PDI 200 with labels describing each electronics and optics enclosure. A description of the connectors on the electronics and optical enclosures is provided in figure 7.2 with the adjoining table showing what connections need to be made for the proper function of the instrument. In general, the electronic connections can only be made to the proper connectors. However care must be taken in connecting the signal cables to the proper locations, namely connectors labeled as Input Signals (BNC connectors) on the ASA Signal Processor must be connected to Input A, B, and C with the labeled cables from the receiver labeled correspondingly as 1A, 1B, and 1C. Care must be taken to carefully aligned a connectors before plugging them in so that the pins are not damaged or misaligned. This is especially true for the SCSI cable connecting the ASA Signal Processors to the computer and to each other.

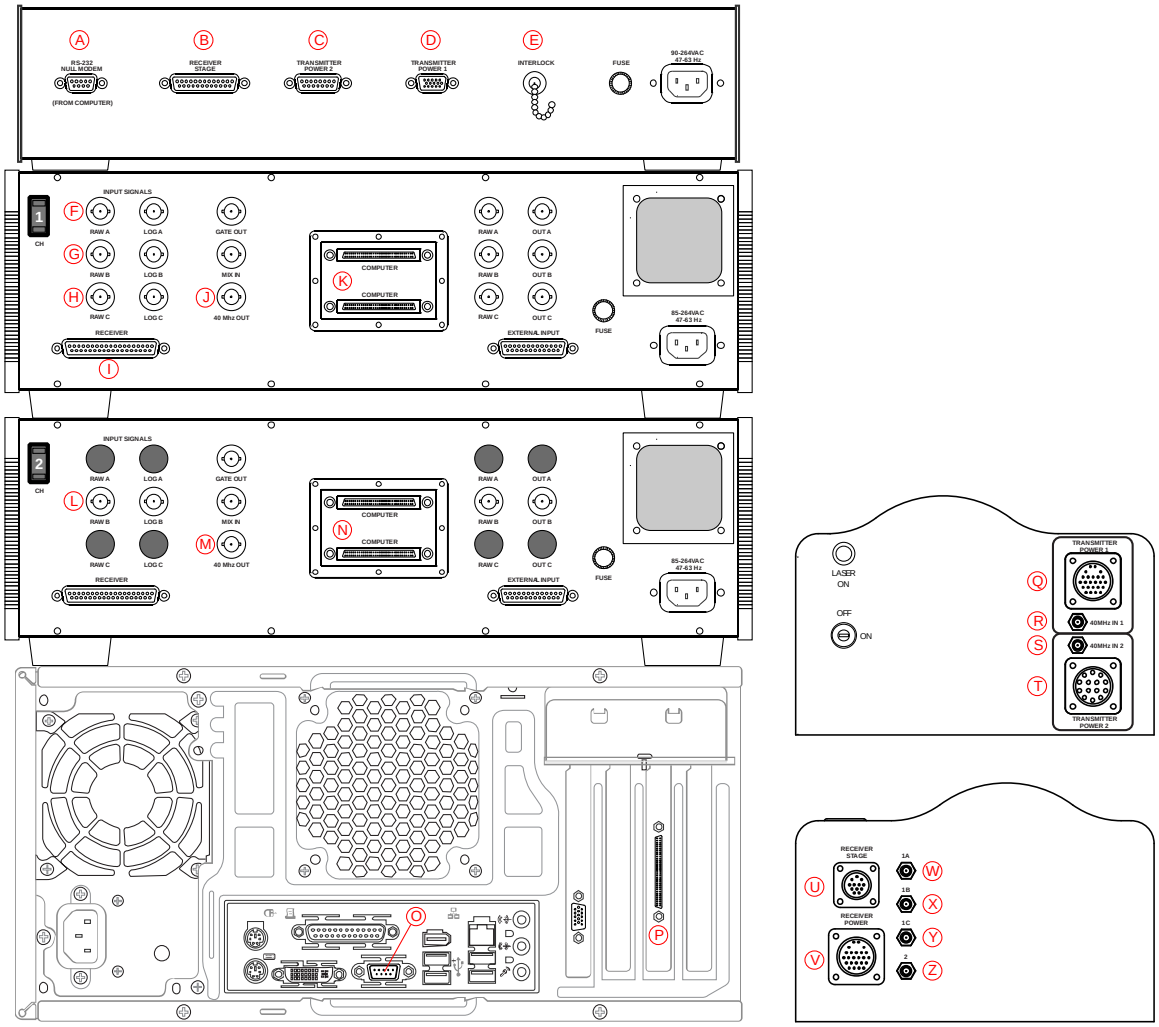

Figure 7.2. Connection diagram for the PDI 200 Instrument

Extension Connection	*Max. Extension Length*		*Label on Cable*		*Label on Cable*	
No Extension		**C**	Transmitter Power 2		Transmitter Power 2	**T**
No Extension		**D**	Transmitter Power 1	**Transmitter Cable Bundle**	Transmitter Power 1	**Q**
50 Ω Coax, BNC connections		**J**	40 MHz 1	< 4m length	40 MHz 1	**R**
50 Ω Coax, BNC connections		**M**	40 MHz 2		40 MHz 2	**S**
50 Ω Coax, BNC connections		**F**	1 RAW A		1A	**W**
50 Ω Coax, BNC connections		**G**	1 RAW B		1B	**X**
50 Ω Coax, BNC connections		**H**	1 RAW C	**Receiver Cable Bundle**	1C	**Y**
50 Ω Coax, BNC connections		**L**	2 RAW B	7 - 10m	2	**Z**
37 conductor cable, d-sub 37 male to female wired straight		**I**	Receiver		Receiver Power	**V**
No Extension		**K** (either)	Proc. 1 to Computer	**SCSI-3 Cable**, 2m	Proc. 1 to Computer	**P**
No Extension		**K** (either)	Proc. 1 to Proc. 2	**SCSI-3 Cable**, 1m	Proc. 1 to Proc. 2	**N**
25 conductor cable, d-sub 25 male to female wired straight	30m	**B**	Receiver Stage	**Receiver Stage Cable**, 10m	Receiver Stage	**U**
9 pin d-sub serial cable		**A**	Serial Port (computer)	**Null Modem Cable**, 3m	RS-232 Null Modem	**A**
		E		**User-Supplied Interlock** (closed = "safe")		

Descriptions of the Connections

In this section, each of the connections on the electronics and optical enclosures will be described and will refer to figures 7.1 and 7.2.

Power Source

This enclosure contains the laser power supplies and the power supply for the motorized module in the receiver that controls the selection of the split apertures. The connections to this box are as follows:

A RS 232 Null Modem

This connection allows communication with the computer so that the lasers can be turned on and off and the slit aperture in the receiver can be moved to the selected location. A null modem cable is provided to connect to the computer.

B Receivers Stage

Power to the receiver translation stage allowing selection of the split aperture is provided through this connector. The appropriately cable with connector labeled Receiver Stage is connected from this point to the connector on the back of the receiver enclosure, labeled Receiver Stage and indicated as U in Fig. 7.2.

C Transmitter Power 1

Power and control for the green wavelength laser including the interlock safety switch is provided through this connector. Power is also provided to the Bragg cells located in the transmitter through this connector. The cable provided with the appropriate connectors and labeled Transmitter Power 1 is connected to the connector on the back of the transmitter labeled Transmitter Power 1 and shown on the diagram in Fig.7.2 as Q.

D Transmitter Power 2

Power and control for the red wavelength laser including the interlock safety switch is provided through this connector. Power is also provided to the Bragg cells located in the transmitter through this connector.

E Interlock

This connector allows a laser interlock switch located on the door or other access to the laboratory to be activated so that when a connection is broken via the interlock switch, the laser will shut off.

ASA Signal Processor CH 1

The ASA signal processor accepts the Doppler burst signals from the receiver and amplifies and filters the incoming analog signals, performs digital and analog signal detection, and presents information on the detected digitized signals to the computer via a high-speed interface card. The signals are processed to produce the size and one component of velocity of the droplets. The following connections are required for proper operation of the instrument.

F, G, and H, Input Signals

The BNC cables provided with the instrument must be connected to the proper BNC connectors on the ASA signal processor. The cables are labeled 1A, 1B, and 1C. The other end of the cable is connected to the receiver enclosure to the SMA connectors labeled 1A, 1B, and 1C indicated as W, X, Y on Fig. 7.2. Be careful to **not** connect to to Log A, Log B, and Log C.

I Receiver

Power for the four photomultiplier tubes in the receiver is provided through this connector. Power and control of the calibration laser is also provided through this connector. The appropriately labeled cable with is connected from this point to the receiver connector labeled Receiver Power and indicated on the diagram in Fig. 7.2 as V.

J 40MHz Out

This BNC provides a 40 MHz signal output to drive the Bragg cells in the transmitter enclosure. The long BNC cable provided must be connected to this point and to the transmitter SMA connector labeled **40 MHz in 1**, shown on a diagram in figure 7.2 has connector R.

K Computer

O Null Modem

The Null modem cable is connected to the serial port labeled as “O” on figure 7.2. The other end is connected to the back of the Power Source enclosure to connector labeled Null Modem and indicated as A in figure 7.2.

Digitized signals and other information are transmitted through this port to the computer. The long shielded SCSI 3 cable (labeled) provided with the instrument is connected to this point on the ASA signal processor and the other end is connected to the interface card slot on the back of the computer indicated has **P** on the diagram in figure 7.2. Care must be taken in making these connections since the pins on the connectors are small and can be easily bent if plugged in carelessly. A second SCSI 3 cable is provided to connect ASA Signal Processor 1 to ASA Signal Processor 2. Typically, the bottom connector on processor 1 is connected to the top connector on processor 2.

RAW A, RAW B, and RAWC BNC Connectors

These connectors are used as monitor points for observing the signals with an oscilloscope. The signals at these points are identical to the signals entering the signal processor at the input signal connectors. It is useful to observe the raw signals with an oscilloscope during alignment of the instrument and during operation to ensure that the quality the signals is adequate and that there are no problems with the incoming signals.

OUT A, OUT B and OUT C BNC Connectors

These monitor points allow the observation of the signals after they have been filtered by the low pass and high pass filters and amplified logarithmically. The signals observable at this point are digitized and that information is passed to the computer for processing using the complex Fourier transform.

GATE OUT BNC Connector

This monitor point allows the observation of the gate signal which rises to approximate level of 5 V when a signal is detected and falls at the end of the signal. This information is useful in observing the performance of the Doppler signal burst detection.

EXTERNAL INPUT

This connection point allows the input of information from other data gathering devices such as pressure monitoring, temperature monitoring, etc. These data are then appended

to the data stream being transmitted to the computer for processing. It can also be connected to a resttable clock so that ensemble averages can be obtained from pulsed injections, for example.

ASA Signal Processor Ch 2

The connections to signal processor 2 are similar to the connections for signal processor 1 except that only one signal input is connected at the input signal BNC connector. Channel 2 only measures the drop of velocity and direction orthogonal to the velocity component measured by Channel 1. The Input Signal is connected to BNC labeled Raw B. The 40 MHz out signal must be connected using the long shielded cable to the transmitter SMA connector labeled 40 MHz In 2. The SCSI 3 cable is connected to the connector labeled N and the other end is connected to the channel 1 ASA Signal Processor.

PDI TRANSMITTER

WARNING: Instrument users must provide protective eyewear suitable for the lasers emission wavelength. The lasers' emission wavelengths are indicated in nanometers (nm). The red solid state lasers emit radiation at 660 nm and the green laser emits at 532 nm. The key in the back of the transmitter enclosure turns the lasers on or off

This enclosure contains the green and red wavelength lasers which produce hazardous light beam intensities. Caution must be taken in operating the system and protective eyewear must be used when performing alignment. Enclosure also contains the appropriate optics and Bragg cells use to shift the frequency and split each laser beam into two equal intensity beams.

Q Transmitter Power 1

This connector accepts the cable labeled Transmitter Power coming from the Power Source enclosure shown in figure 7.1 to provide power for the green wavelength laser and Bragg cells in the transmitter enclosure.

R 40 MHz In 1

40 MHz Bragg cell driver signal from BNC labeled J. on the ASA Signal Processor CH 1 on figure 7.2 is connected to this connector.

S Transmitter Power 2

This connector accepts the cable labeled Transmitter Power coming from the Power Source enclosure shown in figure 7.1 to provide power for the red wavelength laser and Bragg cells in the transmitter enclosure.

T 40 MHz In 2

40 MHz Bragg cell driver signal from BNC labeled M on the ASA Signal Processor CH 2 on figure 7.2 is connected to this connector.

Receiver Base and Alignment

The PDI transmitter and receiver have bases that allow mounting the enclosures to an optical table, optical rails, or other supporting fixtures. The transmitter has a fixed base that can be easily mounted to an optical rail. Final alignment of the receiver to the sample volume is accomplished with the use of the adjustments and mechanisms shown in figure 7.3. This figure shows the components of the base and the alignment mechanisms. Since light scatter detection may be required at various collection angles, depending on the droplet material being measured and the constraints of the experiment, the base was designed to provide a wide variety of configurations. The basic design strategy was to incorporate mechanisms that allow precise movement of the receiver enclosure parallel to the laser beam axis to position the receiver to view the beam intersection point. Traversing along the receiver axis allows precise focusing of the receiver optics onto the sample volume. Elevation screws are provided to tilt the receiver enclosure up or down in the vertical plane to enable aligning the sample volume to the receiver slit aperture.

The left drawing in figure 7.3 shows the base plate which is located on traversing rails to allow motion parallel to the laser beam axis. Mounting holes and slots to accommodate ¼ 20 or M6 low profile socket cap screws are provided to enable flexibility in mounting the base plate to the optical rail or other support mechanism. The slider plate has a protractor scale etched in it to enable positioning of the next level carrier shown in the middle drawing at the appropriate light scatter detection angle. The carrier has four (4) curved slots in it to allow angular positioning. The carrier is placed on the base plate at close to the desired angle and the 4 M4 screws are installed in the holes aligned to the curved slots. The index mark is aligned to the appropriate angle on the protractor etched into the base plate.. Collection angles of 30 or 40° from the transmitted laser beam axis are typical. The base plate mechanism is then mounted to the base of the receiver enclosure

by aligning the dowel pins to the appropriate holes in the base plate and installing the M4 hex head screws provided with the unit.

Also shown in figure 7.3 is the focusing mechanism located on the right-hand side of the base plate mechanism. Focusing is accomplished by rotating the drive screw on the rack and pinion mechanism. A locking lever is provided to hold the mechanism in place once proper focus has been achieved. Drive screws at either end of the rack are provided as a push/pull mechanism to move the receiver enclosure about a vertical plane for aligning the sample volume to this with aperture in the receiver.

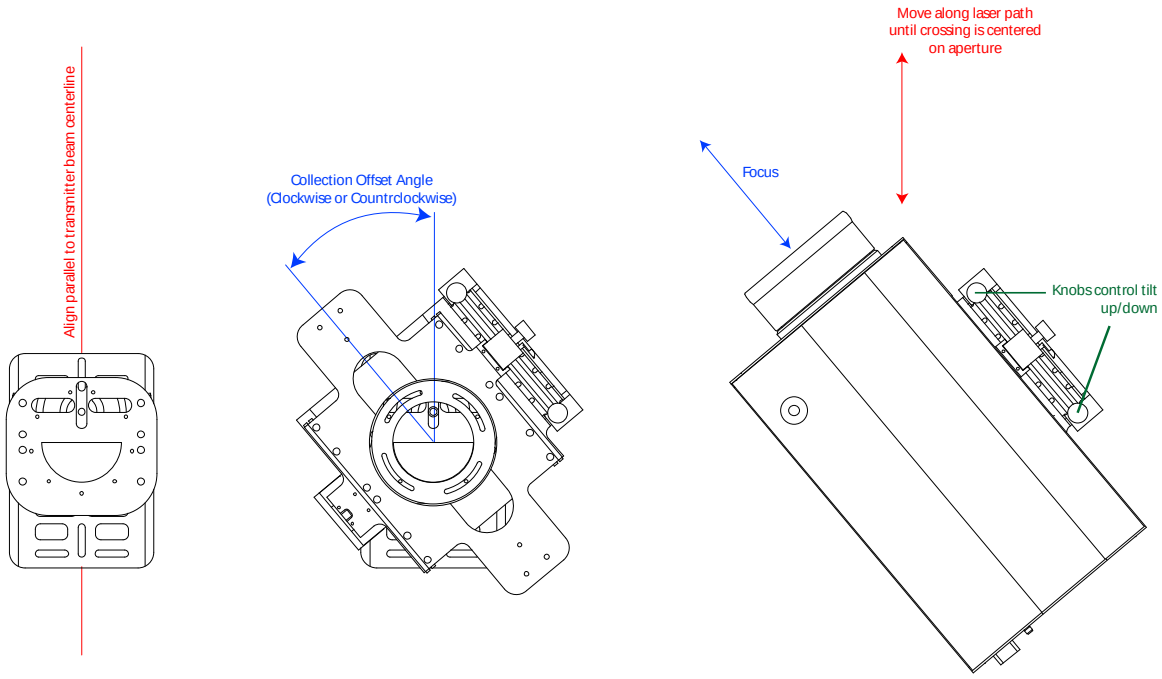

Figure 7.3. Schematic showing the adjustable base of the receiver optics enclosure and the possible orientations.

.

Chapter
8 Software Setup

PDI Device Setup Parameters

In this section, the setup parameters for the system processing electronics and software are described in detail. Although the instrument has a unique automated setup feature (Patent Pending), it is important to know something about the meaning and function of each of these parameters so the user has a better understanding of the system operation. The function of these parameters is also needed in order to make intelligent judgments if manual setup is required. Manual setup may be needed in special cases when the signal-to-noise ratio is low or in very challenging measurement environments. The setup parameters are accessible by using the **F4** function key, by selecting **Acquisition->Device Window…, or simply clicking the mouse on the Device Control icon on the left column** of the AIMS software menu. The parameters in the various tabs are described below.

Acquisition

Acquisition Stop Mode

Data acquisition shown in figure 8.7 may be controlled with three possible commands, Time, # Signals, and Free Run.

Time

This selection is used to set the total time (in seconds) for data acquisition. Acquisition will continue for this elapsed time and then stop irrespective of the number of samples collected.

 # Signals

This selection allows the number of samples to be collected during acquisition (before signal validation). This number is the sum of the measurements for all channels if a two or three velocity component system is used. Typical values are from 5000 to 50,000 signals.

Good statistical representation of the largest drops in the distribution requires a large number of measurements to be made.

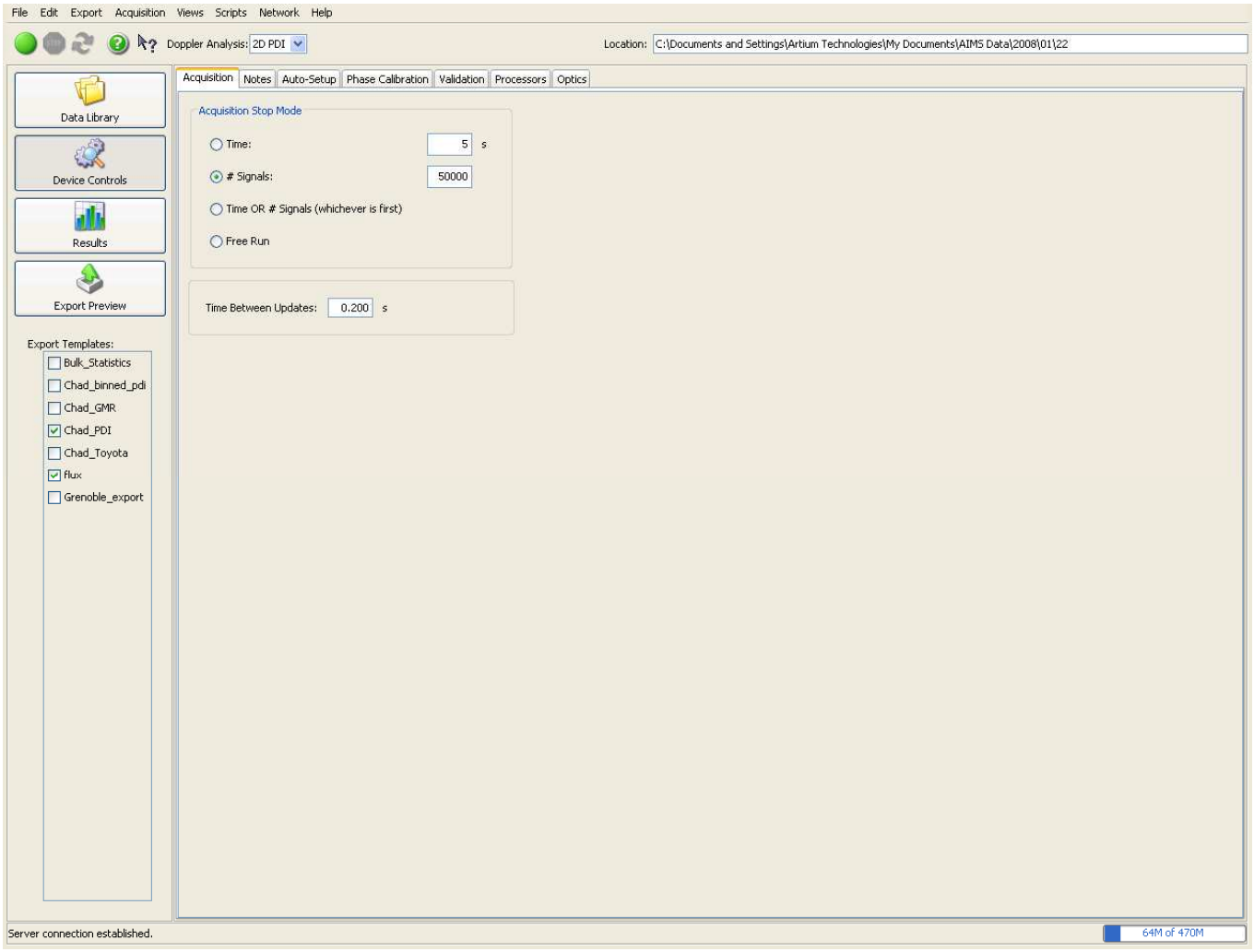

Figure 8.7: Acquisition Tab.

Free Run

When this button is activated and data acquisition is started, the system will continue to take data until the stop button is pressed. This allows the user to observe the histograms of the size and velocity distributions and make a judgment as to when an adequate number of samples have been acquired. It also allows recording of data over extended periods of time when, for example, the spray is changing in time (for example, in-cloud measurements are being made with unpredictable arrivals of the droplets).

Time between Updates

The screens displaying the data will update at the time set on the field in seconds. A setting of zero is a default which means that the software will establish the screen update rate.

Notes

This page is provided so that notes on the experimental setup, information on the experimental conditions and other information that are needed to describe the data acquisition conditions. The information is saved with each data file.

Auto-Setup

This tab allows the user to set up the instrument in either automatic or manual setup modes for channels 1 and 2 by clicking in the box to set or remove a check mark. The check mark indicates Autosetup is active.

Num. Auto-Setup Signals

In auto setup mode, figure 8.1, the instrument will use a set number of signals to measure the flow conditions and use that information to establish the optimum settings for the signal processor. This field controls the number of signals (per channel) that the auto-setup routines will use for the auto-setup of processor parameters. Typically a value between 200 and 1000 signals is appropriate. At typical data rates of 2,000 to 10,000 samples per second, acquiring a thousand samples will only require a fraction of a second. Manual setup typically takes longer since the procedure is to set the instrument parameters, test the result, and possibly repeat the procedure until a suitable setup is attained.

Run Auto Set up Now

This command box allows the user to test the instrument and quickly set up the processor to the appropriate settings using the auto set up logic. Clicking on this box will command the instrument to take a fixed number of signals and determine the best setup for the signal processor, given the spray conditions at hand. This requires that signals are present produced by spray droplets passing the sample volume.

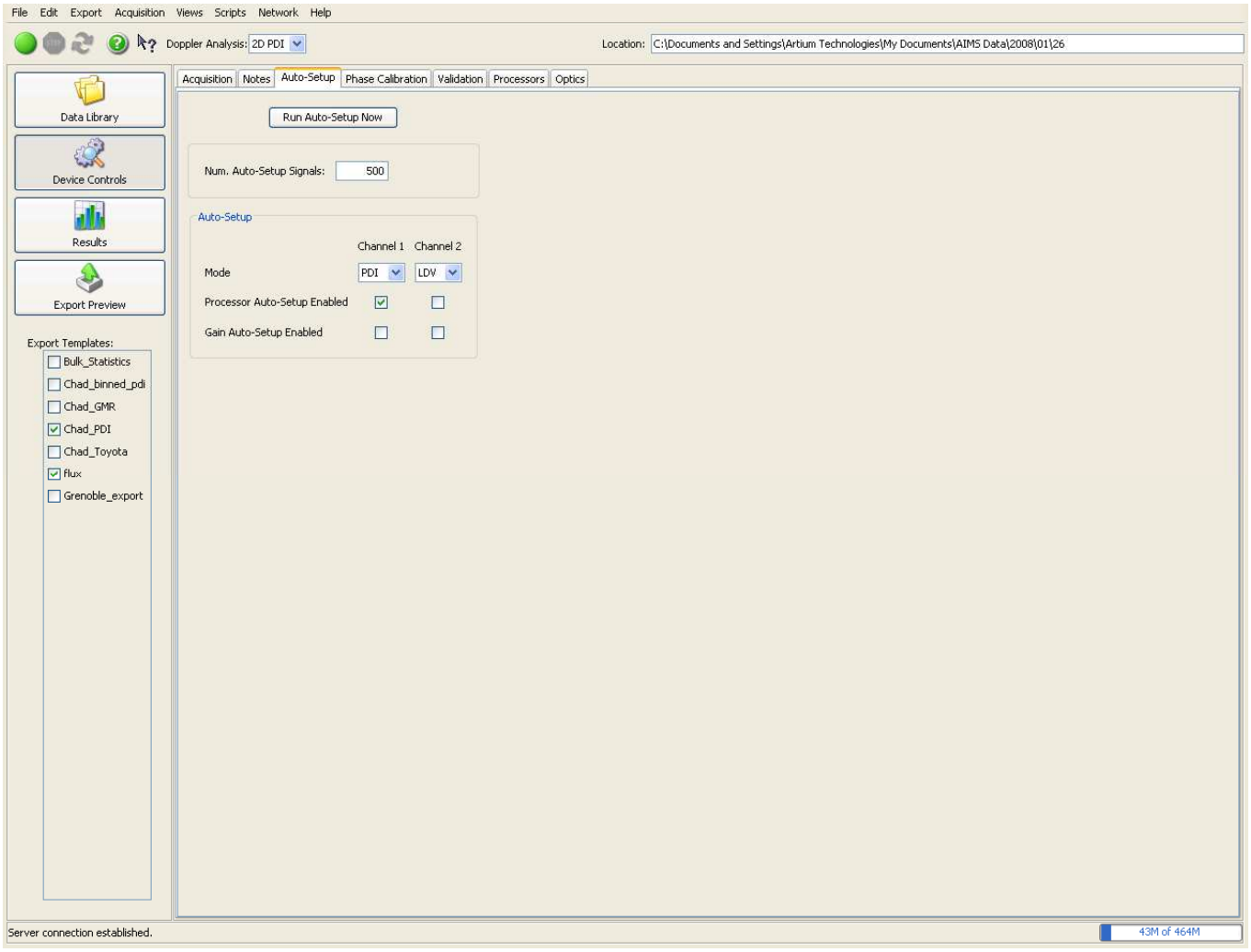

Figure 8.1: Auto-Setup Tab.

Mode

This selection allows one to indicate whether the instrument will be operated as a PDI (measuring size and velocity) or an LDV instrument (measures only velocity) which then affects the Auto-Setup functionality. Channel 2 is typically operated as a velocity only device.

Processor Auto-Setup Enabled

Clicking the Box sets a check mark indicating the Auto-Setup is on for the respective channels. In general, these buttons can be left in the on position (check mark in the box). In some conditions the signal-to-noise ratio may not be adequate or due to other complications, it may be necessary to turn the Auto Setup to off by clicking on the box to

remove the check mark and set the instrument up manually. This is the exception rather than the rule.

Gain Auto-Setup Enabled

Clicking the box for this function sets a check mark indicating that the automatic signal detector gain is operating. In order to get sufficient data to set the PMT gain, several thousand drops may need to be measured. Once again, at data rates of 1,000 to 10,000 per second, this easily wins over manual gain setting strategies. Currently, we are evaluating and perfecting the automatic gain setting algorithms.

Phase Calibration

Calibration Diode

Enabled On/Off

Periodically, the PDI instrument runs through a phase calibration procedure to ensure that there are no unexpected or uncompensated phase delays in the system. Because of the high signal frequencies that occur, small differences in the transit time of electrons through the electronic components can produce phase differences between the signals that might have a significant impact on the measurements. Since accurate particle size measurements depend heavily on the determination of phase differences between the photodetectors, it is critical that these differences due to the electronics are canceled. Phase calibration, figure 8.2 has been incorporated to subtract out the phase differences that may occur due to the photodetector electronics, signal cable length differences and the signal processor. Because the differences in the phase are caused by different transit times and electronics, the measured phase shift will also depend on the signal frequency. Thus, the phase calibration must be conducted at or near the expected signal frequencies produced by the drops passing the sample volume.

Notice: When performing phase calibration, cover the receiver lens with the lens cover so that there are no actual signals interfering with the phase calibration signals. One may also turn off the spray or block the laser beams with the transmitter lens cap.

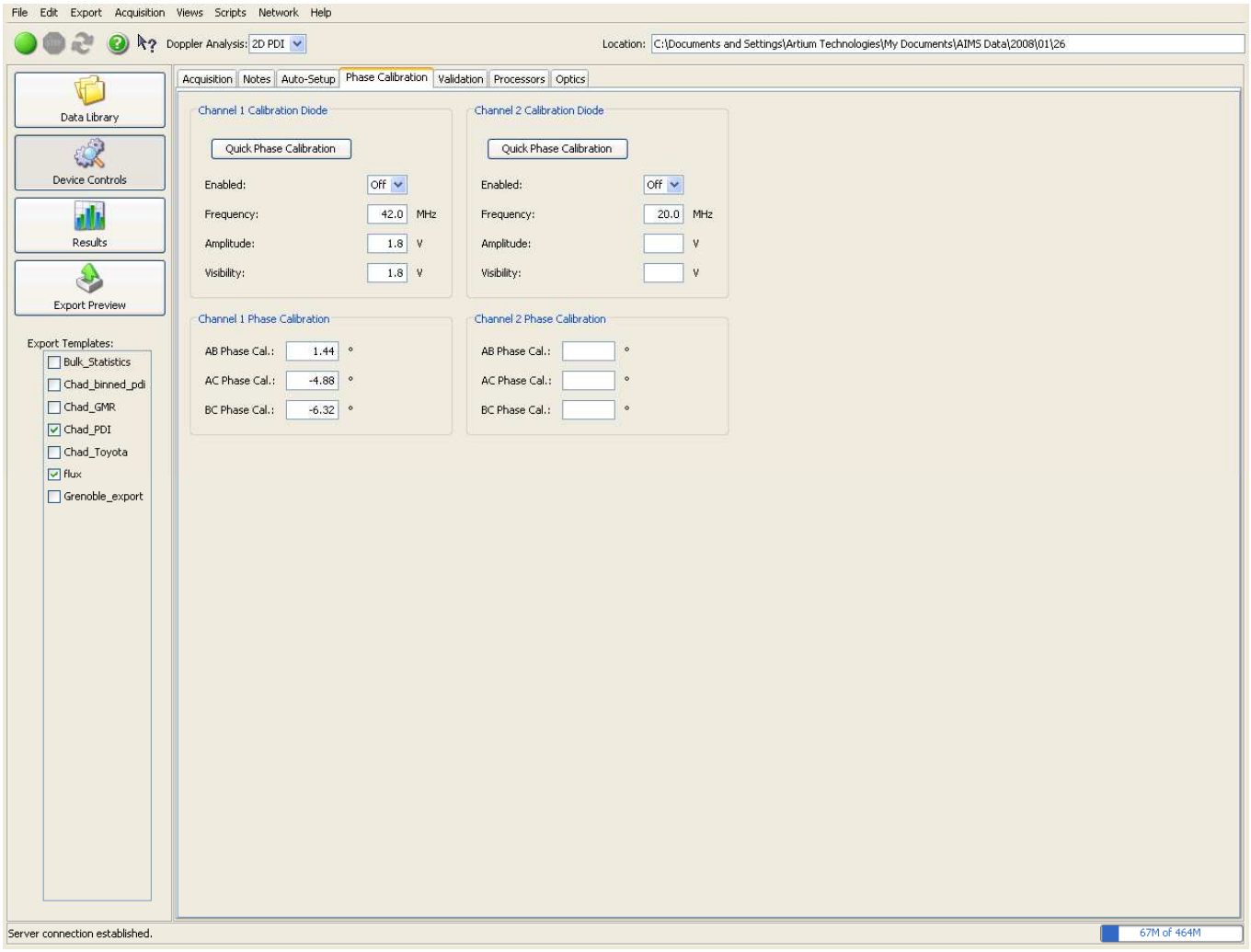

Figure 8.2: Phase Calibration Tab.

The **Enabled On/Off** command turns on the calibration laser diode that generates an identical simulated optical Doppler signal to each of the photodetectors. The instrument measures any phase differences between the signals and sets compensation values so that the relative phase shifts are all zero. Although all of the detectors and preamplifiers have been designed to minimize electronic phase shifts, this final procedure insures that very precise and accurate phase measurements are being made.

In the near future, this calibration procedure will be fully automated and will not need to be performed manually by the user.

Frequency

This command sets the signal frequency produced by the calibration laser diode and should be set to values close to the expected Doppler frequency of the actual signals produced by droplets plus the 40 MHz shift frequency. A value that is relatively close to the expected value is adequate.

An estimate of the signal frequency may be obtained as follows. First, an estimate of the flow velocity is made or a sample measurement may be obtained with the instrument to get the velocity of the spray flow. Doppler signal frequency is given as:

$$f_D = \frac{\overline{V}}{\delta}$$

where V is the mean velocity and δ is the fringe spacing given on the transmitter setup page. The signal frequency is

$$f_r = \frac{\overline{V}}{\delta} + f_s$$

where f_s is the shift frequency of normally 40 MHz. f_r is the approximate value that should be set in the frequency field (in MHz).

Amplitude

The *Amplitude* command is used to set signal amplitude of the simulated signal. Generally, a value between 1 and 3 produces the appropriate signal level. Simulated signals should be observed on an oscilloscope to ensure that they are approximately equal to the mid-amplitude range of the actual signals. Observing the Raw signals using an oscilloscope connected to the RAW signal monitors on the ASA processors, the signal amplitudes should be between 100 and 500 mV.

Visibility

The *Visibility* command adjusts the degree of modulation on the Raw signal monitor at the back of the ASA signal processor (signal directly from the photodetector which has not been high pass filtered). The appropriate values for the setting lie in the range of 1 and 3. A value should be set so that the modulation depth is slightly less than the minimum value of the signal or stated another way, the bottoms of the oscillations do not fall to zero voltage or negative when observed on the oscilloscope.

Quick Phase Calibration

Quick Phase Calibration command may be used to set up the calibration automatically. In most cases, this approach is the fast efficient way to calibrate the detectors. **Remember to set the Frequency** to approximately the expected signal frequency for the measurements. Using this command, the instrument measures a set number of signals and determines the phase shift for each of the detectors and automatically sets these values into the AB, AC and BC Phase Cal boxes under the heading **Channel 1 Phase Calibration**. Using this method, the phase Cal data are not observed. If one wishes to observe the phase Cal results, the manual phase Cal approach may be used. With this approach, the laser diode is activated by setting enabled to **On**. Under the AIMS main data acquisition page, select Views and then Phase Calibration. This page will show the phase shift for each pair of detectors (AB, AC, and BC). Click the Green button on the software user page to acquire data and then take the mean phase values and enter them with the **OPPOSITE SIGN** into the boxes for AB Phase Cal., AC Phase Cal., and BC Phase Cal. It is advisable to take several trials to ensure that the phase cal signal is producing stable results (mean not varying more than a few degrees). It the mean value is varying, ensure that the Phase Cal signals A, B, and C have amplitudes that do not differ by more than +/-30%.

WARNING: Be sure to **turn off** the Cal diode when using the manual calibration procedure. Quick Phase Calibration automatically turns off the calibration diode.

Validation

This tab shown on figure 8.3 allows the user to set the validation criteria for the instrument. Our new PDI instruments have a number of important validation criteria that each signal must pass before it is accepted as a valid measurement.

Channel 1 Basic Processing

Minimum SNR

The ASA signal processor measures the signal-to-noise ratio (SNR) for each signal on each of the three detectors for the sizing channel using the Fourier transform. The SNR is an important criteria used to evaluate whether the signal can be processed reliably and accurately to produce a valid spray drop size and velocity measurement. The addition of the SNR measurements on detector signals from B and C serves two purposes; it lets us know that these channels are receiving good signals and that these signals have

adequate SNR to be processed reliably. **These values are set at the factory at 0.35 and 0.30 and should not need to be changed**.

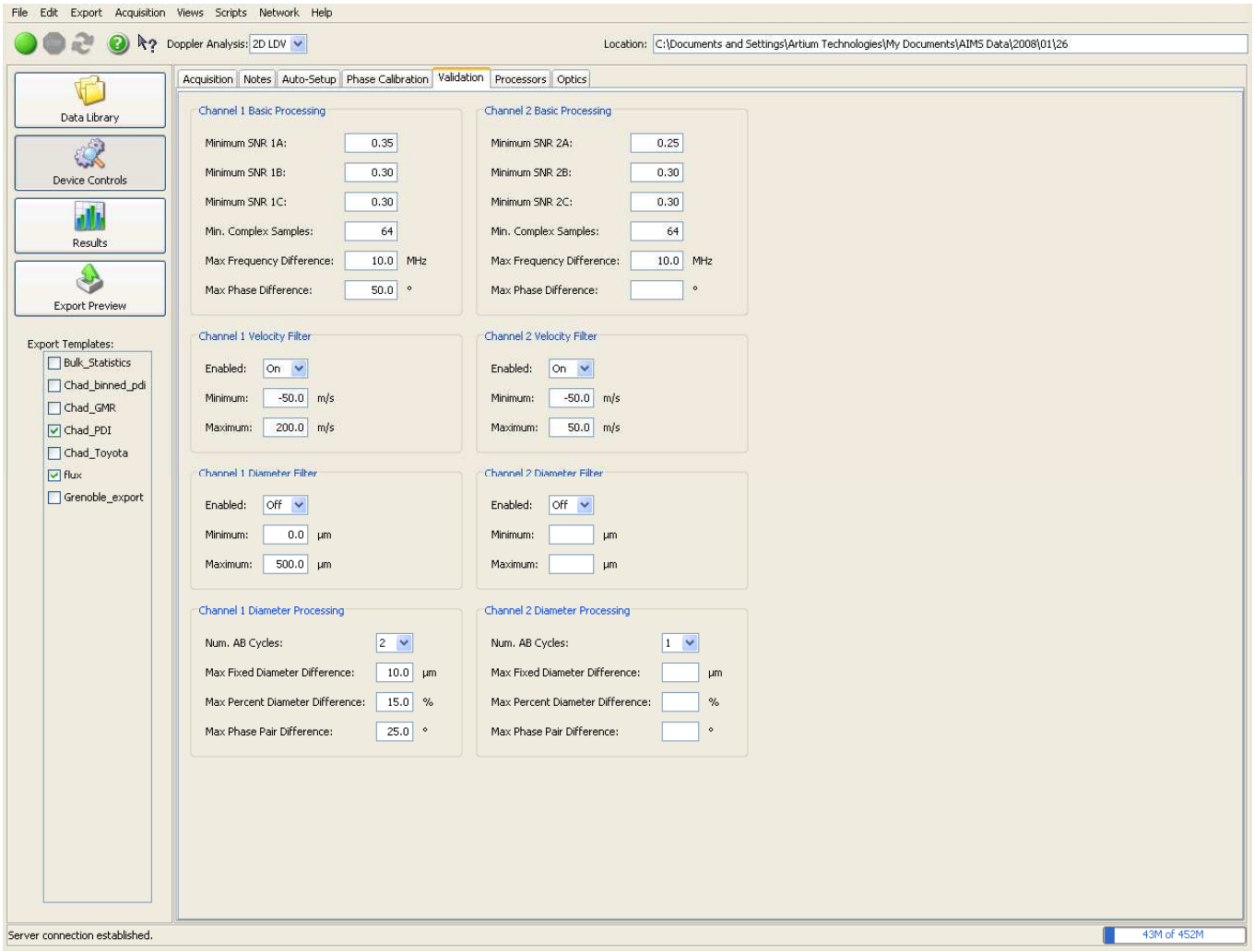

Figure 8.3: Validation Tab.

Min. Complex Samples

The ASA analog to digital conversion of the sampled signals is accomplished with high speed ADC's and both the real (cosine) and imaginary (sine) components of the down mixed signal are sampled for maximum precision and accuracy. Since the duration of the signals will vary depending upon the flow speed and the sample volume diameter, the number of sampled ADC conversions will vary. A minimum number of samples in each signal of 64 has been determined as the minimum number needed for accurate measurements. **This value should not be changed**.

Max Frequency Difference

This is the maximum frequency difference measured over the duration of the signal for each droplet measured. This is a test for the possibility of more than one drop passing the measurement volume for any measurement and such occurrences may be rejected (Patent Pending).

Max Phase Difference

This is the maximum acceptable difference in the phase shift over the duration of the signal. By testing the phase shift over the signal duration, any changes in phase due to mixed light scattering components (reflection and refraction) which can cause significant measurement error can be detected and the sample will be rejected (Patent Pending). This approach is used to ensure that the wrong light scattering component has not contaminated the information on the signal which could lead to significant sizing errors.

Channel 2 Basic Processing

These values are similar to those for Channel 1 except channel 2 does not have a sizing component.

Channel 1 Velocity Filter

Enabled

By turning this function to **On**, it sets the upper and lower limits of the velocity values that can be measured. It can be used to truncate the velocity measurements or to eliminate any potential spurious readings ("outliers") on the signal-to-noise ratio of the incoming signals as low. When the velocity filter is enabled, velocity readings less than or greater than the minimum and maximum values will not be recorded or incorporated into the computations of the mean and RMS velocity values. This constraint is generally not needed.

Channel 2 Velocity Filter

Enabled

This is a similar function operating on Channel 2.

Diameter Filter

When the Diameter Filter function is enabled by turning it to **On,** it serves to limit the minimum and maximum drop sizes that will be measured at this setting. The function can be used to limit measurements outside of the range of interest.

Diameter Processing

Num. AB Cycles

This is the number of phase cycles over which the signal phase may be measured. That is, for 1, the phase on AB may be measured from 0 to 360 degrees. If the value is set at 2, phase AB may vary over a range of 0 to 720 degrees. In most cases, the value is set on 1 since phase shifts that are larger than 360° on AB may lead to a loss of signal visibility. This results because there would be more than one fringe distance over each aperture for the detectors A, B., and C. Using the optional mask on the receiver will reduce the width of the apertures for each detector and allows the use of more than one cycle on phase AB. This enables the instrument to measure over a larger size range with very high sensitivity.

Max Diameter Difference

This is the maximum difference in the measured drop diameter for detectors AB, AC, and BC. This value is typically set to a fixed difference of form 10 to 15 um and 15% of the measured drop size. Recall that the instrument measures a drop size for each of the three pairs of detectors. Detectors AC produce the greatest sensitivity (change in phase relative to droplet diameter) followed by BC and then AB. Artium Technologies uses a unique approach (Patent Pending) using all three detectors to produce 3 drop size measurements for each droplet. These measurements are compared to the weighted mean value of the three measurements and if the difference of the size measured by any pair of detectors falls outside of the acceptable uncertainty band, the measurement is rejected. This validation scheme is very effective in eliminating faulty measurements from the measured drop size distribution.

Probe Volume Min Cutoff

When this function is turned **On**, the system limits the size of the measurement probe volume by rejecting drop signals produced by drops that have passed on the edges of the Gaussian beam intensity distribution. This function serves to better define the size of the sample volume and to reject droplet measurements when larger drops pass the edges of the focused laser beams.

Cutoff Factor

This sets a slope on the lower limits of the probe volume cutoff when this function is turned on. A value of 1 is suitable for this setting.

Cutoff Start Diameter

This sets the drop size where the sample volume limitation begins. Drops passing the sample volume that are smaller than this size typically will not scatter sufficient light from the edges of the Gaussian beam where the incident intensity is too low to produce a detectable signal. The value to set here can be approximately the Sauter mean diameter (D_{32}). This function only affects the values displayed on the data screen and the calculation of the mean values. Since all of the raw data are saved for each measurement, postprocessing may be used along with a different start diameter setting. Thus, if the start diameter has been set incorrectly, information is not being lost and can be recovered in postprocessing..

Processors

The ASA Processors tab shown on figure 8.4 controls the signal processor functions and allows manual setup of the system, if necessary. Each of the signal processor functions are defined in this section and some advice on setting up the system are provided. In general, for normal spray measurements, the auto setup mode should be used. Highly experienced users may want to try other settings and this page allows this procedure.

Channel 1 ASA Processor

FFT Bins:

The calculations of the Fourier transform are normally completed using 1024 frequencies which is also the maximum number of samples collected over the signal duration for signals that are long enough. It is also possible to compute the FFT with more frequencies to obtain a higher resolution on the frequency and phase. In general, a value greater than 1024 is not necessary but values of 2048, 4096, and 8192 may be used in very special cases.

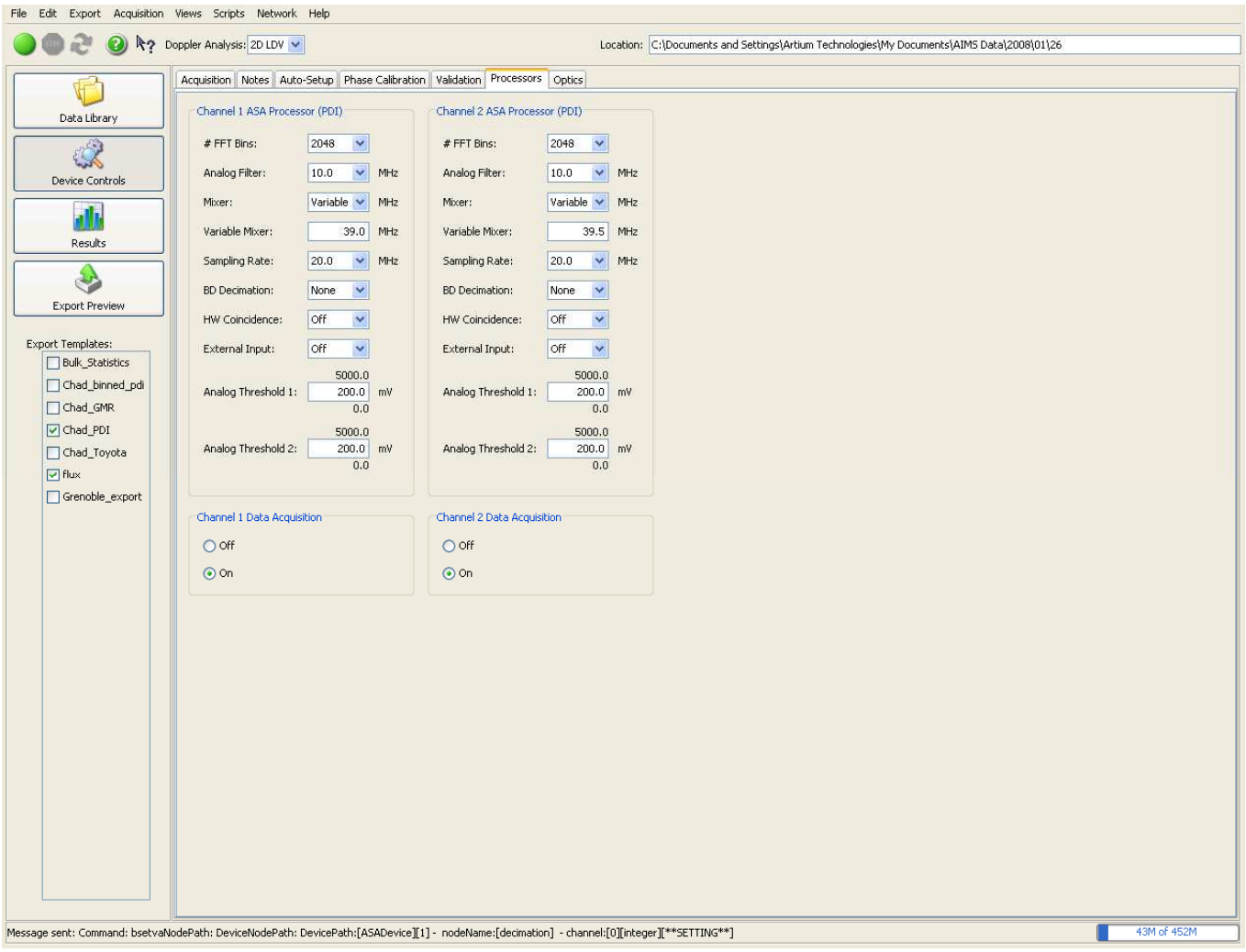

Figure 8.4: ASA Processor Tab.

Analog Filter

The analog filter serves two purposes; it helps to reduce the noise on the signal and removes the sum frequency produced by the frequency mixer. When using a mixer, a local oscillator frequency is mixed with the Doppler signal plus frequency shift. The mixer produces the sum and difference frequencies of these signals. The sum frequency needs to be removed. This is described in detail in the following paragraphs.

The signal consists of a high frequency Doppler component superimposed upon the low-frequency Gaussian pedestal component. The signal frequency is directly related to the velocity of the particle through the relationship

$$v = f_D \delta$$

The fringe spacing of the interference pattern is determined by the wavelength of the laser beam and the beam intersection angle and is given by the following expression

$$\delta = \frac{\lambda}{2\sin(\gamma/2)}$$

The raw signal produced by the photodetectors and received by the signal processor is a combination of the Doppler frequency and the shift frequency, f_s produced by the presence of a Bragg cell. The signal frequency is given as

$$f_r = f_D + f_s$$

The raw signal first passes through a fixed frequency high pass filter set to remove the pedestal component of the Doppler burst signal and any low-frequency noise. The signal is then combined with the mixer frequency, f_m which produces a signal as follows:

$$f = (f_r - f_m) + (f_r + f_{m)}$$

This resulting signal is passed through the low pass or Analog filter to eliminate the high frequency components including the sum frequency, $(f_r + f_m)$, from the mixer and any high-frequency noise. The remaining frequency is given as

$$f_t = f_r - f_m$$

A low pass filter must be set just above the highest frequency, f_t present in the signal with sufficient margin to ensure that the high-frequency excursions in the flow field pass the filter. Using the above expressions along with the knowledge of the highest expected velocity, a rough estimate of the maximum frequency can be made. If the setting is too low, it will be evident from the measured velocity distribution in the first measurement trial. When in manual mode, a few iterations may be necessary to optimize the analog filter setting.

Mixer

The mixer frequency is the value used to drive the electronics mixer that forms the sum and difference of the resultant frequency. This frequency value is set to obtain a reduced

frequency in the desired range for processing as shown in the above expressions. There are fixed mixer frequency settings of 80, 40, 38, 36, and 20 MHz. There is also a variable mixer setting which allows any value in the range of 5 to 45MHz to be set. Setting the proper mixer frequency requires some experience and is best left to the automatic setup. In manual mode the mixer may be set to minimize the signal frequency and allow a low analog filter setting which also serves to filter the noise. However, if the analog filters are set too low, filtered noise may appear to be sinusoidal in nature over short periods of time. This can lead to false detections by the signal burst detection system. After processing the signal using the Fourier transform, the signals will be rejected. However, too many false detections could slow the data acquisition rate or interfere with the detection of real signals.

Variable Mixer

The variable mixer field allows input of any mixer frequency in the range of 5 to 45MHz. The variable mixer capability is very useful when working at low signal frequencies where positioning the frequency in the right range will allow optimization of the processing functions. Once again, the auto setup algorithm does a very good job of picking the right combination of mixer of value, analog filter, and sampling frequency to optimize the signal processing.

Sampling Rate

The sampling rate refers to the frequency at which analog to digital conversions are performed. The processor has the capability of sampling the Doppler burst signals at up to 160 MHz for both the real and imaginary components of the signal. This is an equivalent sampling frequency of 320 MHz. The sampling frequency also needs to be set according to the resultant signal frequency, f_t. For laser Doppler velocimetry applications where only the frequency of the signal is of interest, the sampling frequency must be greater than twice the resultant signal frequency, f_t. When measuring the phase shift between signals, a higher sampling frequency is preferred since it provides better resolution on the phase measurements. With Quadrature Mixing (Mixer) used in our systems, clearly almost any frequency can be set for signal processing. However, the signal bandwidth and duration are critical parameters that need to be considered when selecting the sampling frequency. If the velocity fluctuations are large, the sampling frequency must be set to meet the Nyquist criterion for the highest frequency (sampling frequency greater than twice the signal frequency). A minimum number of samples need to be acquired over the period or duration of the signal. For example, the Gate signal or signal length can be observed on an oscilloscope to estimate the minimum signal duration.

Because of the complexities in setting the appropriate sampling frequency, it is best to use the Auto-Setup which optimizes the selection of the sampling frequency and other processing parameters.

BD Decimation

If the sampling frequency is greater than twice the analog filter setting, it is possible that the digital burst detection system will trigger too frequently on noise. This occurs because the higher frequency noise in the signal has been filtered leaving low-frequency noise. Low-frequency filtered noise over short durations may appear to be coherent or periodic and therefore the burst detector could recognize it as a signal. To avoid this problem while using higher sampling rates, the sampling rate for the burst detection system is reduced by the factor in the BD Decimation field (None, 2, 4). The automatic setup will select the appropriate value. However, if manual setup is used, the rule of thumb is to have the sampling rate divided by the BD decimation equal to twice the analog filter value.

HW Coincidence

This command sets the hardware coincidence circuitry which is used when two or more velocity components are measured. Setting the HW coincidence to On means that the each signal processors must have a signal present at the same time to be recorded. This means that each of the velocity component systems is measuring the same particle at the same time as it passes through the probe volume. This allows the determination of the vector velocity in two or three dimensions for each droplet. The PDI system also has software coincidence which may be applied after the measurements have been acquired. Software coincidence sorts the measurements by time of arrival and looks for signals from each of the velocity measurement components that overlap. This indicates that the particles were in the sample volume at the same time. Hence, the vector velocity for each particle may be determined.

External Input

The setting alerts the system to the presence of some other device that inputs information such as temperature pressure etc. that will be measured at the same time as a particle size and velocity are measured. This information is attached to the size and lost information on the function is turned on.

Analog Threshold 1

Analog Threshold 2

There are two signal detection systems in the ASA signal processor; a digital and analog detection system. The analog threshold allows setting a voltage threshold level at a specific value for signal detection. This is necessary if, for example, there is a low level coherent noise signal in the background. In this case the digital burst detection system will detect a signal when a Doppler signal is not present. Setting the analog voltage threshold level above this coherent background noise level will prevent the processor from detecting the background. Analog Threshold 1 sets the start detection level and Analog Threshold 2 sets the stop detection level on the Log Amplified signals. These values do not need to be equal but in general, are both set to 100 mV which represents a level of about 1 to 2 mV on the Raw Signals. Typically, values of from 100 mV to 200 mV are used. It is not generally necessary to adjust this value.

Channel 1 Data Acquisition

This software switch activates this channel. If the switch is set to Off, the channel will not show any data.

Channel 2 ASA Processor

Similar conditions apply to velocity Channel 2 except that this channel typically measures the cross stream velocity which may be lower than the streamwise velocity and only the velocity is measured, not size.

Channel 2 Data Acquisition

This software switch activates this channel. If the switch is set to Off, the channel will not show any data.

Optics

This page shown in figure 8.5 provides information on the optical setup of the PDI instrument and allows setting those optical parameters that may need to be changed to adjust the system for the prevailing spray conditions.

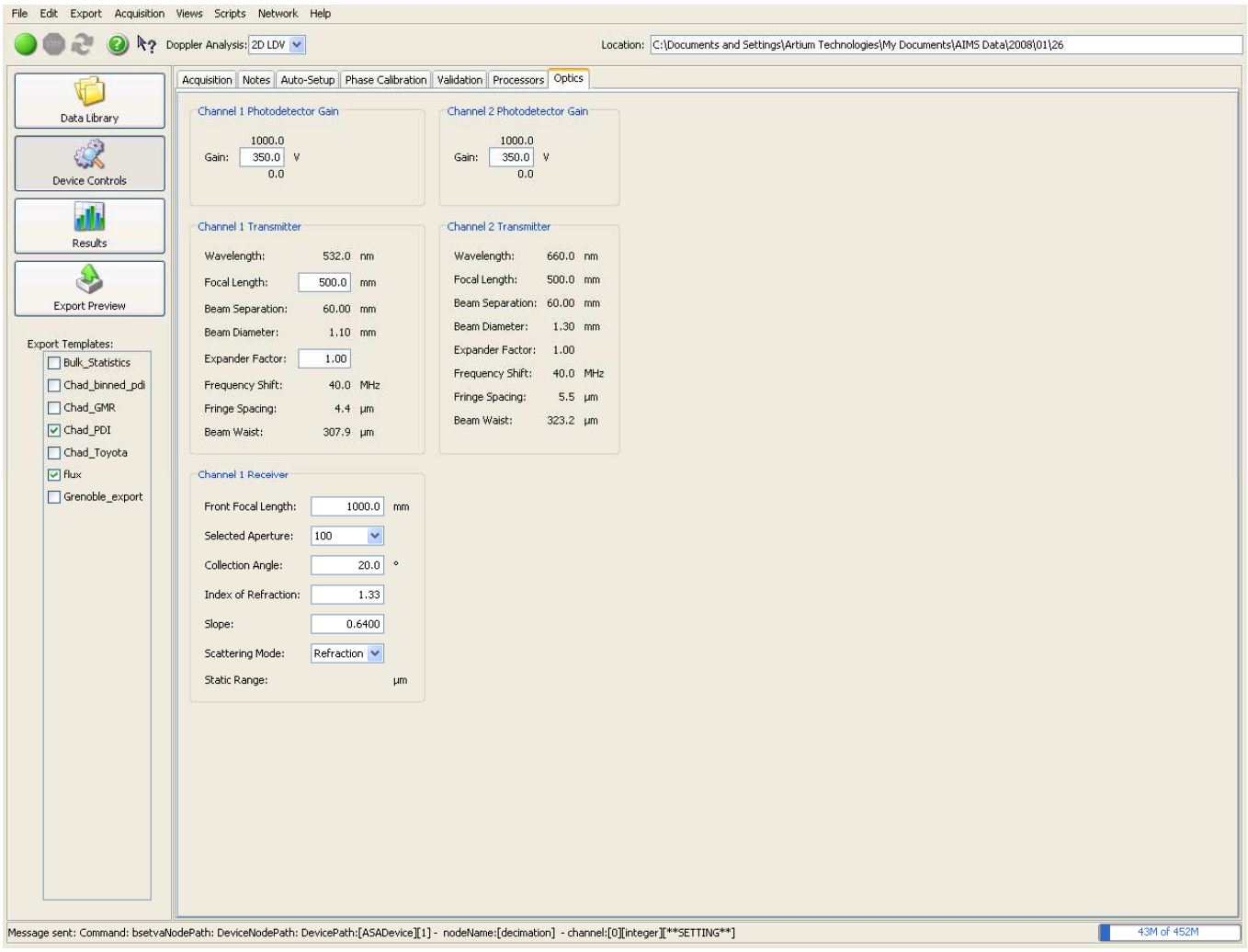

Figure 8.5: Optics Tab.

Photodetector Gain

Channel 1 Photodetector Gain

This allows setting the photodetector gain or high voltage to an appropriate value that depends upon the drop size distribution to be measured, the focal lengths of the receiver and transmitter, and other factors. The photodetectors or photomultiplier tubes convert the scattered light imaged onto them into electrical signals which are then processed to produce the velocity and size information. A value of 350 V is typically used as a start. A simple rule of thumb is to increase the gain by 50V until a value is reached where the saturation lights (red lights on the front of the signal processor box) start flashing occasionally. The voltage can then be reduced by 25 V.

This function is set automatically by measuring the signal amplitude for each drop size class and adjusting the gain so the signal amplitude corresponds to the proper value for

that drop size within the distribution. In some cases, the automatic setup may fail so it is useful to know how this function is set.

Channel 2 Photodetector Gain

When a two component system is used, the second channel is adjusted using this function. The second channel is set up similar to channel 1 but with some differences. The second channel only measures drop velocity and uses the entire receiver lens whereas the channel 1 uses 3 segments, one for each segment of the receiver lens for each detector. Therefore, the collection efficiency is at least three times greater than for channel 1. However, the laser power is less for this channel. The detector gain will be different due to this fact and the fact that the laser power for this channel is one third of that for channel 1. The gain setting for this channel will also be automated in the near future.

Transmitter (Channel 1)

Wavelength

Specify the light wavelength for the lasers used in the transmitter system. Typically, a green laser of 532 nm and a red laser of 660 nm are used for channels 1 and 2 respectively. These values are set at the factory and do not need to be changed.

Focal Length

This value is the focal length of the **transmitter lens** currently installed in the system. Transmitter lens of 320, 500, 1000, and 2000 mm focal lengths are available for the standard Artium transmitter. It is very important that the correct focal length (focal length of the lens actually used in the transmitter) is displayed in this field. The calculation interference fringe separation in the sampling volume is based on this length (along with the beam separation). In general, longer focal length lenses are needed when measuring larger drops (see the sizing table) and shorter focal lengths are used when measuring small drops. When the transmitter lens is changed, the new value must be entered into this filed. **Significant error will occur if this change is overlooked**.

Beam Separation

This is the spacing in millimeters of the two beams exiting the transmitter without a transmitter lens in place. The beam spacing is set at Artium and should not be changed

since this determines the fringe spacing of the interference fringe pattern formed at the probe volume (along with the lens focal length) and is a part of the system calibration.

Beam Diameter

This is the diameter of the laser beam entering the transmitter lens. The value is set at Artium and does not need to be changed. Beam diameter, along with the laser wavelength and transmitter focal length, determines the probe volume diameter. It also provides information to the automatic aperture width setup function.

Expander Factor

If the transmitter has an external beam expander, the beam expansion factor is input into this field. Normally this value is set to 1.00. A different value is required only for special optical designs.

Frequency Shift

All PDI transmitters are equipped with acousto-optic frequency shifters (also know as Bragg cells). Frequency shifting is needed to resolve the particle direction, whether in the positive or negative direction, and to enable high pass filtering to remove the pedestal component of the Doppler burst signal. Frequency shifting also allows the compression of the relative signal bandwidth for highly turbulent flows and flows with recirculation. Typically, a frequency shift of 40 MHz is added to the Doppler signal frequency. This value is set at Artium and should not be changed.

Fringe Spacing

Once the transmitter focal length and the beam spacing have been input in their appropriate fields, the software automatically calculates and interference fringe spacing produced at the sample volume. The fringe spacing δ is calculated as follows:

$$\delta = \frac{\lambda}{2 \sin \gamma / 2}$$

where λ is a laser wavelength and γ is the beam intersection angle set by the beam spacing and transmitter lens focal length.

Beam Waist

The beam waist is the diameter of the focused Gaussian beam at the sample volume for the1/e^2 intensity level. The beam waist d_w is calculated approximately as follows:

$$d_w = \frac{4\lambda f}{\pi D}$$

where f is the transmitter focal length and D is the diameter the beam entering the transmitter lens. This value is calculated automatically once the transmitter focal length and beam diameter are input into their appropriate fields. The value is only a guide whereas the actually diameter of the sample volume is measured for each measurement using in situ methods. The actual probe volume diameter will depend on the instrument setup and the measurement conditions. Fortunately, the instrument measures the probe diameter in situ for each measurement which also takes into account the measurement conditions.

Transmitter (Channel 2)

Similar settings are provided for the Channel 2 transmitter optics which shares the same transmitter lens. The transmitter focal length must always be the same as for Channel 1 so it is set with the input of Channel 1.

Receiver

Front Focal Length

The PDI receiver module has removable lenses that can be changed to accommodate the various drop sizes to be measured. A range of focal lengths from 350 mm to 2000 mm are available (options). When the receiver lens is changed, the focal length of the lens used **must be entered into this field**. Since this is a critical parameter, **significant measurement errors will occur if it is not set properly**. A general rule of thumb is to use the shortest focal length possible since this provides the greatest measurement resolution and accuracy and smoothes the slight fluctuations in the otherwise linear phase versus diameter response function.

Slit Aperture

The slit aperture is the width of the spatial aperture used in the receiver to limit the size of the sample volume.

Selected Slit Aperture

In Artium PDI models, the slit aperture located in the receiver can be changed via a computer controlled small traverse stage. There are currently five values that can be selected from 50 µm, 100 µm, 200 µm, 500 µm, and 1 mm. This aperture limits the size of the sample volume. For dense sprays a small slit aperture is needed to ensure a high probability of only having one droplet in the sample volume at any time. For dilute sprays or at the edge of sprays where the droplet number density is low, a wider aperture may be selected to optimize the data rate. In the near future, we plan to automate this function so that the appropriate aperture is selected automatically depending on the average arrival rate of the droplets at the sample volume. This will serve to optimize the data collection and ensure reliable data under automatic traversing and data acquisition.

Note: Some systems do not have adjustable aperture widths in which case this parameter is fixed.

Collection Angle

The collection angle is the angle at which the receiver is set relative to the transmitted laser beam, figure 8.6. The transmitted laser beam is at 0° in the collection angle is measured from the forward direction of the transmitted beam. Thus, 40° collection means that the receiver makes angle 40° with the transmit ted beam. The collection angle will affect the slope value (response of the instrument to droplet diameter) given in the next field.

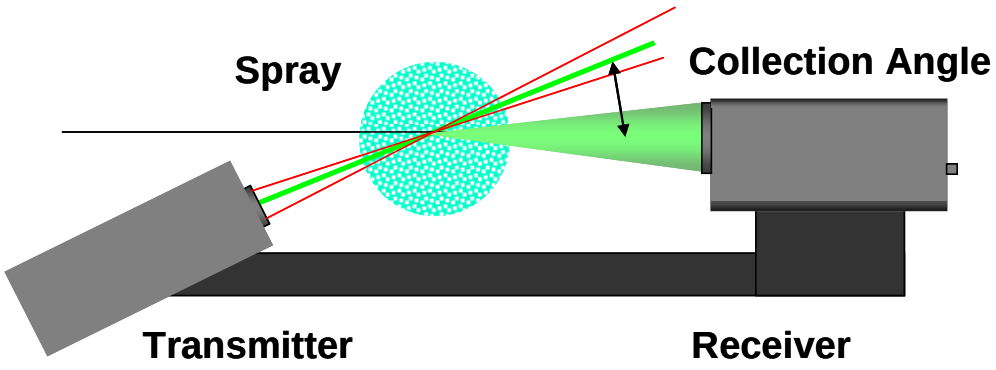

Figure 8.6: Receiver Collection Angle.

Slope

The slope is a parameter that incorporates receiver solid angle of light collection, light scatter detection angle or angle at which the receiver is set, laser wavelength, drop index of refraction, and the fringe spacing at the sample volume. It is essentially the response

function for the phase of the detected signal as a function of drop size. Slope values for discrete collection angles and the other parameters mentioned have been pre-computed and are displayed in a table. Selecting the receiver focal length, droplet material index of refraction, and collection angle, will automatically install the correct slope value in this field.

Main Laser

Enabled

For Artium flight probe systems, the laser is located at a remote location within the probe mounted on the exterior of the aircraft. This field is used for turning the laser on and off. In non-flight probe systems this field does nothing.

Traverse Control

Figure 8.8 shows the traverse control menu allowing automated scanning of the spray flow field.

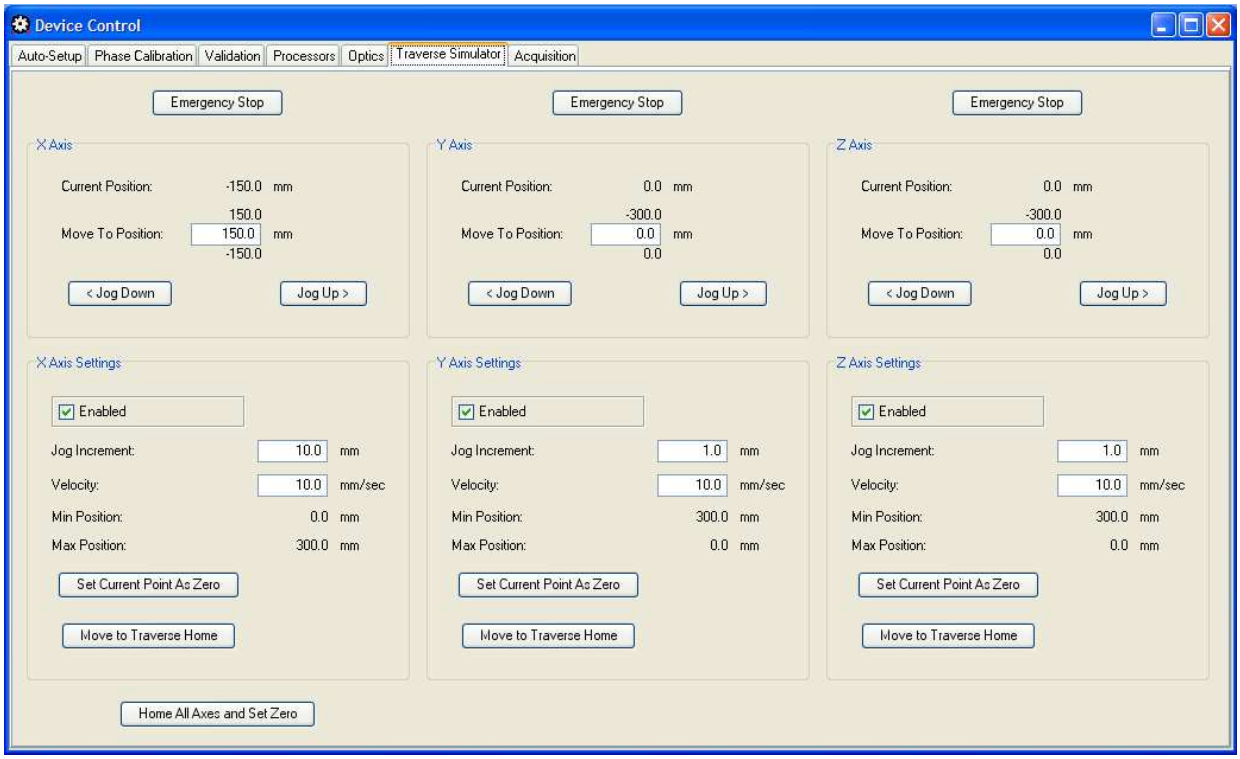

Figure 8.8 Traverse Control Menu

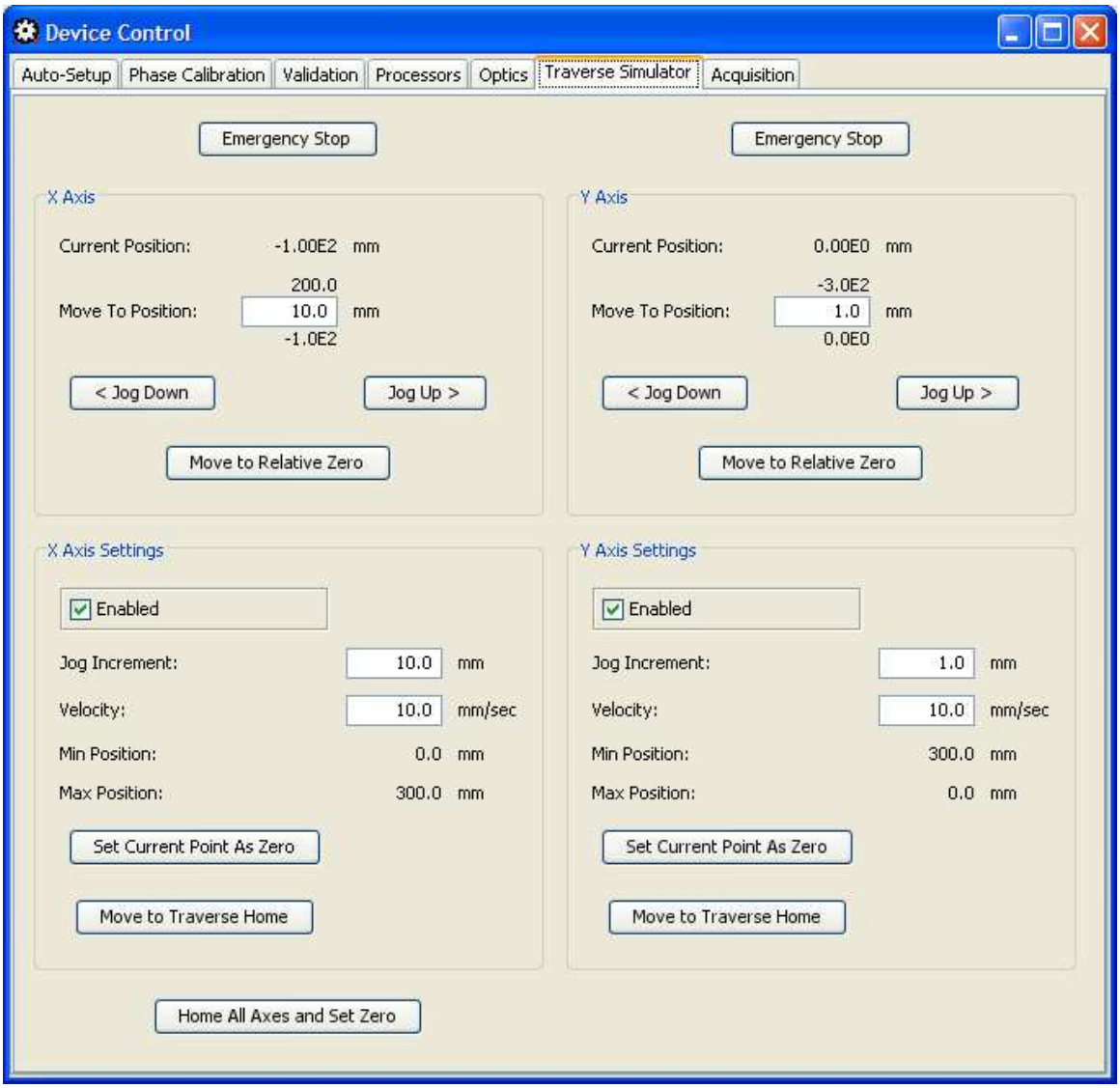

Figure 8 9: Traverse Control Tab.

Each traverse axis has a limit on travel, figure 8.9. For convenience, AIMS can shift the zero point of the axis to correspond to a more convenient location. For example, if the absolute limit of a traverse axis is 0 to 300mm, we can visualize it as:

```
Absolute Scale:      0mm                              300mm
                     X-------------------------------X
```

In this example, if we had a nozzle at 110mm that we wanted to characterize, it would be easier if the zero point was at 110mm. AIMS can shift the zero point to 110mm and you would enter "0" to move the traverse to the point under the nozzle. This is visualized as:

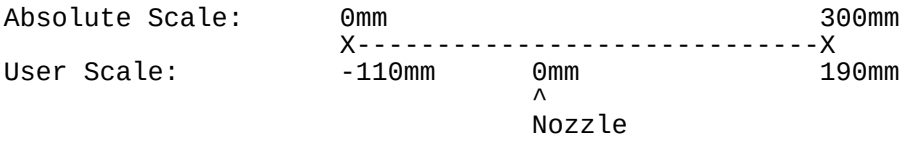

For more information, see Set Current Point As Zero or Home All Axes And Set Zero.

Emergency Stop

Clicking on this button while the traverse is in motion causes all traverse motion to cease as quickly as possible. On traverses that support it, all motion is stopped at once.

X-, Y-, and Z-Axis

These sections control the manual movement of the traverse.

Current Position

The current position (as reported by the traverse controller) of the axis, in mm.

Move To Position

To manually move the traverse, enter the desired absolute position in this field. As the traverse axis moves, the current position will be updated in the Traverse Current Position field. The maximum and minimum values for this field are shown above and below the field, respectively.

Jog Down

Moves the traverse "down" (decreasing) a relative amount from the current position. The amount of the jog move is controlled by the Jog Increment.

Jog Up

Moves the traverse "up" (increasing) a relative amount from the current position. The amount of the jog move is controlled by the Jog Increment.

X-, Y-, and Z-Axis Settings

Enabled

When this is unchecked, the traverse controller is told to disable the axis. Commands to move the traverse will be ignored.

Jog Increment

The amount (in mm) the axis/stage will move relative to the current position when the Jog Down or Jog Up buttons are pressed.

Velocity

Speed (in mm/sec) to use when the traverse is moved.

Min Position

Minimum absolute position of the traverse in millimeters.

Max Position

Maximum absolute position of the traverse in millimeters.

Set Current Point As Zero

Sets the current position of the traverse axis/stage as zero. The conversion between user position and absolute position is explained in Units.

Move to Traverse Home

Tells the traverse axis/stage to move to its home position. This position is at one end of the axis/stage and is usually referenced/indicated by a limit switch. This can be used to set the traverse axis/stage to a known (and constant/fixed) position.

Home All Axes And Set Zero

This homes all of the traverse axes/stages and then sets the current point (when the moves are finished) as zero.

Chapter
9 Optical Setup and Alignment

PDI-200 MD

The PDI 200 is a two component phase Doppler interferometer that uses two diode pumped solid-state (DPSS) lasers as the light source. The lasers emit at two wavelengths, green (532 nm) and red (660 nm). By using solid-state lasers, single mode polarization deserving fibers are no longer required. DPSS lasers also eliminate the need for very large inefficient air or water-cooled argon ion lasers. Figure 9.1 shows the major components of the two component phase Doppler interferometer. The transmitter and receiver have been designed using large optical apertures to provide the greatest sensitivity to the drop size measurements and minimize the uncertainty in the measurement of the smallest particles in the size distributions. The advanced ASA signal processors incorporate proprietary means for reliable signal detection, quadrature mixing and sampling of the signals, and signal processing using the complex Fourier transform (real and imaginary signals are sampled and processed). In this section, setup of operation of the optical system will be described.

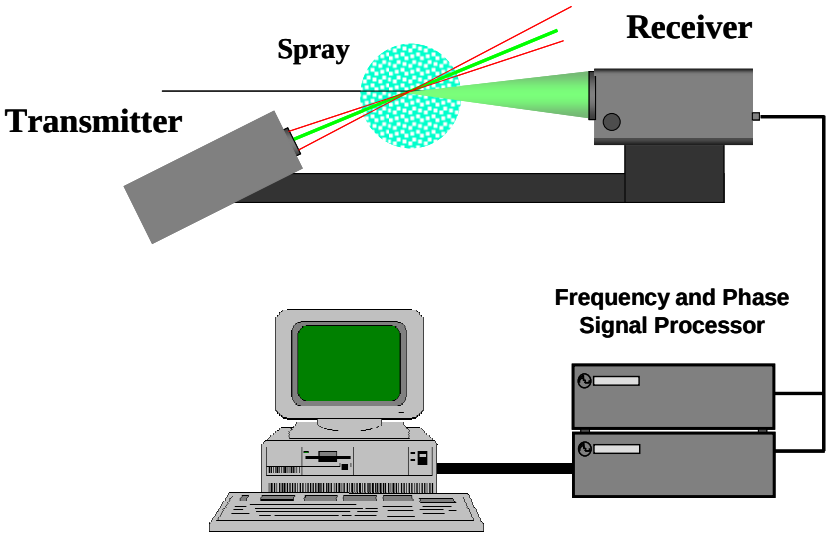

Figure 9.1: Schematic of a Two-Component Phase Doppler Interferometer showing the optical system and electronics for signal processing.

Optical Configurations

The preferred setup arrangement for the PDI system is in the off axis forward scatter configuration as shown in Figure 9.2. This arrangement provides the greatest sensitivity to the drops and minimizes the adverse effects resulting from the detection of the unwanted scattering mode, namely reflection. Only when no other possibility exists should the backscatter arrangement shown in figure 9.3 be used. Transmitter lenses are provided with nominal focal lengths of 300 mm, 500 mm and 1000 mm. The shorter focal length provides the greatest sensitivity to the small droplets. However, as a result of facility constraints and spray field size, it may be necessary to use the longer focal length of 500 mm.

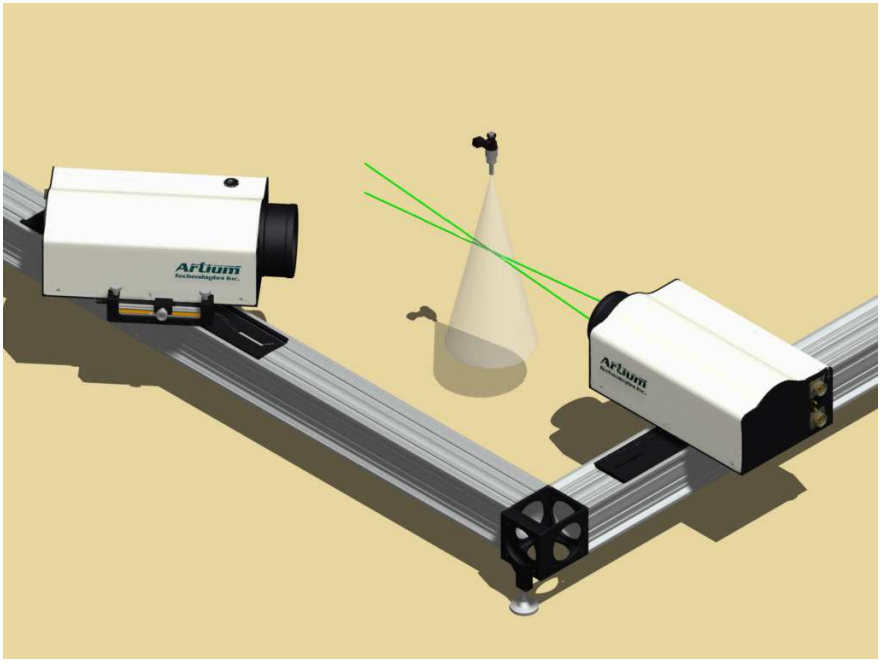

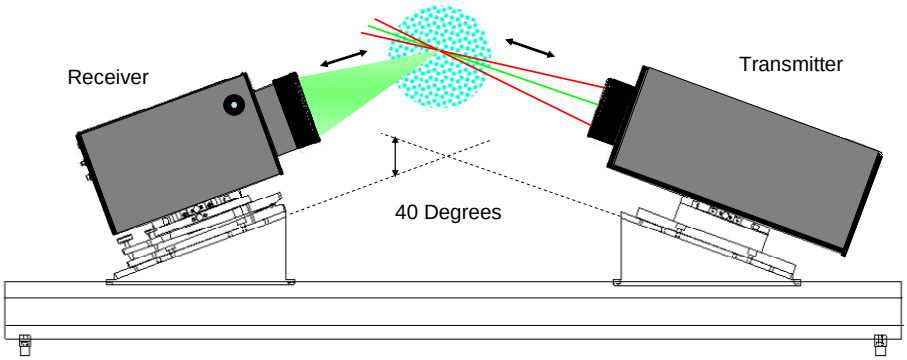

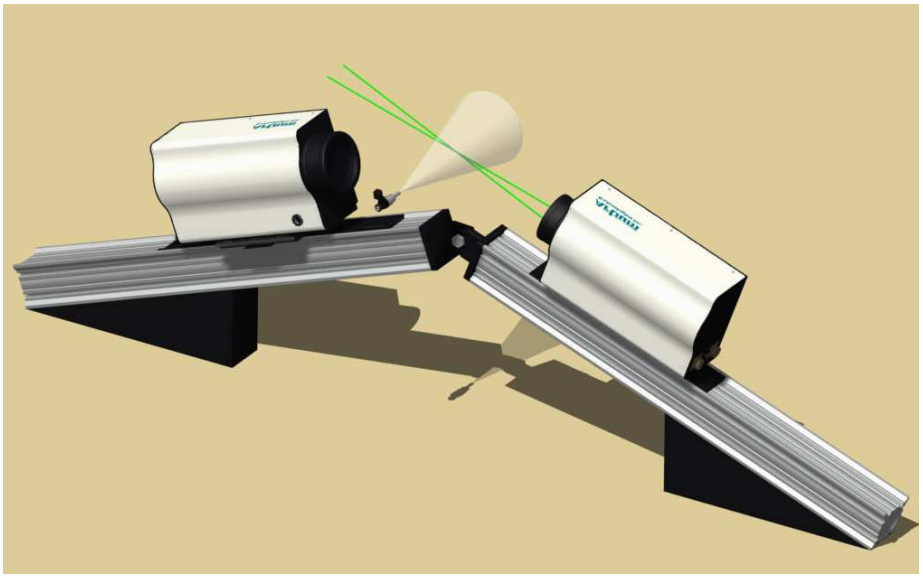

Figure 9.2: Transmitter and receiver optics setup for optimal measurements of a horizontal spray.

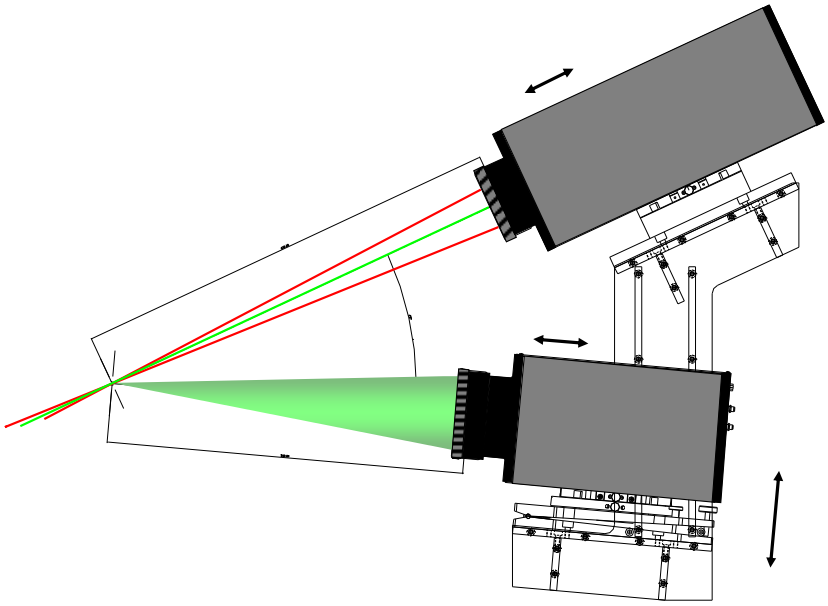

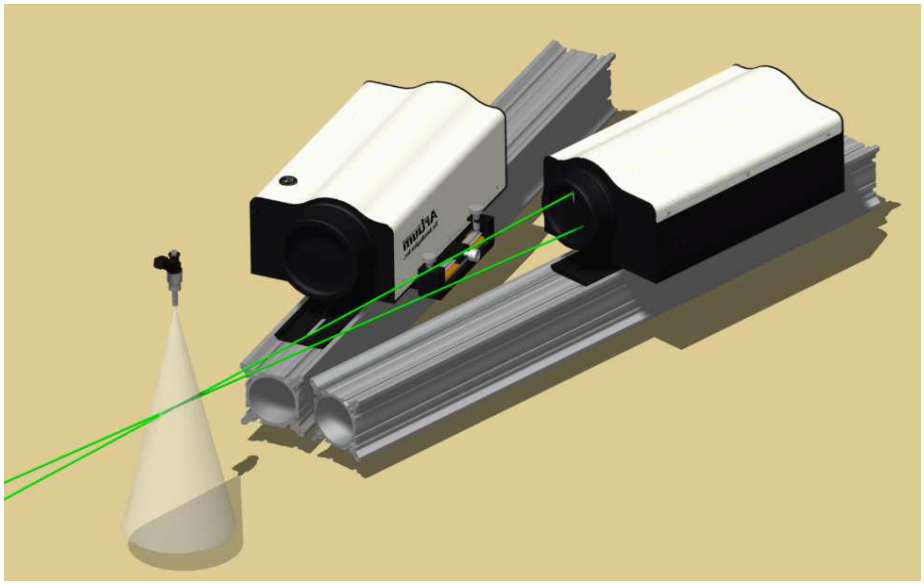

Figure 9.3: Schematic showing the transmitter and receiver set for off axis backscatter light detection. Intersection angle depend on the indexer a fraction of the material measured.

The beams spacing has been set as wide as possible to ensure the greatest sensitivity to the drops even for the 500 mm focal length lens. A table is provided in this section to be used as a guide to setting up the system to accommodate the spray drop size distribution. The software also presents the size range that can be measured when the transmitter and receiver focal lengths are input in the appropriate boxes.

For sprays directed vertically downward, the instrument can be set up in a horizontal plane. When the spray is horizontal, it may be better to set the instrument up so that the intersection angle between the transmitter and receiver are in the vertical plane. However, either configuration can be used for either spray orientation. **The only constraint that must be observed is that the receiver and transmitter are in a plane that is orthogonal to the plane formed by the two green beams used for drop sizing.** This is true for both forward scatter and backscatter, Figure 9.3, orientations. The most common off-axis configuration has the receiver located at 40° from the transmitted beam direction as shown in figure 9.2. Other angles may be used but are not recommended.

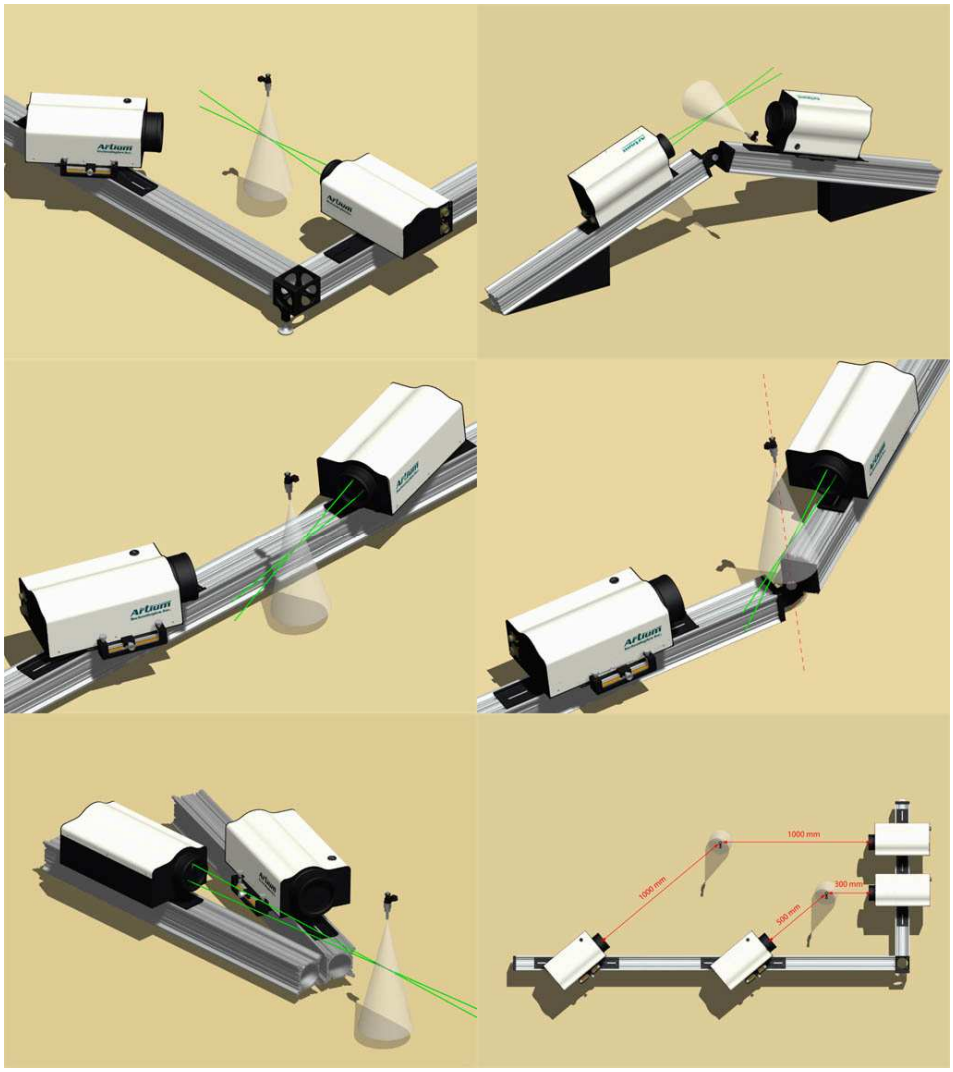

Figure 9.4 Examples of possible optical configurations that may be used.

Optics Setup Table

The following table is offered as a basic guide to selecting the optics that will cover the size range, spray pattern size, and measurement conditions. By inputting potential optical setups into AIMS, the Optics Tab will also provide the measurable size range with the various optical combinations. One must iensure that the actual optical setup is used, once a lense combination for the receiver and transmitter are selected. In general, shorter focal length lenses on the transmitter produce a smaller probe volume diameter and higher resolution and accuracy for measuring small drops. Longer focal length lenses produce a larger probe volume and lower sensitivity to the small drops in the size distributions. Shorter focal length receiver lenses with the same diameter (typically 100 mm) produce strong signals with good SNR and greater sensitivity to the smaller drops. We also provide

detector masks that fit onto the front of the receiver lens that extend the size range to larger drops for the same Receiver focal length. This range of optical combinations should allow measurement of drops in the size range of 0.5 to 1,500 μm.

Nominal PDI Parameters For Sizing and Velocity Measurements

Receiver 30 Degrees, Slope = 0.760

Transmitter mm	Fringe Spacing,μm	Receiver Focal Length, mm	dmin) (AB 5 deg.), μm	dmax (AB 450 deg.), μm	Velocity min m/s	Velocity max m/s
350*	3.1	400	0.5	80	-75	200
350*	3.1	500	0.7	100	-75	200
350	3.1	1000	2.0	200	-75	200
350	3.1	2000	4.0	400	-75	200
500	4.33	400	1.0	120	-100	400
500	4.33	500	1.5	150	-100	400
500	4.33	1000	3.0	300	-100	400
500	4.33	2000	6.0	570	-100	400
1000	8.66	500	3.0	300	-200	800
1000	8.66	1000	6.0	570	-200	800
1000	8.66	2000	13.0	1100	-200	800
2000	17.3	500	6.0	570	-400	800
2000	17.3	1000	13.0	1200	-400	800
2000	17.3	2000	25.0	2200	-400	800

* Recommend Shift Receiver angle to 40 degrees

Receiver 40 degrees, Slope = 0.672

Transmitter mm	Fringe Spacing,μm	Receiver Focal Length, mm	dmin) (AB 5 deg.), μm	dmax (AB 450 deg.), μm	Velocity min m/s	Velocity max m/s
350	3.1	400	0.5	90	-75	200
350	3.1	500	0.8	110	-75	200
350	3.1	1000	2.5	230	-75	200
350	3.1	2000	5.0	450	-75	200
500	4.33	400	1.5	130	-100	400
500	4.33	500	1.5	160	-100	400
500	4.33	1000	3.5	320	-100	400
500	4.33	2000	7.0	640	-100	400
1000	8.66	500	3.5	320	-200	800
1000	8.66	1000	7.0	640	-200	800
1000	8.66	2000	14.0	1300	-200	800
2000	17.3	500	7.0	640	-400	800
2000	17.3	1000	14.0	1300	-400	800
2000	17.3	2000	30.0	2600	-400	800

PDI Transmitter Setup and Alignment

This section describes the basic techniques used in setting up the optical systems and aligning the instrument shown schematically in figure 9.5. When using modular systems, careful alignment is important for proper operation of the system and for acquiring reliable measurements.

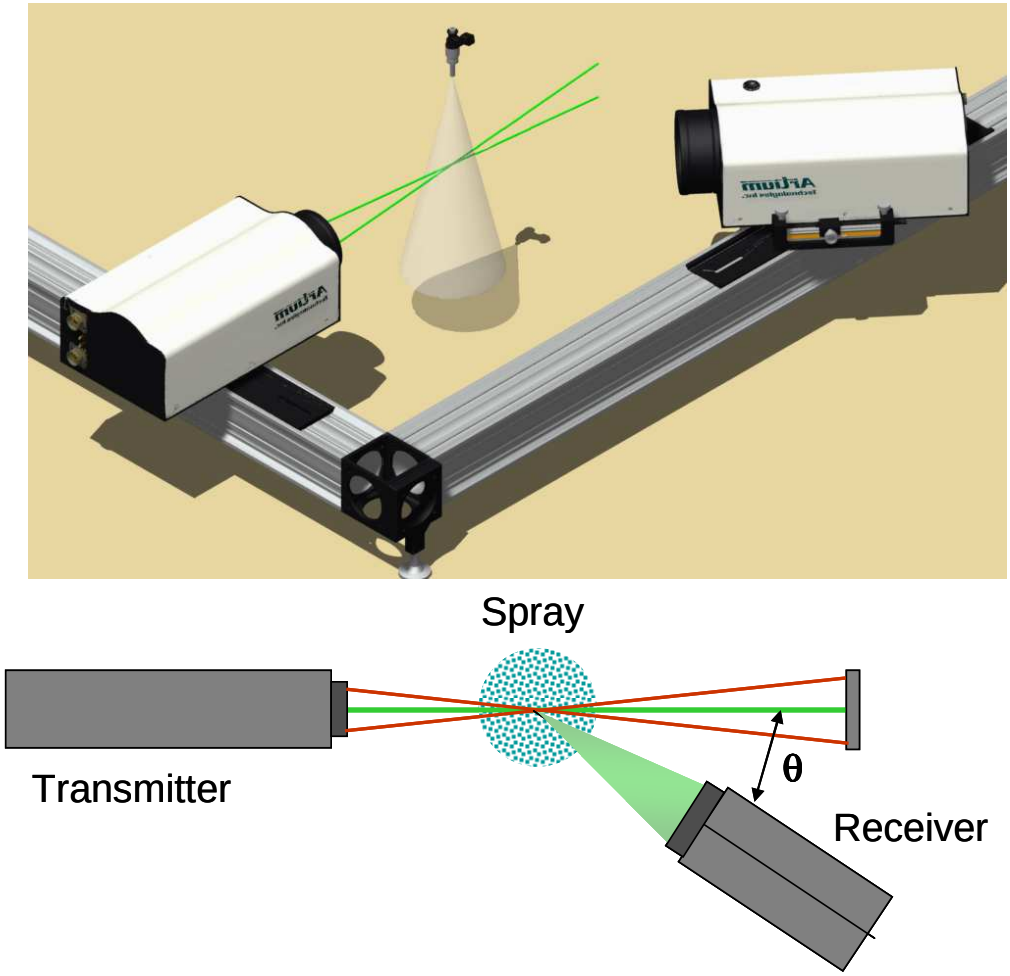

Figure 9.5: Schematic of the PDI Optical Components.

The optics internal to the transmitter have been aligned at the factory and should not require further alignment unless the system has been severely jostled or exposed to severe shocks that could cause misalignment. Periodically, it is useful to check that the beams are properly aligned and all four beams converge to a single overlap point at the

sample volume. A short focal length lens, holder, and stand have been provided to make this process relatively easy to perform.

Caution: The short focal length lens is reflective and may easily reflect laser light into your eyes. Use safety glasses for the initial set up of this test.

Figure 9.6 shows the front face of the transmitter and an enlarged view of the beam intersection forming the sample volume of the PDI instrument. For proper measurements, all four beams must intersect at the same point. If the beams do not overlap, good Doppler signals will not be produced and the signal-to-noise ratio will be compromised leading to less than optimum operation of the instrument.

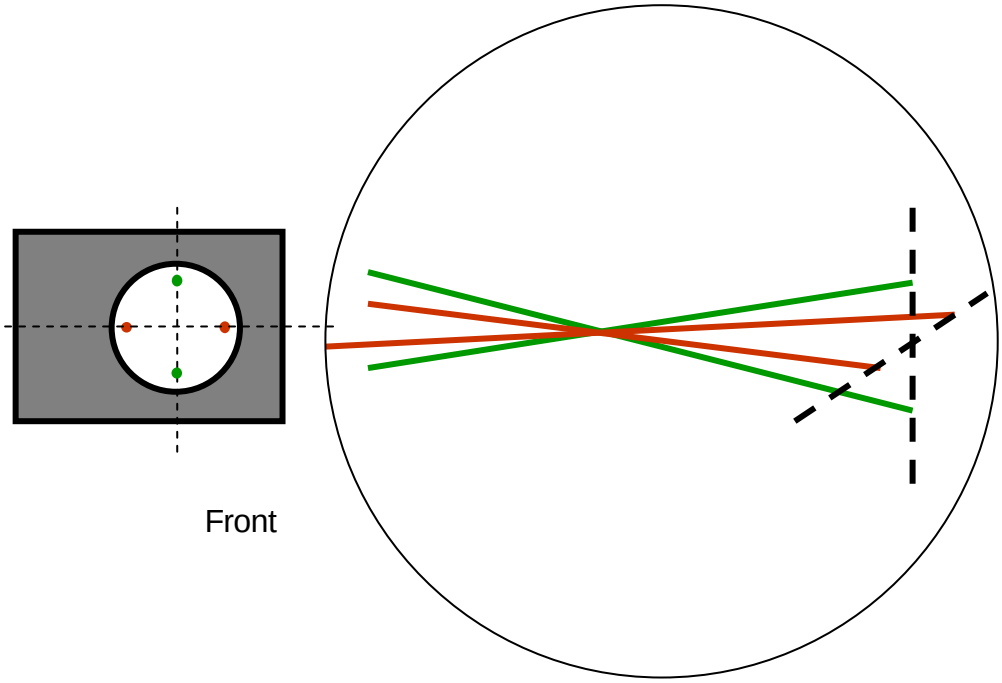

Figure 9.6: Schematic showing the laser beams exiting the transmitter enclosure and an enlarged view of the beam intersection that forms the sample volume.

To determine whether the beams are properly overlapped at the sample volume, the short focal length lens (installed on its stand) should be placed on a platform that will allow it to be moved back and forth along the beam axis.

The short focal length lens is then positioned in the laser beams and moved slowly back and forth along the beam axis while observing the magnified image of the beams on a distant wall or other suitable viewing surface. As the objective is moved away from the beam intersection point, four beams will be observed on the viewing screen. While moving the microscope objective slowly along the beam axis, the four spots will converge into a

single spot, as shown in figure 9.7, if the beams are properly aligned. If the beams do not converge into a single spot, go to the Appendix, for detailed description of how to align the beams.

The **polarization** of the pairs of beams should be checked occasionally to ensure that it is in the correct orientation for each beam. This can be easily checked with a linear polarization filter placed anywhere in the beam path. **Be careful to avoid reflections from the polarizer surfaces.** The maximum extinction of the transmitted beam should occur when the polarization axis (marked by lines on the polarizer frame) is parallel to the plane of the sizing (green for a two-component system, red or green for a one-component system) beams. This is required for each of the four beams (two for a one component system). That means the polarization direction of the beams is in a plane orthogonal to the plane of the laser beams used for sizing the particles.

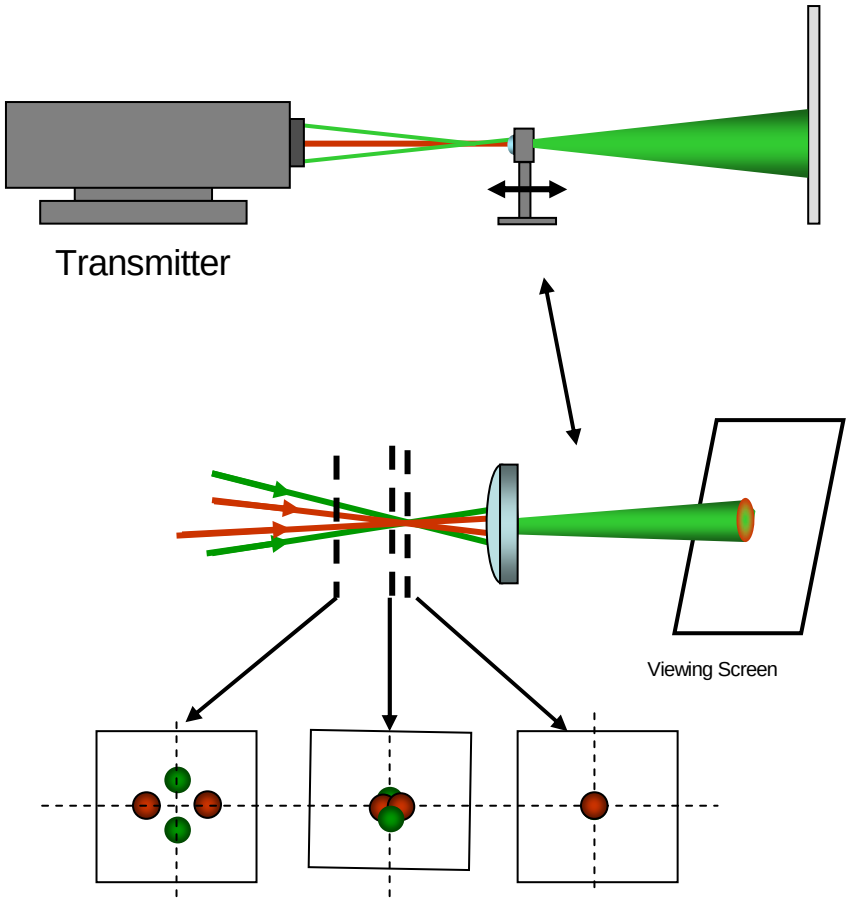

Figure 9.7: Schematic showing how a simple lens can be used to magnify the sample volume to determine that the laser beams are all completely overlapped at the sample volume.

If the beams are not completely overlapped to with 10% of the beam diameter), it may be necessary to adjust the beam that is not in the overlap circle of the other three beams. Although this procedure should not be necessary after installation, it is possible that a strong shock to the receiver could move one beam relative to the other.

Caution: Although there is an interlock switch that will turn off the laser when the cover is removed, it is best to turn off the laser before starting to remove the cover. Use proper laser safety glasses (attenuate 532 nm wavelengths) when working around laser beams.

The first step is to remove the cover be removing the 6 small screws at the bottom edge of the cover that hold it to the base plate. Use a 2.0 mm ball driver to remove the screws. Carefully remove the cover by grasping the lower edge of the wider vertical side and lifting upward. Although there is an interlock switch that turns off the laser when the cover is removed, it is best to turn off the laser first before removing the cover. Turn on the laser power again. The interlock switch will now need to be defeated by taking it down with a piece of transparent tape or other tape so that the laser will come on. Position the short focal length lens near the crossover so that the beams are slightly separated when projected on a dark piece of paper or other black surface. Using a dark surface will reduce the amount of light reflected making it easier to observe. Use laser light protection goggles or glasses while performing this operation.

Loosen the set screws that lock the drive mechanism of the wedge prisms as shown in figure 9.8a using a 1.5 mm ball driver. Insert a pair of 2 mm drivers in the drive gears as seen in Figure 9.8b and very slowly rotate one driver relative to the other. Rotating these gears rotates a wedge prism that causes the beams to move in arcs at the sample volume. Carefully rotating one of the gears relative to the other will produce the motion required Some experience is required to do this precisely but the alignment is relatively easy at this point. With all four beams appearing on the viewing screen or wall, choose the beams that are closest together and align the other beam that is farthest from that location on to the other beams. Using this approach, there will be little or no danger of steering all four beams off of the axis of the transmitter optical system. However, a slight displacement from the optical axis of the transmitter will not create any problems. Once the beams have been carefully aligned to overlap each other at the sample volume, tighten the locking setscrews carefully. Locking the set screws can cause the wedge prisons to move slightly. Several iterations may be required to get perfect alignment but once this is complete, it should not be required again unless there are severe shocks to the transmitter package.

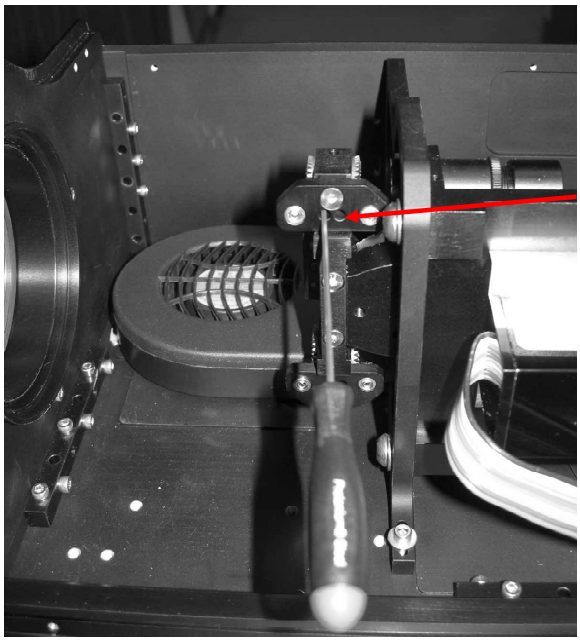

There are set screws to lock the adjustment gears in these 2 holes. Use a 1.5 mm ball driver to slightly loosen the set screws.

Figure 9.8a. Photograph showing the location of the locking set screws for the beam alignment mechanism.

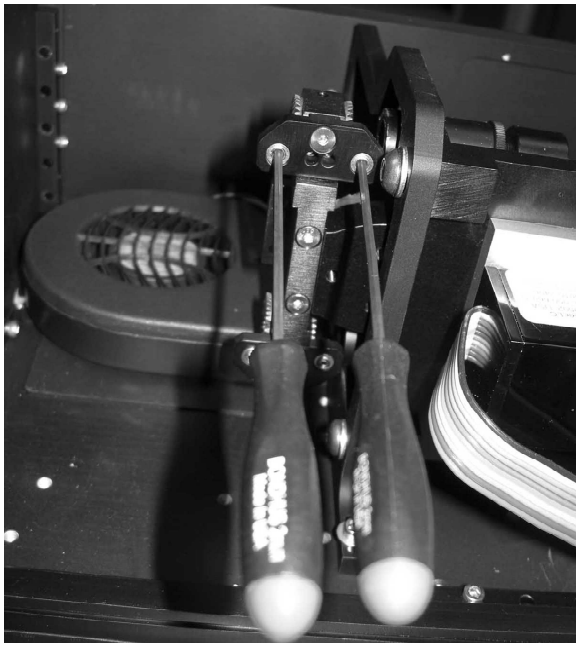

Use a pair of 2 mm drivers inserted into the small gear drive sockets. Rotating the drivers slowly will drive the carriers for the wedge prisms used to steer the beams. Rotating the drivers in opposite directions will move the beams in an approximate straight line in some direction. By rotating the drivers at different amounts of rotation will move the beams on different paths. Some experimentation on one beam will provide information on how the drives must be rotated to locate the beam at the desired spot.

Figure 9.8b . Photograph showing the ball drivers inserted into the drive gears used to adjust the wedge prisms that move the beams.

Figure 9.8 Beam alignment used to bring the beams to perfect overlap at the sample volume.

PDI Receiver Setup and Alignment

There are several basic techniques for setting up and aligning the optical systems to obtain reliable and accurate measurements. The goal is to set the receiver so it admits light that originates at the intersection of the two laser beams and passes to the photodetectors through a small slit aperture. The interference pattern used to obtain information on particle velocity and size is formed at this small region is shown in figure 9.9.

The easiest layout is when the optics are in a horizontal plane with both the transmitter and receiver mounted on a optical bench or optical rails with the spray in the vertical direction. In this case, a target consisting of a piece of transparent tape attached to a post may be set up at the measurement point or other suitable reference point. The transmitter is then set such that the beam intersection falls on the transparent tape. This can be determined by slowly moving the transmitter back and forth and observing the laser beams on the tape **(use laser safety glasses)**. Away from the intersection of the two beams, two spots can be observed (four spots, 2 red and 2 green will be observed when using a two-component system). As the transmitter is moved forward and back, these two spots will converge to one spot and then diverged two spots again. The beam intersection where only one spot appears is where the two beams overlap. This defines the location of the measurement volume.

The receiver is then positioned precisely at 40° to the transmitted beam (other collection angles may be used but the collection angle used needs to be input into the Software setup on the **Optics** page). It does not matter if it is 40 degrees on either side of the transmitted beams since the light scatter is symmetric about the forward direction. However, the angle must be in the plane orthogonal to and passing through the bisector of the green laser beams. If the receiver angle is off by plus or minus a few degrees, it will not significantly affect the measurements. The centerline of the receiver also needs to intersect the laser beam spot on the transparent tape. This requires some adjustment and manipulation by sliding the receiver from side to side while maintaining the 40° angle to the measurement point. While moving the receiver, the image of the spot of the laser beams may be observed by looking through the eyepiece at the receiver aperture module. An internal light activated by a pushbutton switch on the front of the receiver has been provided to illuminate and identify where the aperture is located during the alignment setup under low light conditions.

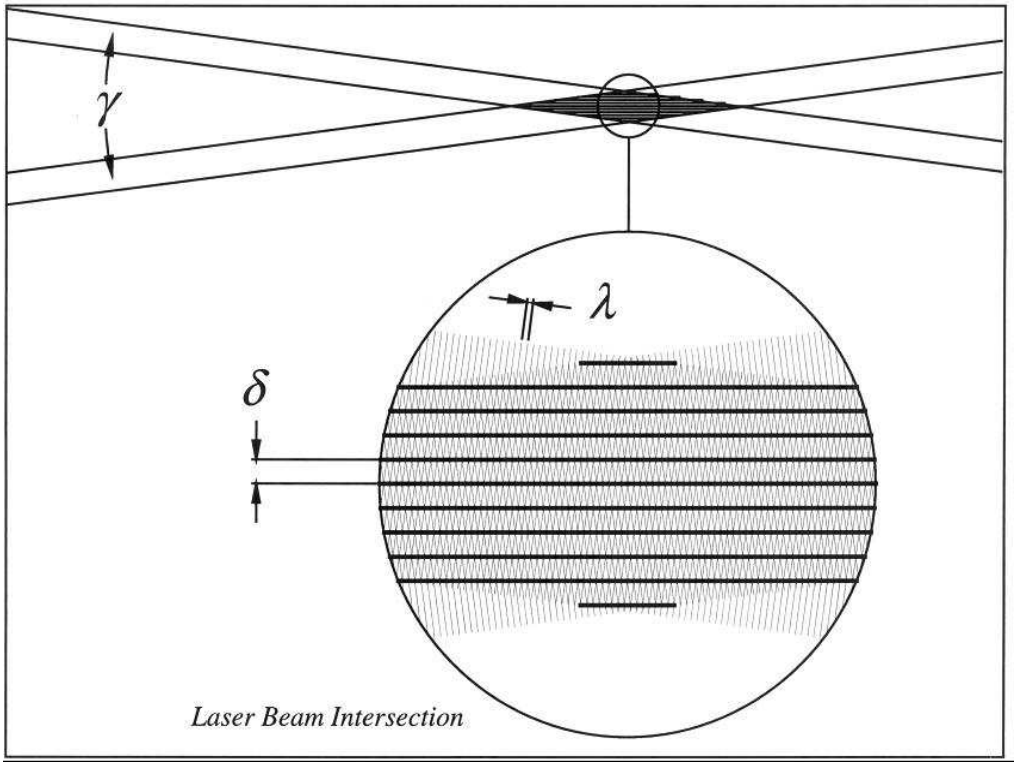

Figure 9.9: Schematic showing the laser beam intersection and the interference fringe pattern created at the sample volume.

The receiver should not be rotated to achieve alignment to the laser spot since this changes the light collection angle. After the system is roughly set up, slight adjustment of the receiver along the direction of the transmitted beams may be used to align the slit aperture to precisely over the beam intersection point. This process may require one or two iterations of setting the receiver, focusing the spot to the slit aperture plate and then using fine adjustment of the beams to move the laser beam intersection region by sliding the transmitter back and forth slightly so the only a single spot is observable on the tape used to scatter light and in the receiver.

Careful focusing of the receiver is required to achieve the best measurement results. Rough adjustment of the focus can be accomplished by setting the base of the receiver at the proper distance from the measurement point indicated by the spot of the laser beams on the transparent tape. The receiver is then moved back and forth to focus the spot onto the face the aperture module using the fine adjustment provided. This is done by unlocking the rack and pinion drive and adjusting the drive screw to on the right hand side to move the receiver fore and aft while observing the image of the spot through the

eyepiece. Figure 9.10 shows the various alignment conditions that you will see while setting up the receiver.

When two spots are seen, figure 9.10a, the beam crossover is not at the target (transparent tape set to scatter light) so the transmitter needs to be adjusted back and forth along the beam path while observing the spot on the tape. A single spot on the tape indicates that the beam crossover is at the target. One spot should be seen as shown in figure 9.10b. Once a single spot is achieved, the receiver can now be focused by loosening the upper pair of screws on the base and sliding it slowly back and forth to produce a minimum spot diameter. Set it at the minimum diameter as shown in figure 9.10c. Once this is achieved, the spot can be moved to the center of the aperture in use, figure 9.10d. This is the aperture that is aligned with the two marks above and below the row of apertures. The system is now aligned well enough to start testing with a spray.

Install the spray centered approximately where the post with the transparent tape was positioned. Turn on the spray and observe the image of the laser beam in the spray as seen through the receiver lens. A length of the beam intersection will scatter light to the face of the aperture module, just as if we were directly looking at the laser beams in the spray. Proper alignment is when there is a single focused beam waist across the aperture. figure 9.10 shows two cases.

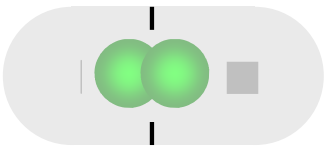

a) Laser Beam Images out of focus and not overlapped

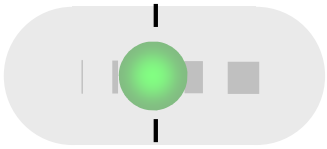

b) Laser Beam Images out of focus but overlapped

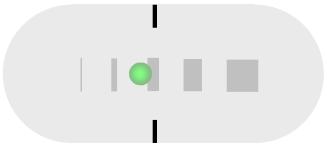

c) Laser Beam Images in focus and overlapped but not centered on aperture

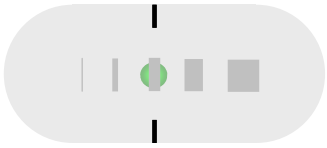

d) Laser Beam Images in focus and overlapped and centered on aperture

Figure 9.10: Schematic showing the aperture module with the images of the laser beam spots on the face of the module at various stages during alignment.

Using the eyepiece on top of the receiver that produces a magnified image of the aperture and the laser beams, complete the fine adjustment of the focus and the alignment over the aperture, figure 9.11.

Aligning to the Correct Aperture:

There are 5 apertures (50, 100, 200, 500 and 1000 μm) on the aperture substrate seen through the viewing port. To avoid confusion as to which slit aperture is the right one, start the AIMS software and select a slit aperture on the Device Control page and then the Optics Tab. For example, select 200 and then align the image of the scattered light from the beams when either a transparent tape scattering target is at the sample volume or a spray is operating to that aperture. It is obvious which aperture is 200 μm wide since they are in descending order by size.

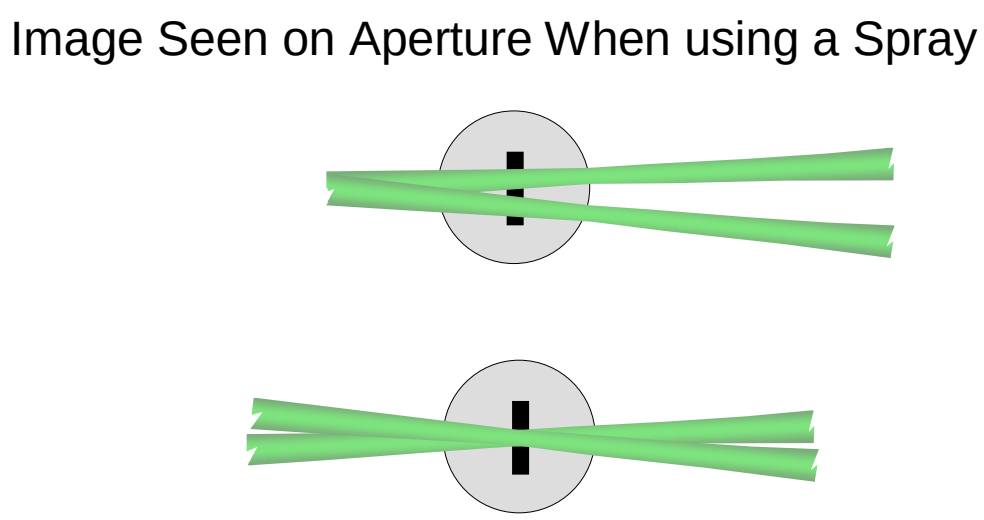

Figure 9.11: Schematic showing the image of the light scatter by the focused laser beams. In the upper case, the beam crossover or intersection is not focused at the aperture. In the lower case, the image of the beams is properly focused with the beam intersection point at the aperture.

SUMMARY OF STEPS IN ALIGNING THE OPTICS

- Set up a light scattering target using a piece of transparent tape on an appropriate stand.
- Set up the receiver and transmitter at 40° and separated at distances approximately equal to the focal lengths used in the transmitter and receiver.

- Position the transmitter so that the beam intersection falls on the surface of the transparent tape indicated by single laser beam spot (**use laser safety glasses**).
- Adjust the receiver so that the image of the spot falls on the face of the aperture module within the receiver while maintaining the 40° collection angle as close as possible.
- Move the receiver back and forth along its optical path to focus the laser beam spot on the face of the aperture module.
- Align the spots so it falls into the aperture indicated the software setting as the active aperture.
- Observe the focus on alignment using the magnification eyepiece on top of the receiver to perform fine adjustment of the focus and the alignment into the aperture.
- Turn on the spray and ensure that the image of the laser beam through the spray is in focus and the crossover is centered on the aperture.

Chapter
10 PDI Calculations

Calculations

This chapter describes the methods by which the software interprets the raw information received from the instrument and computes information to obtain droplet velocity and size. The software resolves the stored raw data into the velocity and size measurements for the each particle and then computes the remaining statistical parameters. This section describes the calculations completed by the computer. The nomenclature for this chapter is as follows:

Δ	Spatial Wavelength
δ	Fringed Spacing
ϕ_{12}, ϕ_{13}, ϕ_{23}	Phase shift in degrees between detectors 1 and 2, 1 and 3, and 2 and 3 (also called A, B, and C)
Θ	Receiver Collection Angle
γ	Laser Beam Intersection Angle
α, α_r	Aperture width, resultant aperture width
D_{max}	Diameter of the largest particle size
D_{10}, D_{20}, D_{30}, D_{32}	Mean particle diameters: Arithmetic, Area, Volume, Sauter
d	Diameter of spherical particle
f, f_D, f_m,f_r,f_s, f_t	Frequency: Doppler, mixer, raw, shift, transformed
I, ,I_i, I_o, I_s	Light Intensity: incident, maximum at r = 0, scattered
i	Histogram Bin Number
j or n	Number of samples in histogram bin
K	Optical constant
ND	Number Density
n, n_c	Number of samples in each bin: corrected size count
PA	Probe Area
PV	Probe volume That
PVC	Probe Volume Correction
PVO	Probe volume cut off
RL_1, RL_2	Receiver Lenses: Collimating, Focusing focal lengths
r_w or w	Laser beam radius measured from the centerline of the beam: $I = I_o/e^2$
S, S_{12}, S_{13}	Effect of detector separations: between detectors 1 and 2, and 1 and 3
Σ	Sizing Slope Factor
τ	Particle or droplet transit time through the probe volume
t, t_{tot}	Time: total run time
v	Velocity
VF or F	Volume Flux

Velocity Measurement

The particle velocity is measured by the method typically used for laser Doppler velocimetry. That is, as a particle crosses the interference fringes created by the two intersecting coherent laser beams, figure 10.1, it refracts or reflects the local light intensity onto the receiver. The light intensity pattern projected onto the receiver and directed to the photomultiplier tubes produces a typical Doppler burst signal, figure 10.2. The signal consists of a high frequency Doppler component superimposed upon the low-frequency Gaussian pedestal component. The frequency of the signal is directly related to the velocity of the particle through the relationship

$$v = f_d \delta$$

The fringe spacing of the interference pattern is determined by the wavelength of the laser beam and the beam intersection angle and is given by the following expression

$$\delta = \frac{\lambda}{2\sin(\gamma/2)}$$

The raw signal produced by the photodetectors and received by the signal processor is a combination of the Doppler frequency and the shift frequency produced by the presence of a Bragg cell. The signal frequency is given as

$$f_r = f_D + f_s$$

The raw signal is passed through a high pass filter set at 10 MHz (or 20 MHz) to remove the pedestal component of the Doppler burst signal and any low-frequency noise. The signal is then combined with the mixer frequency and sent through a low pass filter to eliminate the high frequency components including the sum frequency from the mixer and any high-frequency noise. The remaining frequency is given as

$$f_t = f_r - f_m$$

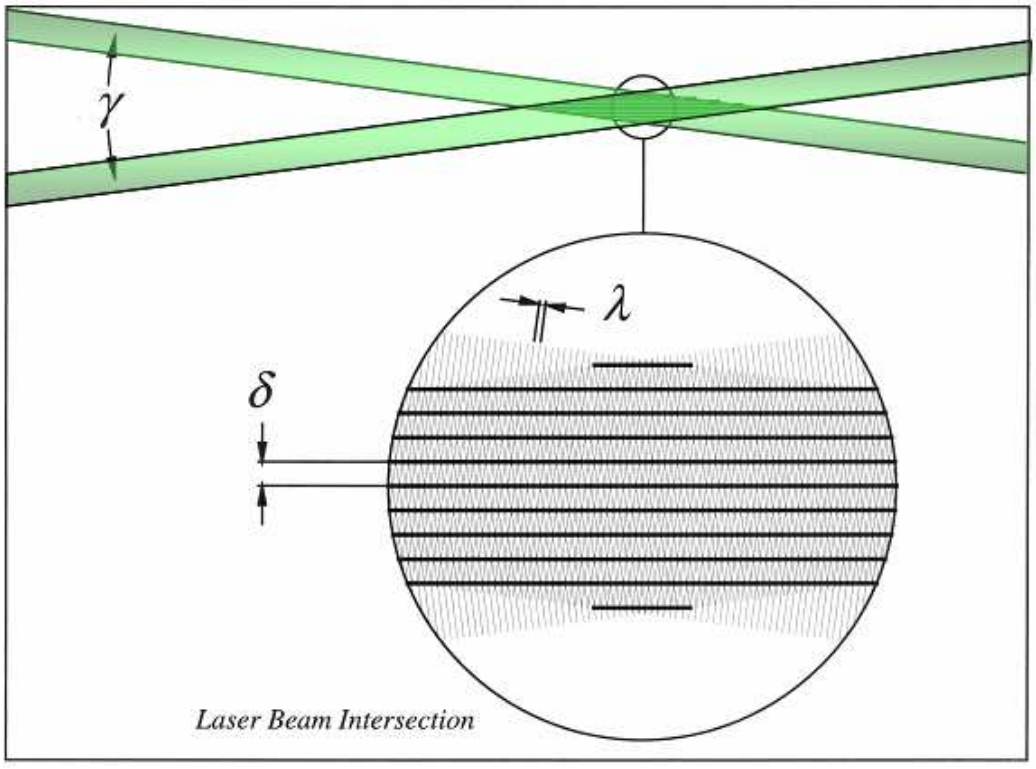

Figure 10.1: Schematic showing the laser beam intersection and the formation of interference fringes in the probe volume.

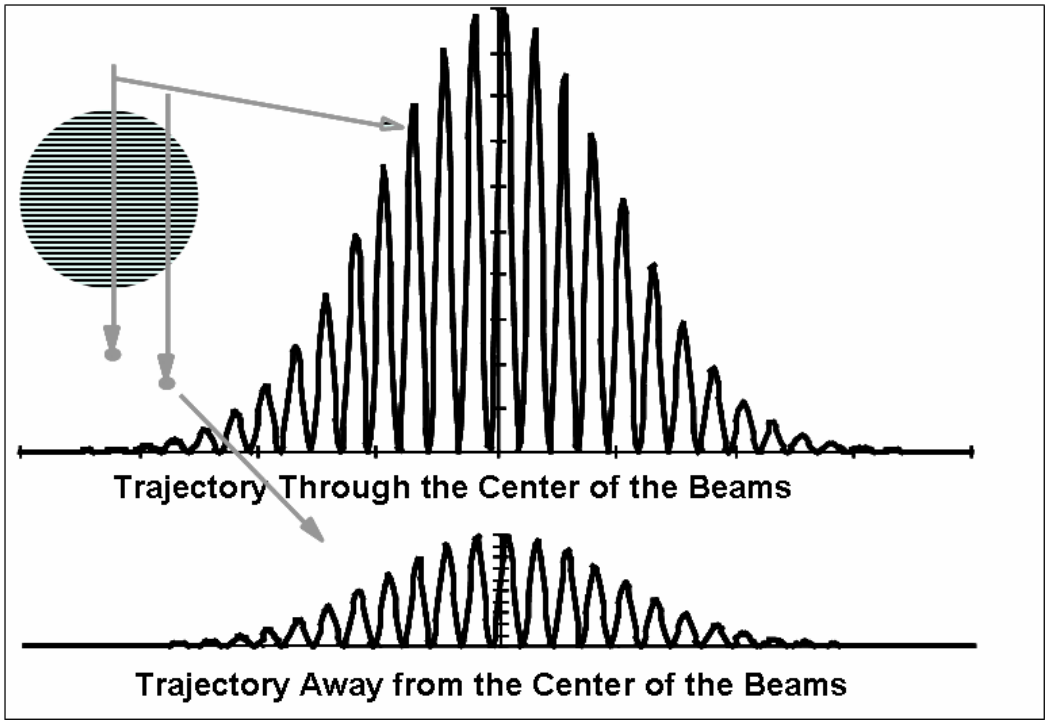

Figure 10.2: Simulated Doppler signals.

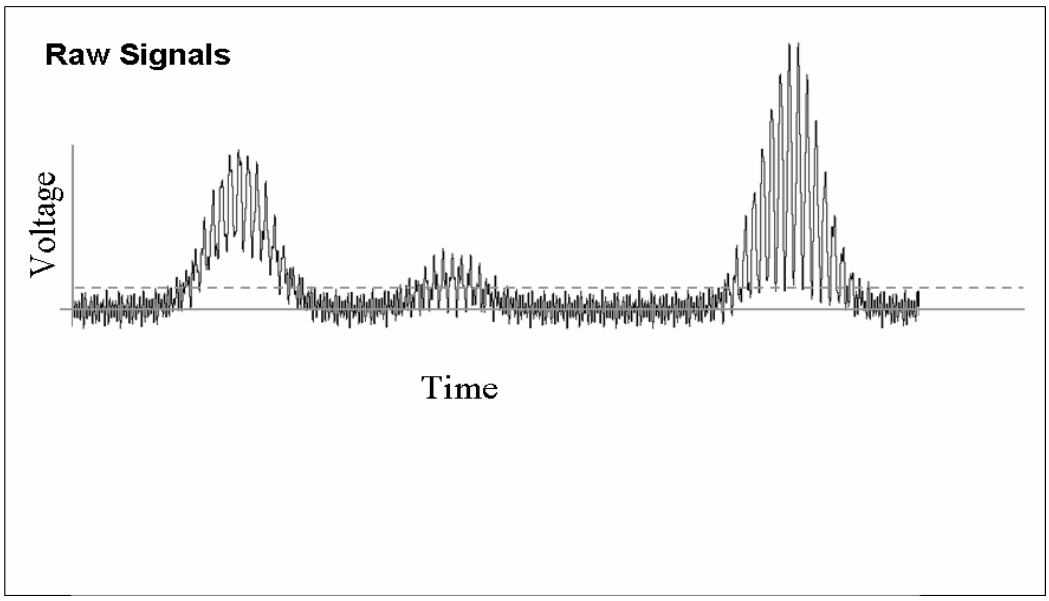

Figure 10.3: Typical Doppler burst signals for different trajectories through the probe volume.

This frequency is processed usingt the FFT programed in the system computer. The Doppler frequency is then obtained from the known mixer and shift frequencies and measured raw frequency using following expression

$$f_D = f_t + f_m - f_s$$

Size Measurement

This section describes how the diameter of the particles is determined using the phase Doppler interferometer method. The particle magnifies the interference fringe pattern onto the receiver to different degrees relative to a particle size. The degree of magnification is measured by comparing the spacing of these fringes on the receiver detectors (spatial wavelength Δ) and the fringe spacing. The diameters of the particles are determined using this relationship along with the receiver focal length and the sizing slope factor given as

$$d = \frac{F\delta_r}{s\Delta}.$$

A spatial wavelength, Δ is determined by using the phase shift of the signal between the detectors in the time domain along with the calibrated spacing of the detectors. The spatial wavelength, Δ is obtained from the weighted average of

$$\overline{\Delta} = 360\left[\frac{k_{12}S_{12}}{\phi_{12}} + \frac{k_{13}S_{13}}{\phi_{13}} + \frac{k_{23}S_{23}}{\phi_{23}}\right] / \left[k_{12} + k_{13} + k_{23}\right]$$

Artium Technologies, Inc. uses several proprietary methods for resolving the sizing slope factor for all possible transmitters/receiver configurations. The slope is calculated assuming spherical particles and therefore, the particles to be sized should be spherical or near spherical if accurate results are to be obtained.

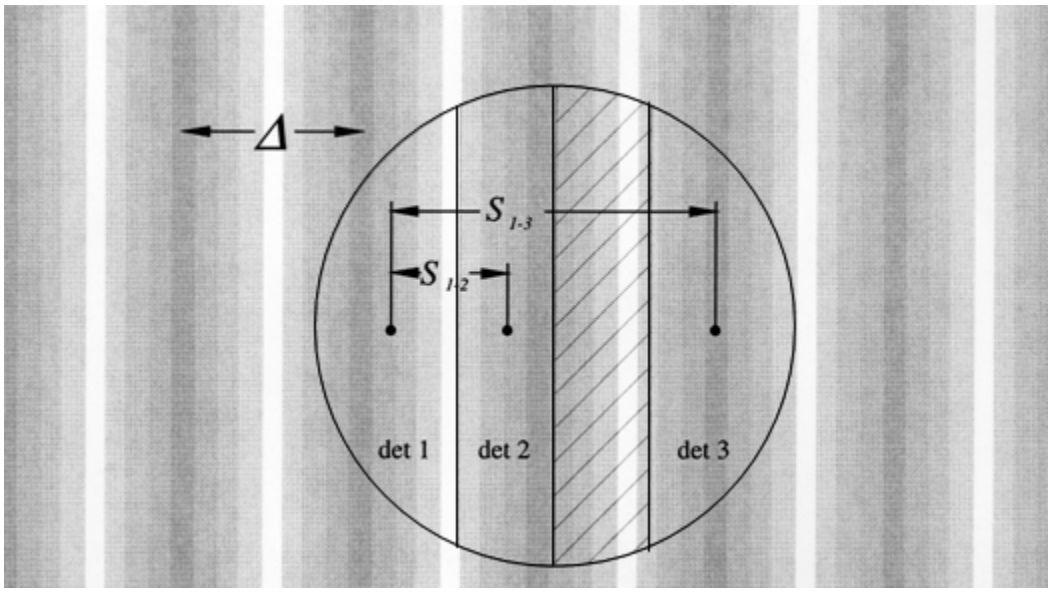

Figure 10.4: Schematic showing the interference fringes produced by the scattered light and projected onto the receiver lens.

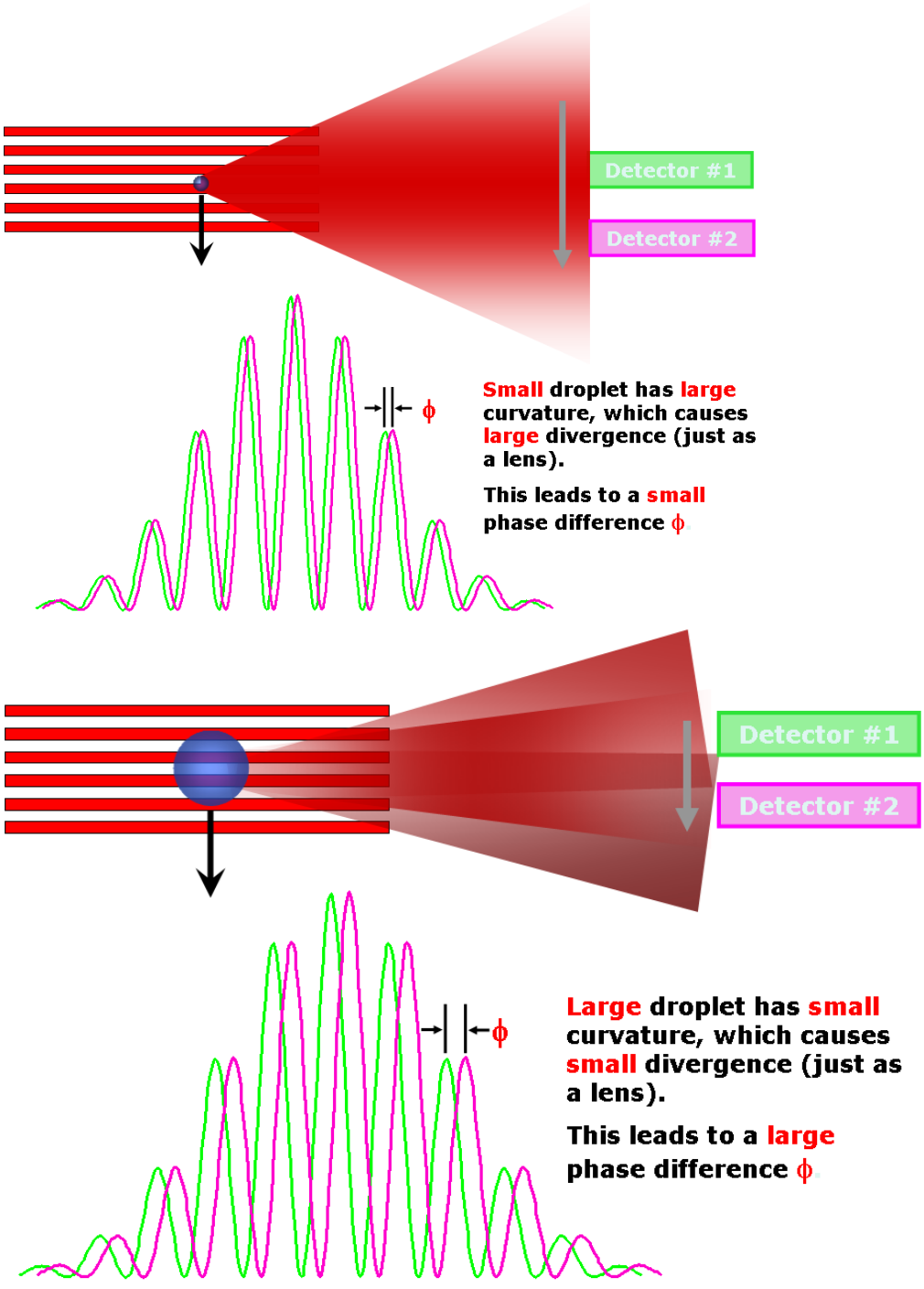

Figure 10.5: Schematic showing the interference fringes formed by the scattered light and the pattern overlaid on the receiver lens and a description of how the droplets produce different phase shifts at the pairs of detectors.

Probe Volume, Probe Area, and Probe Volume Correction

The probe volume is a volume through which particles must pass to be measured by the PDI systems. Probe volume is defined by the focused laser beam diameter and the slit aperture width in the receiver. The shape of the probe volume can be estimated as a slice of a cylinder with oblique ends. The width and angle of the slice are determined by the slit aperture width in the receiver, optics, and the angle of the receiver relative to the transmitted beams. The intersecting beams are at a small enough angle such that they can be assumed as cylindrical in shape within the region seen by the receiver.

The cylindrical diameter of the probe volume increases in diameter for increasing size classes of particles. This is due to the relation between the amount of incident light scattered by particle (proportional to the diameter of the particle squared) and particle size in conjunction with a Gaussian nature of the laser beam intensity profile illuminating the particles. The amount of light incident on the particle is determined by the distance the particle passes from the center of the laser beams and its location along the trajectory through the beams. For two intersecting laser beams the incident light is

$$I_i(r) = I_o e^{\frac{-2r^2}{r_w^2}}$$

The intensity of the light scattered by particle is proportional to the particle surface area. Combining the size relation with the above Gaussian equation results in the expression

$$I_s(r,d) = KI_i(r)d^2 \approx KI_o e^{\frac{-2r^2}{r_w^2}} d^2$$

which is equal to the amount of light incident on the receiver optics relative to a particle size and position.

A minimum amount of light incident on the receiver is needed in order for the instrument to detect a particle. This intensity cut off determines the maximum radius r at which each particle size can be detected yielding a cylindrical diameter D as a function of the ratio of the probe volume diameters to particle diameter is

$$D^2(d) = D_{\max}^2 - 4r_w^2 \ln\left(\frac{d_{\max}}{d}\right)$$

which is used when calculating the probe volume correction, PVC.

The maximum probe diameter is either assumed to be equal to a nominal value by using an analytical method for probe volume correction or is determined in situ by the transit time method. The transit time is the time a particle spends in the probe volume which depends on its speed and the diameter of the probe volume. The measured transit time multiplied by the particle velocity yields the particle path length within the probe volume. Artium Technologies Inc. uses a proprietary method of combining the transit time of all particles passing through the probe volume to determine the maximum probe diameter.

The probe area is determined from the maximum probe diameter of the maximum size bin and is given as

$$PA = \frac{D_{\max} a_r}{\sin \varphi}$$

The resultant aperture size at the laser beam intersection is related to the aperture size within the receiver and the focal lengths of the receiver lenses. The resultant aperture size is given as

$$a_r = a\left[\frac{RL_1}{RL_2}\right].$$

The number of particles in each size class of the distribution is multiplied by the probe volume correction factor to reflect the change in sampling volume with particle size and is given as

$$n_c(d) = n(d)PVC(d)$$

The probe volume correction factor is simply the ratio of the probe area for the maximum particle size bin ratio to the probe area of each individual size bin d. Since the aperture and the angle of light scatter detection, Θ, remain constant, the ratio is determined only by the maximum probe diameter of each particle size class.

$$PVC(d) = \frac{D_{\max}}{D(d)}$$

The in situ probe volume measurement and correction is dependent on certain factors in order to perform properly. First, the laser beams must have a nearly Gaussian intensity distribution at the beam intersection. The trajectory of the particles should be predominantly normal to the direction of the beams for a two component system (two orthogonal velocity components measured). For a one component system, the predominant trajectory of the particles should be in the direction of measurement of the velocity. If these conditions are not met the analytical method to define the probe volume correction may be more accurate.

Mean and Median Calculations

In this section, the various mean diameters used in the presentation of data are presented. These mean values are commonly used in spray analysis.

Arithmetic or Linear Mean Diameter (D10)

$$D_{10} = \frac{\sum_i n_{c(i)} d_i}{\sum_i n_{c(i)}}$$

Area Mean Diameter (D20)

$$D_{20} = \sqrt{\frac{\sum_i n_{c(i)} d_i^2}{\sum_i n_{c(i)}}}$$

Volume Mean Diameter (D30)

$$D_{30} = \sqrt[3]{\frac{\sum_i n_{c(i)} d_i^3}{\sum_i n_{c(i)}}}$$

Sauter Mean Diameter (D32)

$$D_{32} = \frac{\sum_i n_{c(i)} d_i^3}{\sum_i n_{c(i)} d_i^2}$$

Total Number

$$tN = \sum_i n_{c(i)}$$

Number Fraction

$$fN = \frac{\sum_i^N n_{c(i)}}{tN}$$

Total Length

$$tL = \sum_i n_{c(i)} d_i$$

Length Fraction

$$fL = \frac{\sum_i^N n_{c(i)} d_i}{tL}$$

Total Surface

$$tS = \pi \sum_i n_{c(i)} d_i^2$$

Surface Fraction

$$fS = \frac{\pi \sum_i^N n_{c(i)} d_i^2}{tS}$$

Total Volume

$$tV = \frac{\pi}{6} \sum_i n_{c(i)} d_i^3$$

Volume Fraction

$$fV = \frac{\frac{\pi}{6} \sum_i^N n_{c(i)} d_i^3}{tV}$$

Number Density and Volume Flux Measurements

Number Density is a measurement of the number of particles per unit volume present in the measurement space. There are two methods used to calculate number density and they are referred to as the swept volume method and the transit time method. The total corrected count (corrected for probe volume) is divided by this volume to calculate the number density and is given as

$$ND = \frac{1}{(PA)(t_{Tot})} \sum_i \frac{n_{c(i)}}{\overline{|v_i|}} .$$

A separate average absolute velocity is calculated for each size bin to eliminate the velocity biasing on the sampling statistics and is given as

$$\overline{|v_i|} = \frac{\sum_j |v_{i,j}|}{n} .$$

With the transit time method which is favored, the number density is determined using the transit times for the particles as they pass the sample volume. The transit time is the measure time that the particle spends within the probe volume. This method uses the computed ratio of time duration when there is a particle in the probe volume to the total sample time for the measured distribution at that point. Transit time ratio divided by the probe volume yields the number density given as

$$ND = \frac{1}{t_{Tot}} \sum_i \frac{\sum_j Tt_{i,j}}{PV_i}.$$

This method is applied for each size class to accommodate the size biasing of the probe volume as a function of drop size.

Both methods rely on an accurate probe area calculation. The transit time method will work best as long as the beams are partially Gaussian at the intersection. The swept volume method works well if the trajectories of the particles are normal to the direction of the beams in a two component system or if the trajectories of the particles are in the direction of the velocity component measured for a one component system.

Volume flux is calculated using the following expression

$$VF = \frac{tV}{t_{Tot} PA} = \frac{\pi}{6} \frac{tND_{30}^3}{t_{Tot} PA}.$$

Mass flux can be calculated by multiplying the volume flux by the density of the spray drops or particles being measured.

Liquid Water Content (LWC)

The liquid water content is the volume of liquid water in a given volume of space. Liquid Water Content in gm/m^3 is given as

$$LWC = \frac{\pi}{6} \rho D_{30}^3 ND$$

where ρ is the density of the liquid.

Chapter
11 Data Analysis

Test Data Analysis

After the PDI-200 MD hardware has been properly connected and the various software parameters have been properly set, data acquisition may be initiated by clicking on the green button in the software user interface page or pressing the F9 key. The following figures show the various data screens that can be viewed by selecting the appropriate tabs. These screens provide information on the drop size, velocity, mean values, and temporal information on the spray. A short description of the information on each screen is provided to aid the user in interpreting the data being acquired. By right clicking on any of the plots, the plotting parameters may be changed and the graph limits adjusted as desired.

1D PDI Statistics

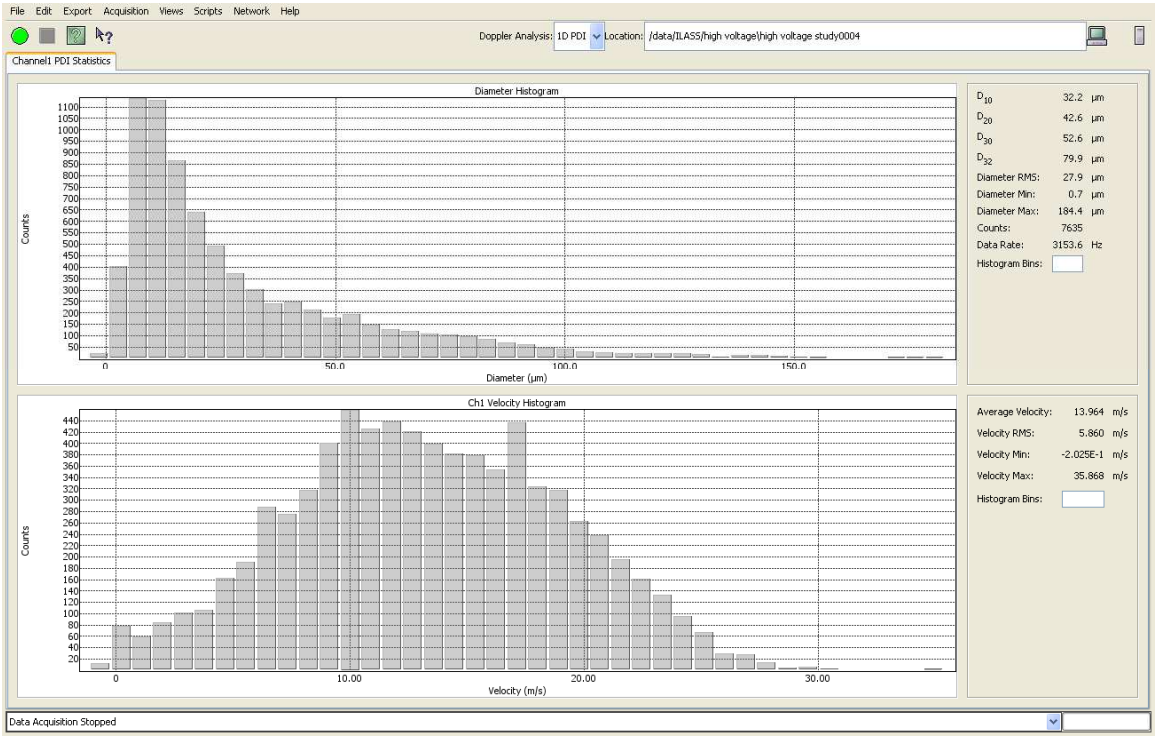

Figure 11.1: Diameter histogram and velocity histogram.

Figiure 11.1 shows the screen that displays the histograms of the size and velocity distributions for the measured spray. Note that for the example shown, the spray size distribution has a characteristic log normal shape but it appears to have a slight increase in counts at around 75 µm. Note also that the velocity distribution appears to be bimodal. This behavior can be further understood by also looking at the size velocity correlation shown in a subsequent screen, Figure 11.5. In short, smaller drops for this spray relax to the ambient flow speed whereas larger drops continue to move at a greater speed because of their initial momentum. Reduced mean values are shown in the right hand column along with the number of drops measured and the data rate.

1D PDI Statistics (PVC)

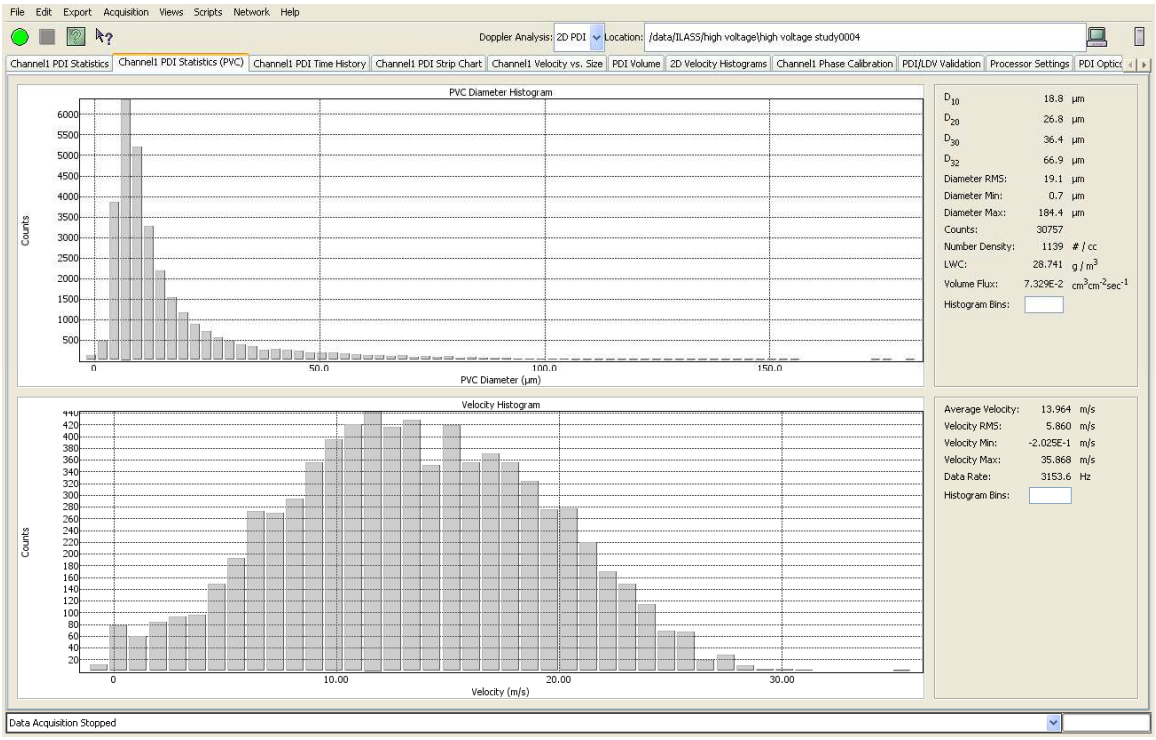

Figure 11.2: Probe volume corrected diameter histogram and velocity histogram.

Figure 11.2 is similar to Figure 11.1 except that the data have been corrected for the effect of varying sample volume on the drop size. Since smaller droplets have a smaller effective sample volume, the number in each size bin must be increased by a factor equal to the ratio of the sample volume for the largest drops to the sample volume for the drops in each size bin. This normalization approach compensates for the sample volume affect by increasing the number of drops in the smaller size bins. As noted from the mean values, especially D10, the mean size is decreased by the sample volume correction. It is

important to note that the sample volume correction is necessary for an accurate measurement of the size distribution. This is the size distribution that should be reported.

1D PDI Time History

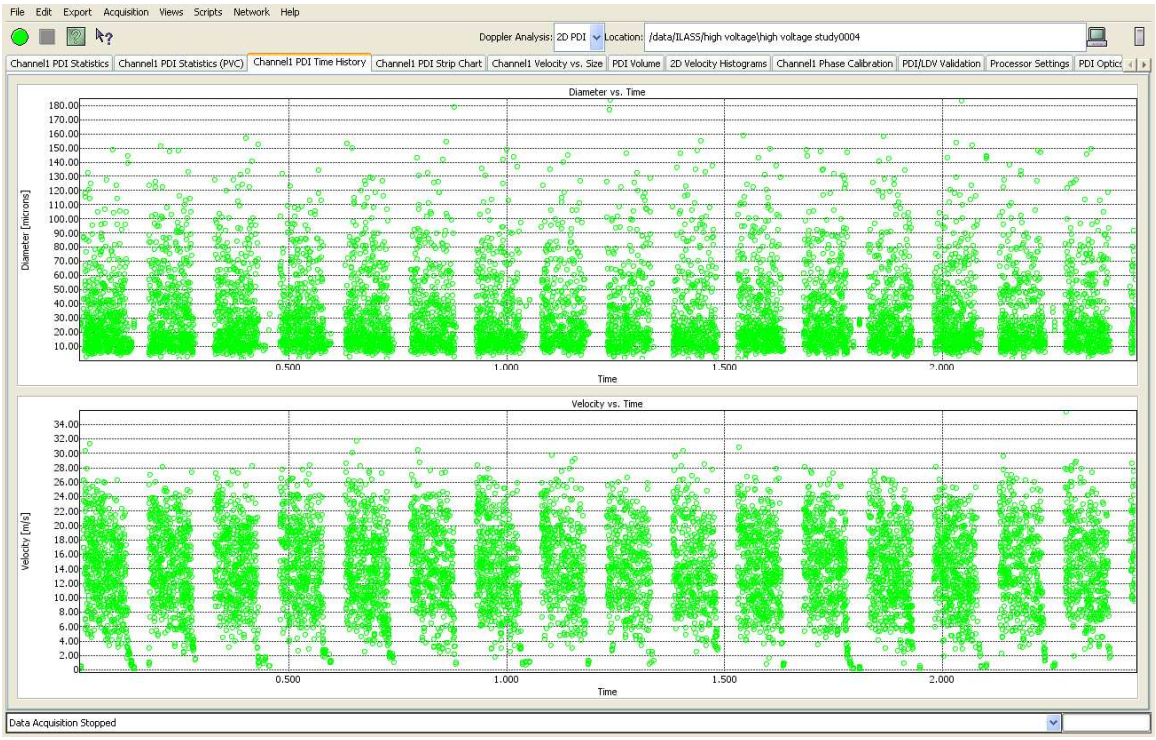

Figure 11.3: Time history plot of diameter and velocity.

Figure 11.3 shows each drop size and velocity measurement as a function of the time of arrival. Each point on the plot represents one drop measurement. This information is useful in determining if there is any unsteadiness, clustering, or other temporal phenomenon in the spray. For example, pulsatile sprays can be observed to reveal pulse variations in the spray. If the spray is interacting with turbulent flows, spray drop clustering may be observed in this plot. By right clicking on the plot, any section of the time record can be selected and expanded to observe the details.

1D PDI Strip Chart

Figure 11.4 also shows the diameter and velocity information as a function of time but displays it as a strip. This display is useful for viewing long time records over a short elapsed time period to observe any time-dependent details in the spray.

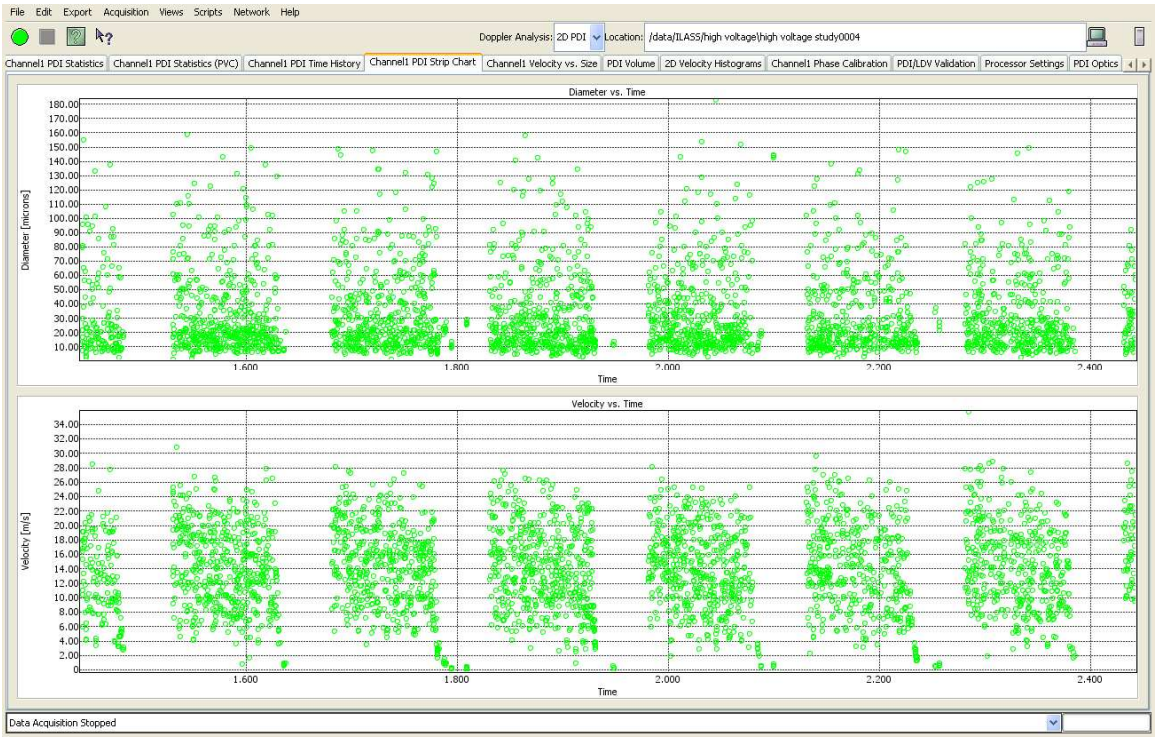

Figure 11.4: Strip chart plot of diameter and velocity.

Velocity vs Size

Figure 11.5 shows a very useful plot for observing the droplet dynamics. Each point on the graph is a single drop measurement of the drop and velocity. In this case, it is easy to see that the small drops have relaxed to the slower ambient flow velocity and that the larger drops have a higher velocity because of their greater initial momentum.

Since the PDI instrument responds to droplet flux, the relative velocity of the drops will affect the size distribution. To convert the size distribution to a concentration dependent distribution, the number of counts in each size bin needs to be normalized to remove the effect of the drop velocity for each size class. This needs to be done, for example, when the results are being compared to imaging techniques or to a line-of-sight ensemble light scatter detection method. The shape of this size versus velocity plot also helps to explain the shape of the size distribution described previously. Counts in the bins of the size histogram are affected by the relative velocities of the drops in the different size classes.

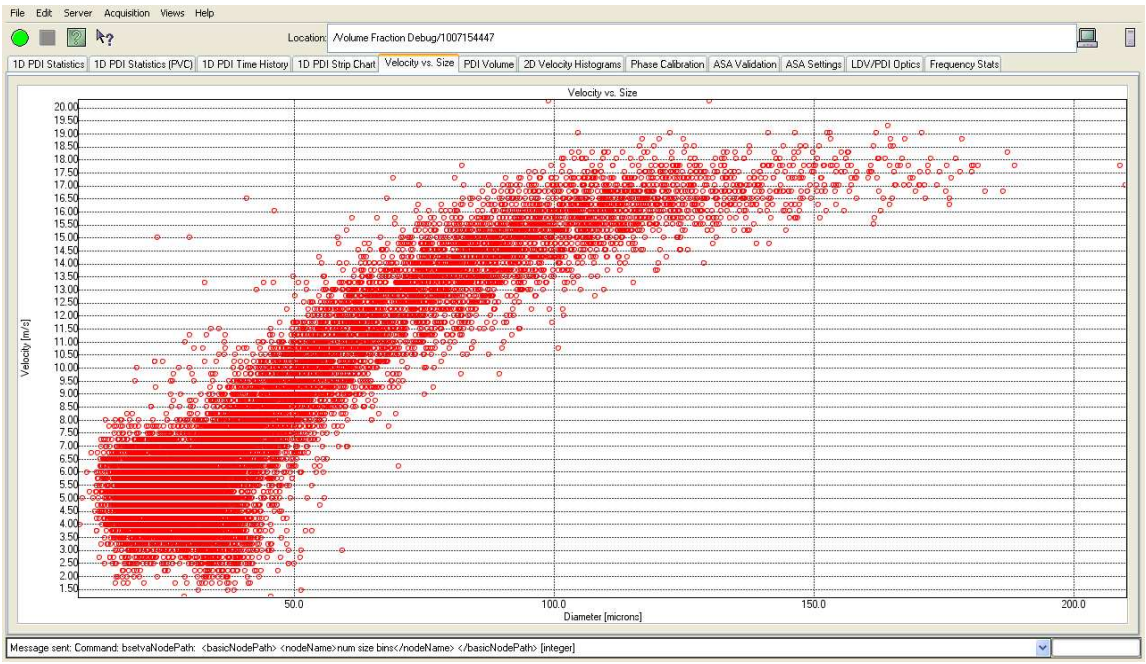

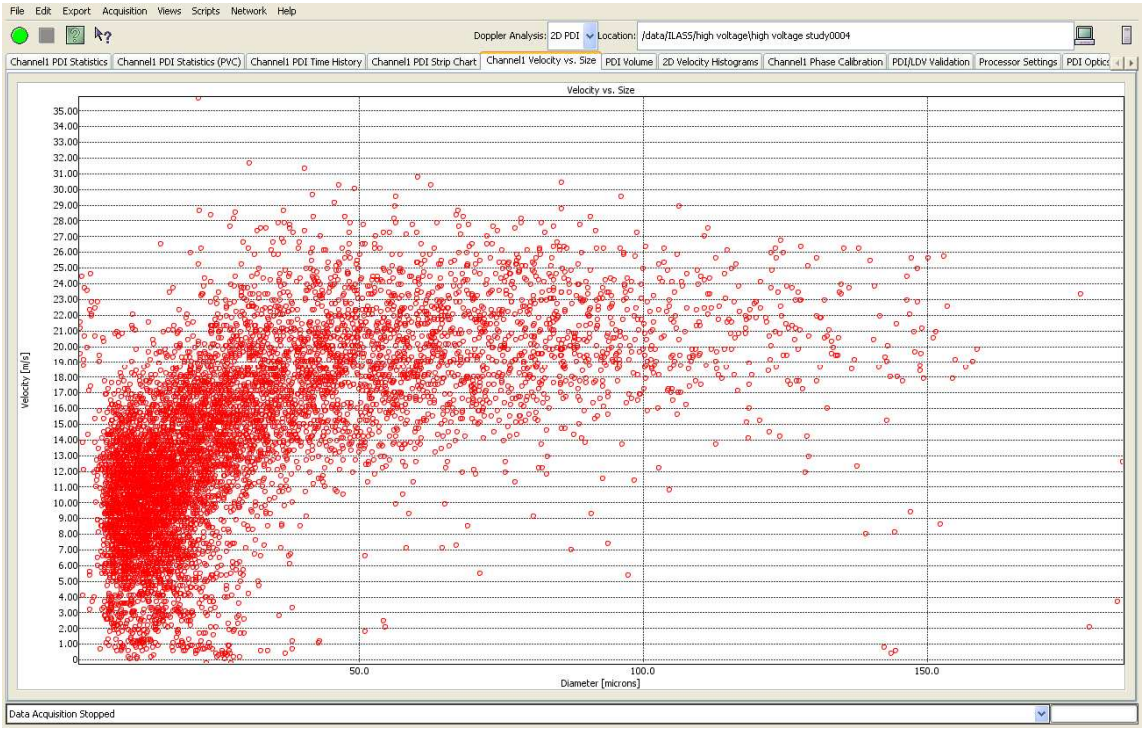

Figure 11.5: Examples of Velocity vs Diameter plots

PDI Volume

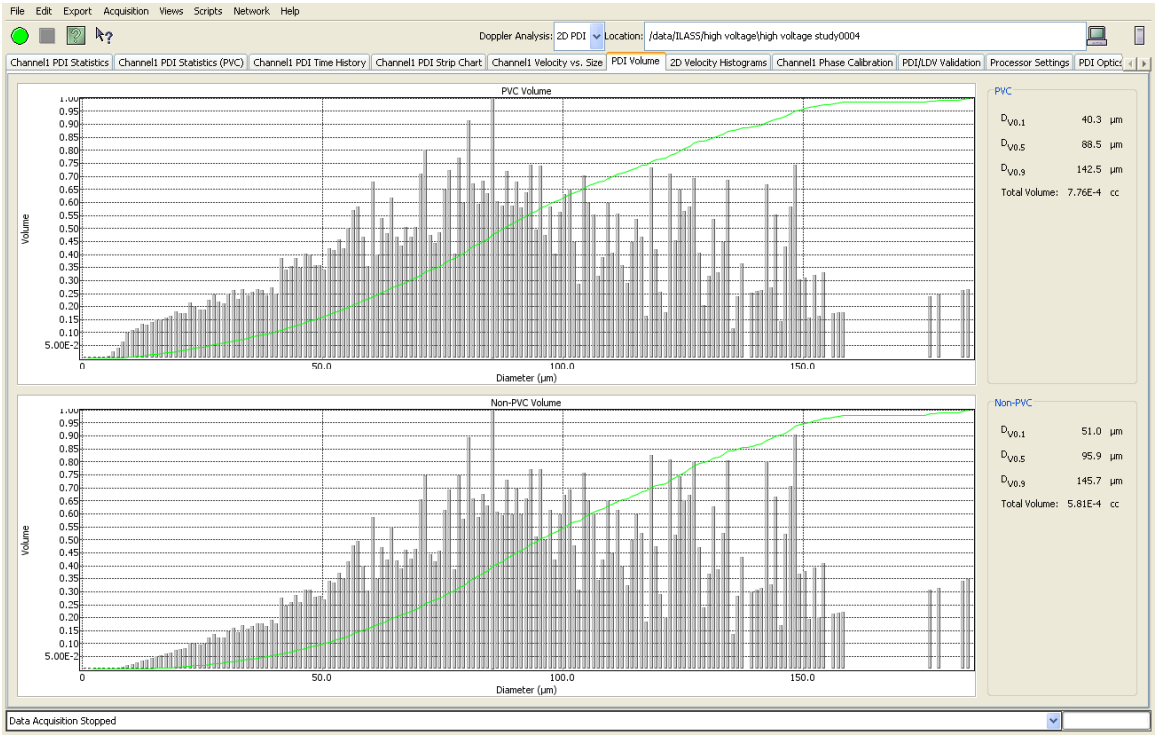

Figure 11.6 : Volume distribution (PVC and non-PVC).

Figure 11.6 shows the volume contribution for each size class of the spray drop size distribution. Also shown in the plot is a cumulative volume contribution for the various size classes. The 0.5 point on the plot is used to obtain the median volume diameter (MVD). The upper plot shows the size distribution that has been corrected for the probe volume affect (PVC) whereas the lower plot is the volumetric contribution for the uncorrected raw data (Non-PVC). The PVC corrected data is what should be used in reporting the measurements.

2D Velocity Histogram

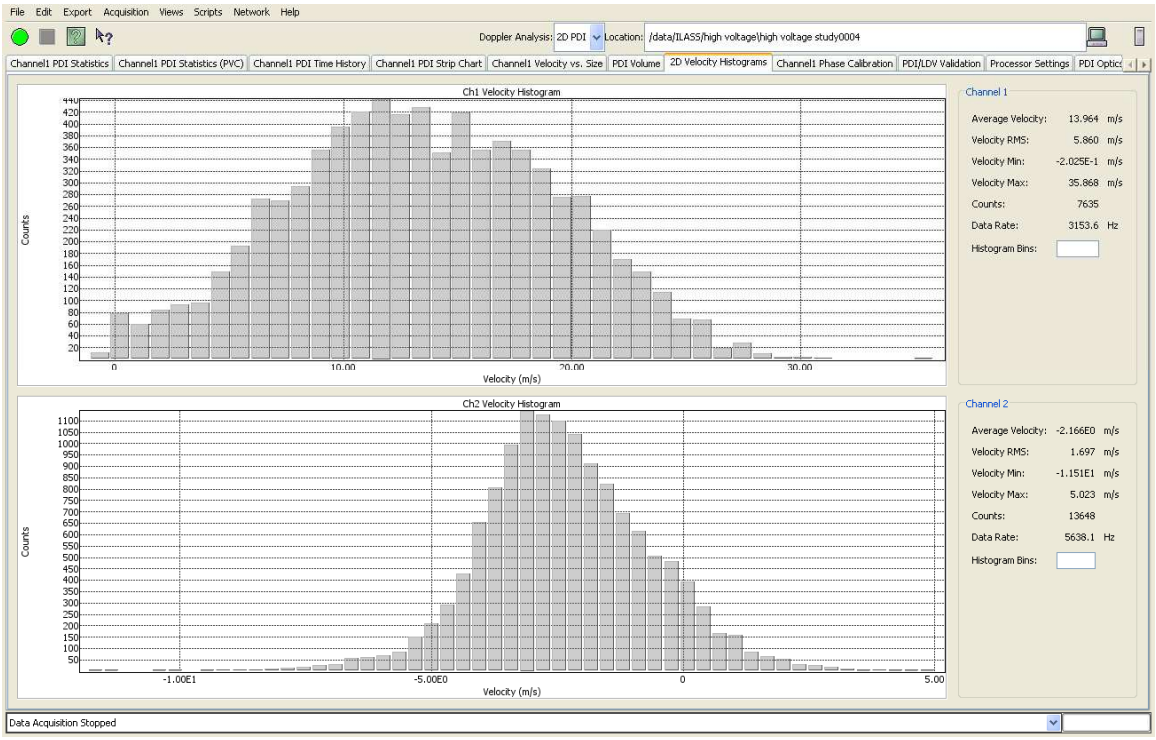

Figure 11.7: Channel 1 and channel 2 velocity histograms.

Figure 11.7 shows the velocity distributions measured with Channel 1 and Channel 2 (x- and y-components of velocity). The mean and rms velocity statistics are provided along with the number of drops measured (counts) and the data rate for each channel..

Phase Calibration

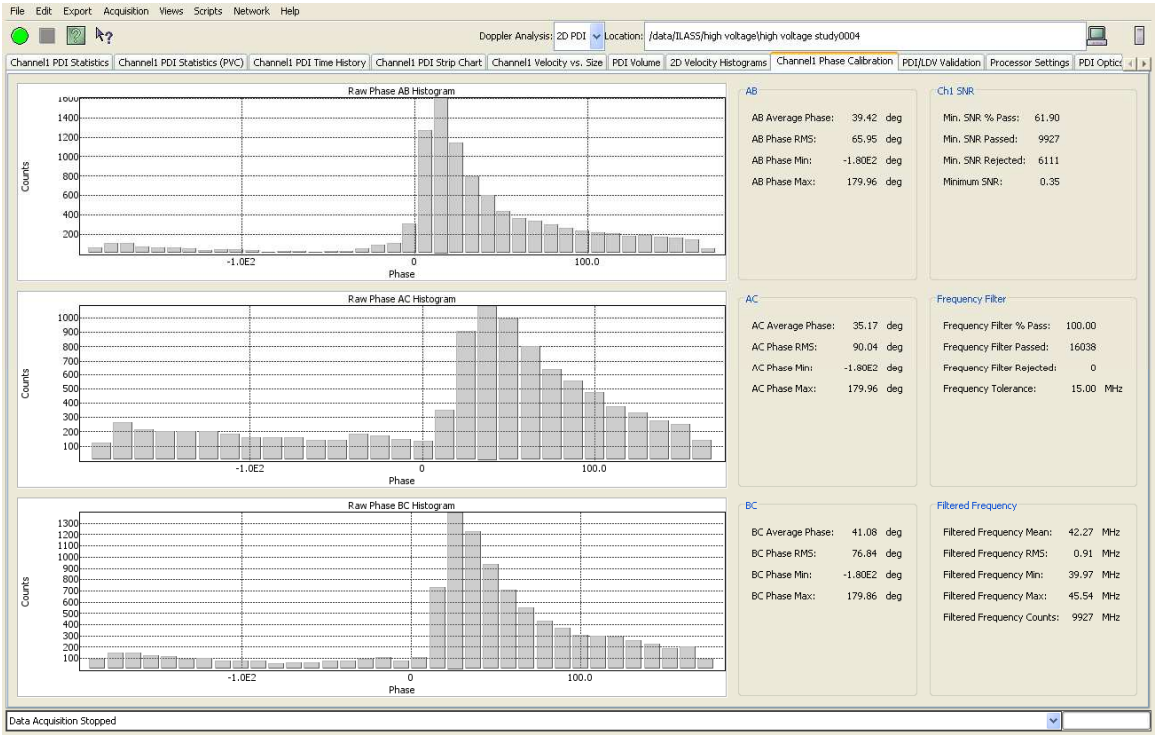

Figure 11.8: Phase calibration plots.

Figure 11.8 shows the phase angle measurements between detectors AB, AC, and BC. This plot is generally used to observe the phase shift when calibrating the instrument using the phase Cal diode. In the present case, the phase shifts are shown for the spray and the wrap around (phase beyond 360 degrees) can be seen. Using the information from the various detector pairs allows us to reconcile these phase shifts into their true values and relate them to the appropriate drop sizes.

ASA Validation

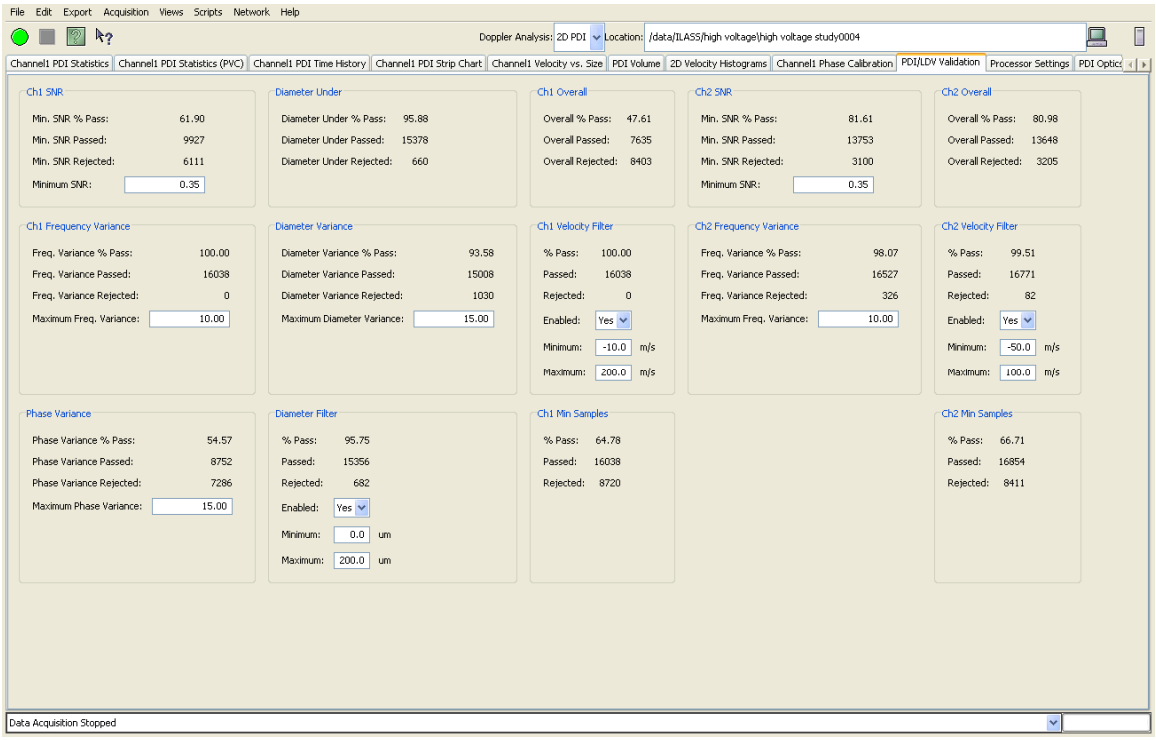

Figure 11.9: Data validation results.

Figure 11.9 shows the screen that provides information on the percentages of attempted measurements that pass the various criteria before a measurement is accepted as a valid estimation of the drop size and velocity. The validation percentage provides an indication of the quality of the signals being detected but low validation rate does not necessarily mean that the instrument is making faulty measurements. Our proprietary digital Doppler signal detection method is programmed to detect signals based on their coherency (whether or not they have sinusoidal characteristics). Since we do not want to miss any droplets the detection is set to attempt measurements of even low amplitude, low SNR signals. The small drops will produce the weakest signals with low amplitude and low SNR but we do not want to bias the measurements by missing the small drops in the distribution. Furthermore, false signal detections will be discarded once the signals are processed with the full complex FFT and the remaining validation criteria have been applied. If the detection is set too conservatively, the validation will be very high but at the expense of missing the small drops.

Our innovative burst signal detection system has been designed to reliably detect even the smallest signals while minimizing false signal detection. Thus, the validation rates are

usually high. However, in difficult sprays (dense sprays, sprays with very small drops but that are large in area, etc.) the validation rate may be expected to fall somewhat.

Each of the validation criteria have been described in the Device Control section under the Validation Tab. The rates shown here are in response to the criteria described in that section.

ASA Settings

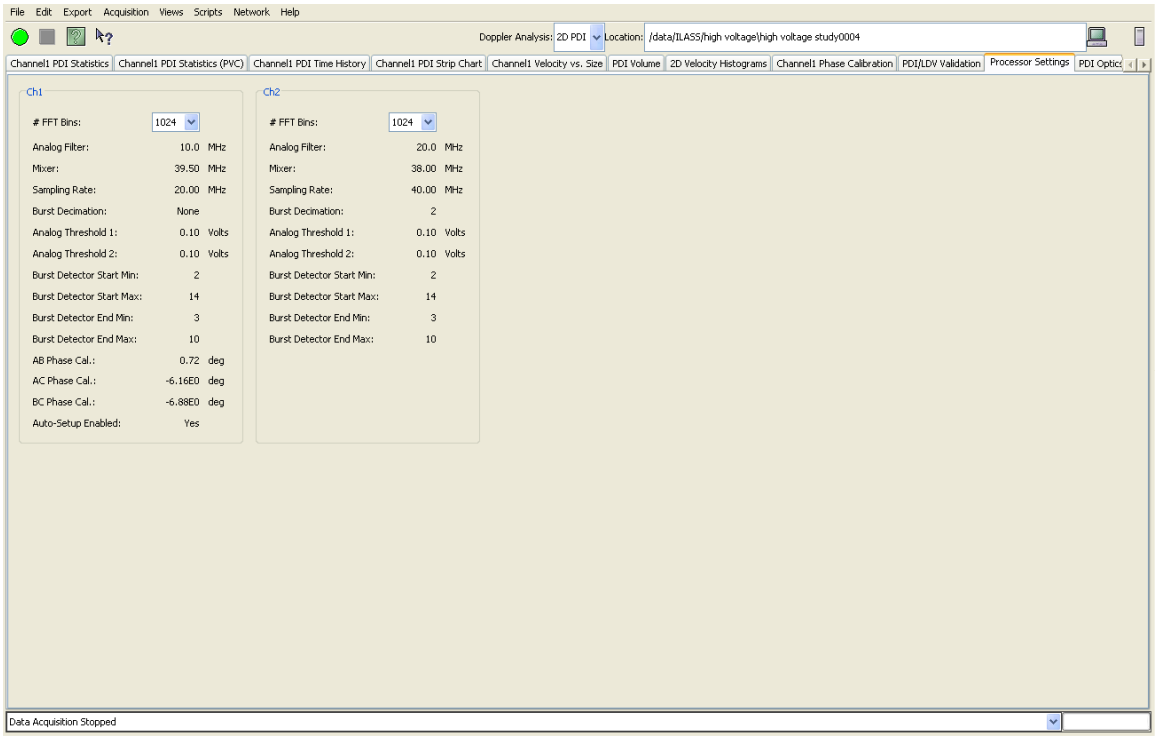

Figure 11.10: ASA settings.

Figure 11.10 shows the screen that provides a summary of the ASA signal processor settings for this measurement point. This information is saved with the data file and allows the user to recover the settings for that data and if desired, repeat the measurements with those settings.

LDV/PDI Optics

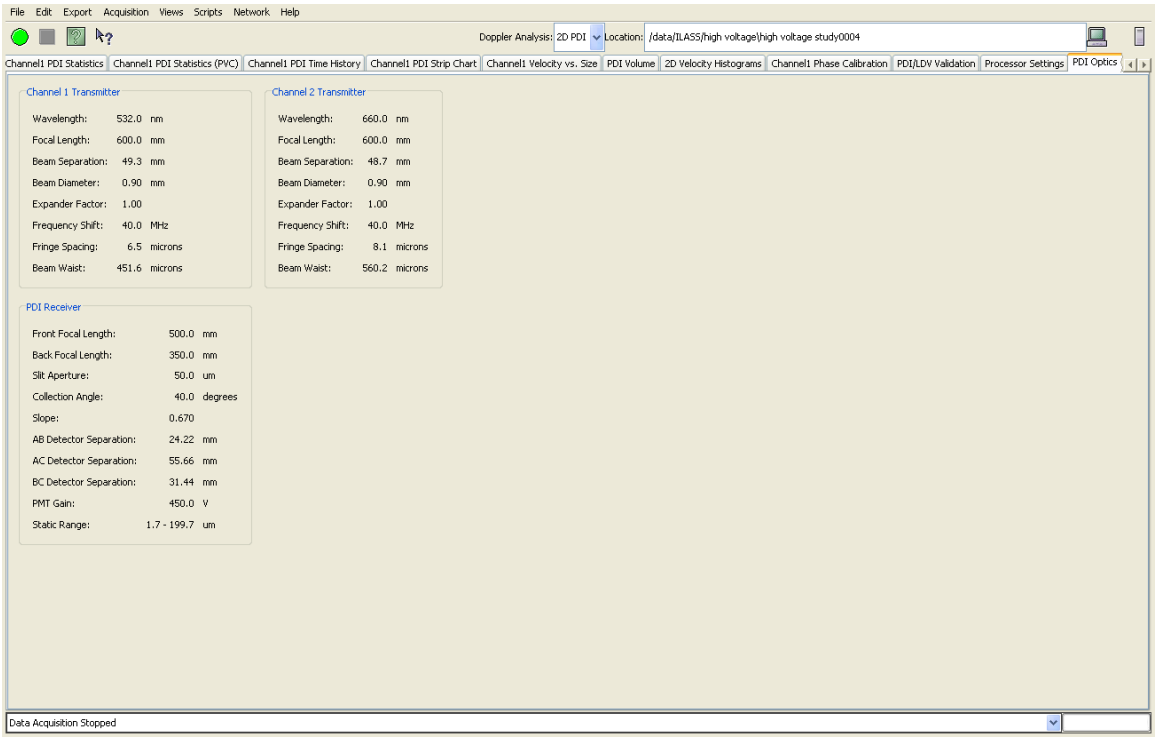

Figure 11.11: LDV/PDI Optics Settings.

Figure 11.11 provides the information on the optical setup used to acquire this data point. This information is stored with each measurement so that the user may, for example, recover this information and if desired, repeat the measurement at the same conditions or assess whether the setup was correct or not.

Frequency Stats

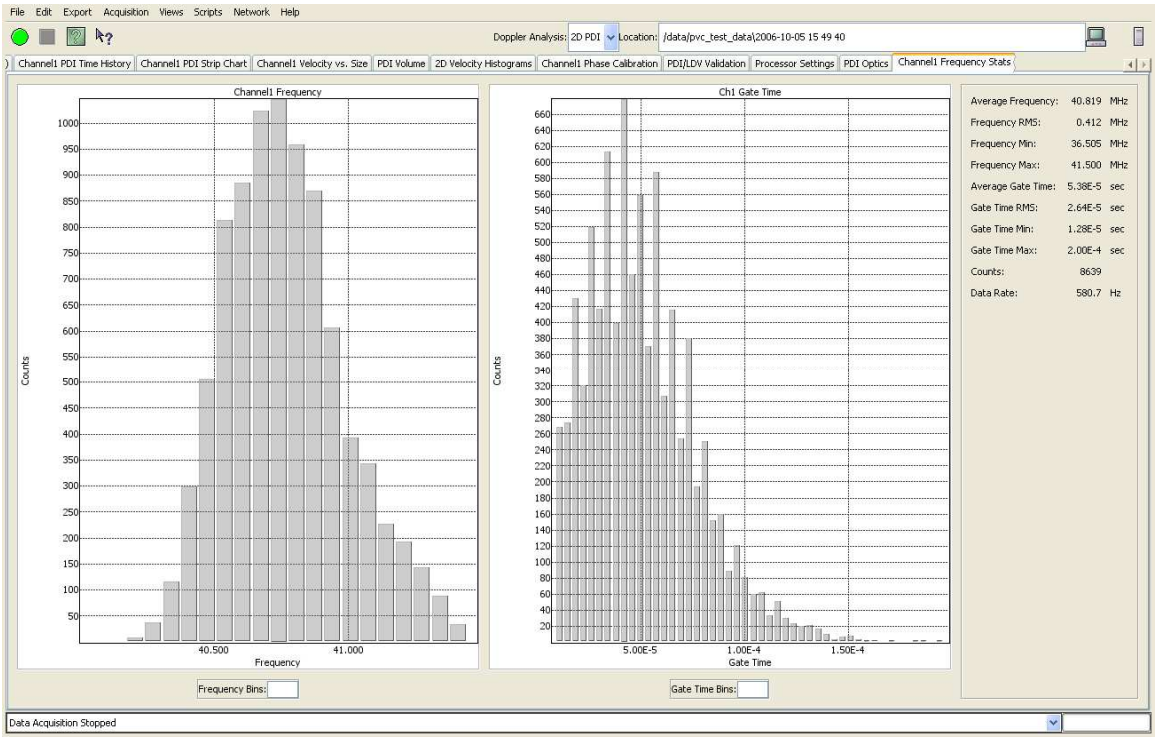

Figure 11.12: Frequency statistics.

Figure 11.12 shows the page that is used for diagnostic purposes. It shows the actual signal frequency for the measurements and the Gate Time or time the particle spent in the sample volume for each measurement. Experienced users would observe these data along with the setup information to determine if the setup was consistent with the measurement conditions. Using auto Setup eliminates the need for studying the information on this screen. However, if there was a failure of the system or the results were in question, the information on this page can be used to help reconcile the problem.

Appendix

A Theory of Operation

Phase Doppler Interferometry

Bachalo (1980) theoretically described the light scattering from spherical particles and showed that the phase shift of the light scattered from two intersecting beams could be used to accurately and reliably measure the diameter of spherical particles. With the use of pairs of detectors to enable the measurement of the interference fringe pattern formed by the far field interference of the scattered light, a method for reliably and accurately measuring spray drop size even in difficult measurement environments was realized, Bachalo and Houser (1984). Following the initial development of the phase Doppler interferometry method, significant research and development has been devoted to the improvement of this important instrument and numerous publications have been written on the subject [Bachalo et al. (1993); Dodge (1987)]; Sankar et al. (1991); Sankar and Bachalo ((1995); Bachalo and Sankar (1988); Bachalo and Houser (1985); Bachalo et al. (1988); Ibrahim et al. (1990); Ibrahim et al. (1991); Ibrahim and Bachalo (1992); Ibrahim and Bachalo (1994);].

The Phase Doppler Interferometer (PDI) instrument, formerly known as the Phase Doppler Particle Analyzer (PDPA), has advanced as the standard laser-based diagnostic instrument for simultaneously measuring the size and velocity of individual spherical particles in polydisperse flow environments. The success of the method may be attributed to the measurement principles upon which it is based, namely, light scattering interferometry. Light scattering interferometry utilizes the wavelength of light as the measurement scale and, as such, the performance is not as easily degraded as it is for systems using light scattering intensity information for the estimation of the particle size. In addition, the method does not require frequent calibration. Over the decades, the instrument has proven to need only an initial factory calibration. The parameters affecting the measurement which include the laser wavelength, beam intersection angle, transmitter and receiver focal lengths, and the detector separation do not change with age and require deliberate intervention by the user or serious mistreatment of the instrument before

they lose adjustment. Another important characteristic of the method that is often missed is related to the signals generated by the device. Unique sinusoidal signals are produced which can be easily detected even in the presence of noise using the Fourier analysis.

As an aid to understanding the measurement method, it will be useful to consider the simplest form of light scattering by a sphere. A geometrical optics description of the light scattering phenomena is illustrated in Figure A1. At the first interface, part of the incident light is reflected from the surface of the sphere and these rays are referred to as p = 0 following the convention of van de Hulst (1957). The light transmitted and refracted by the sphere is referred to as p = 1 rays and rays reflected from the interior surface and refracted in the backward direction are p = 2 rays. The relative light energy reflected from and transmitted through the sphere may be calculated using the Fresnel reflection coefficients.

A schematic of the optical and electronics components for a basic PDI system is presented in Figure A2. The optical requirements are identical to that of a one-component laser Doppler velocimeter (LDV), except that three detectors are used in the receiver, and the receiver must be located at a known off-axis angle to the transmitted beams. The preferred light collection position for the receiver is at an off-axis angle of from 25 to 45 degrees to the transmitted beam direction measured from a plane passing through the two intersecting beams. The optical axis of the receiver should be in a plane that passes

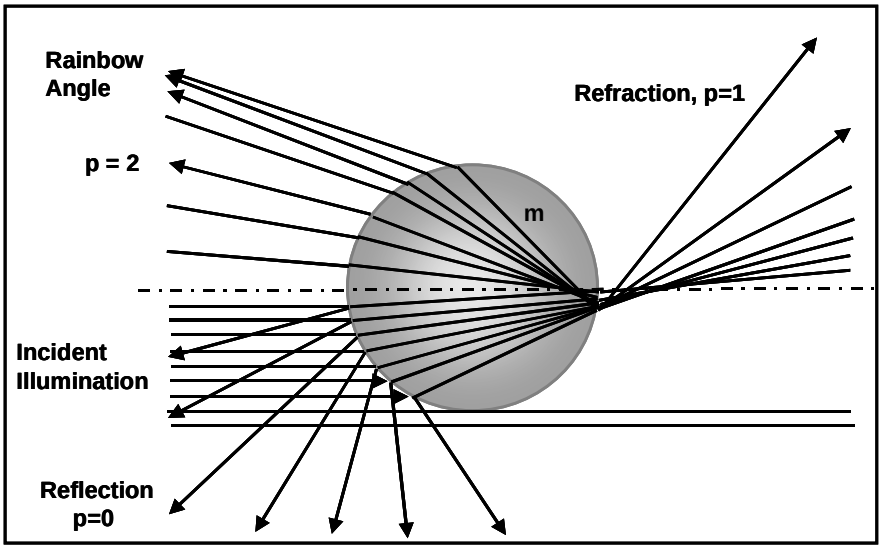

Figure A1: Simple ray diagram showing the deflection of the light rays incident on a spherical particle illustrating the p = 0, 1, 2, and 3 rays.

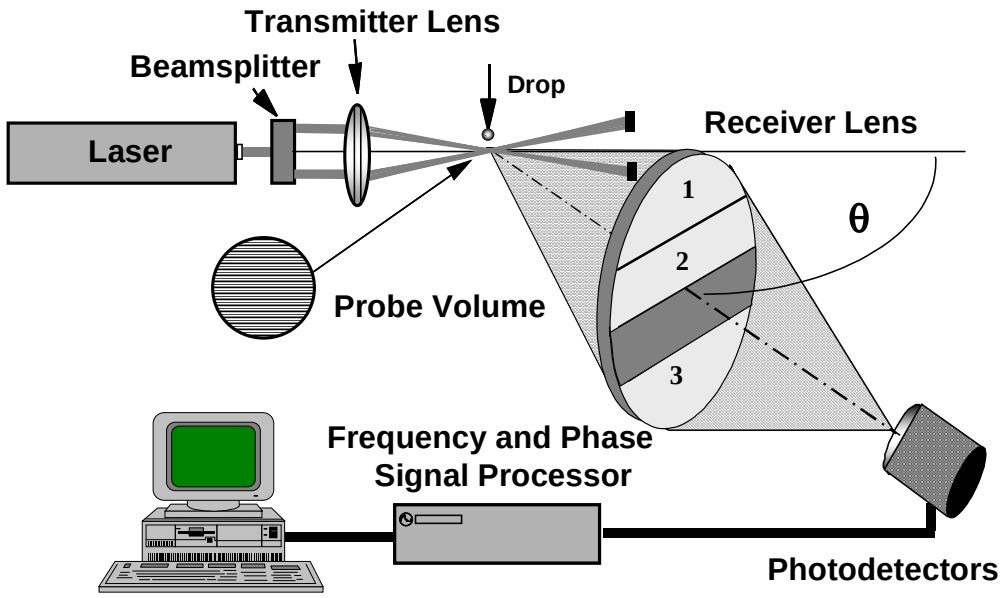

Figure A2: Schematic of the basic Phase Doppler Interferometer (PDI) system.

through the intersection of the beams, and is orthogonal to the plane formed by the two intersecting beams. Other receiver angles and configurations have been suggested but we do not recommend that they be used unless no alternative exists due to some other constraints of the experiment.

In the basic PDI optical system, the laser beam is split into two beams of equal intensity. The beams are then focused and made to intersect using a transmitter lens. Frequency shifting is used to compress the frequency dynamic range and resolve the direction ambiguity that would occur for drops passing in a reverse direction. Particles passing through the beam intersection will scatter light that is collected by the receiver lens. A single aperture is used in the receiver to allow only light scattered by particles crossing a small region of the beam intersection to reach the photodetectors. Shown in figure A3 is a schematic depicting a spherical particle located at the intersection of the two laser beams. An enlarged view of the sphere with a light ray from each beam incident upon it is also shown. Since the rays from each beam enter at different angles, they must pass on different paths to reach a common point P. The sphere has an index of refraction, m, that is different than the surroundings. Thus, the difference in the optical path length of ray 1 from beam 1 relative to ray 2 from beam 2 will produce a phase shift between light waves traveling in the directions shown by ray 1 and ray 2 to the point P. An interference fringe pattern will form in the distant space surrounding the drop. Under ideal conditions, the interference fringe pattern will have a sinusoidal intensity distribution and will form a hyperbolic set of curves when projected onto a plane. The wavelength of the pattern at a

given location will be inversely proportional to the drop diameter. This phase shift can be calculated easily and exactly using the geometrical optics theory. Given a specific location in space (points on the receiver lens aperture) the phase shift between the light scattered from each beam will vary in proportion to the drop diameter.

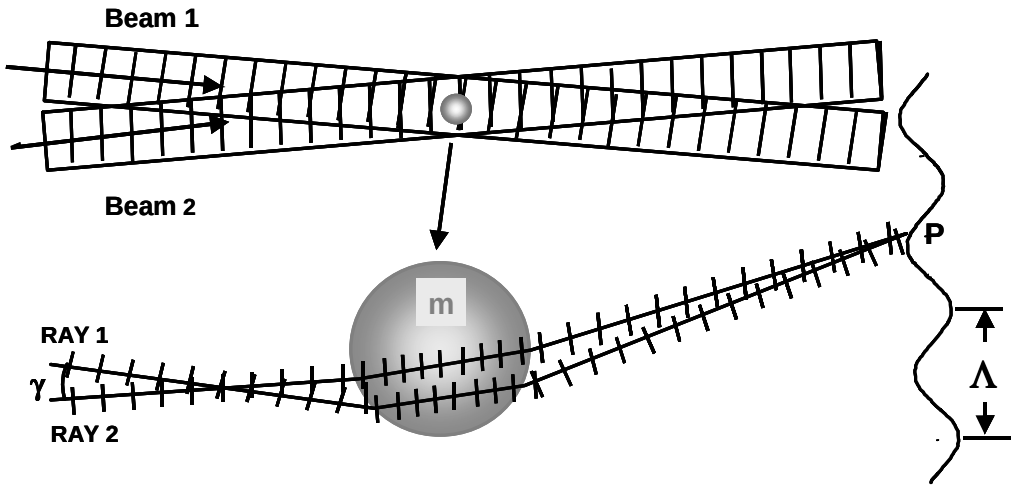

Figure A3: Simple diagram showing the light rays and waves incident on a spherical particle and the phase shift resulting from the passage of the light through the drop on different optical paths.

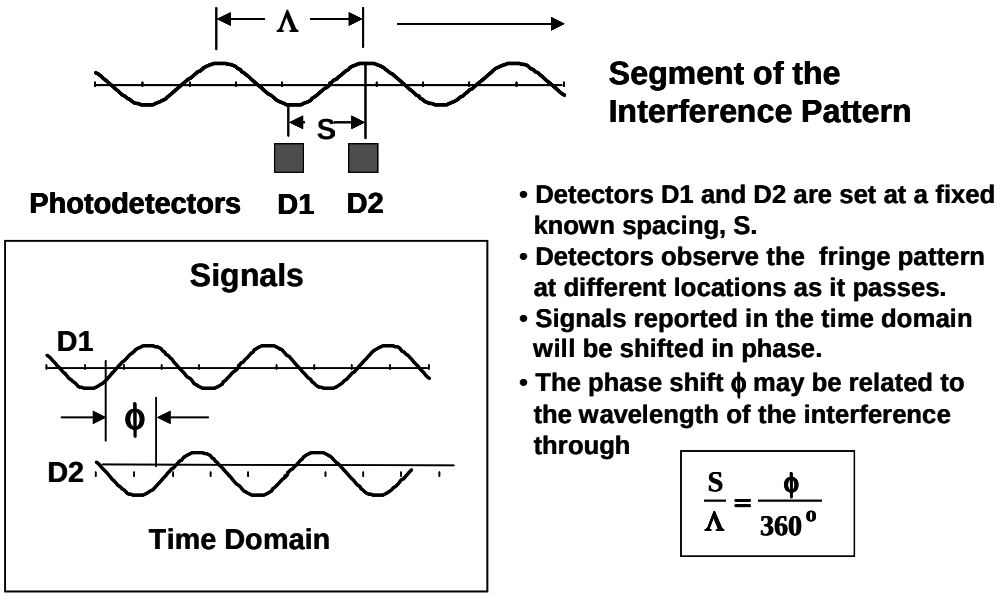

Figure A4: Scheme used for rapidly measuring the spacing, L of the interference fringes produced by the scattered light.

Measurement of the spacing of the interference fringes produced by the scattered light is accomplished in a straightforward manner using pairs of detectors, figure A4. For this approach, pairs of detectors are located in the fringe pattern, or an image of it, and the separation S between the detectors is known. When the particle or drop is moving, the usual Doppler shift in the frequency of the scattered light occurs. The difference in the Doppler frequency shift between the light scattered from beam 1 and beam 2 causes the fringe pattern to appear to move.

As the pattern sweeps past the detectors at the Doppler difference frequency, each detector produces a signal that is similar in frequency but shifted in phase. The phase shift is related to the spacing of the scattered fringe pattern through the following relationship:

$$\frac{s}{\Lambda} = \frac{\phi}{360^{O}}$$

where s is the detector spacing and ϕ is the phase shift between the signals. The wavelength Λ is the spacing of the interference fringes formed by the scattered light and is inversely proportional to the drop diameter. Three detectors are used to avoid ambiguity in the measurements, to provide redundant measurements of the pattern, and to improve the resolution for the small particles. The ambiguity could occur when the fringe spacing, Λ is less than the detector separation. In this case, the phase shift would be greater than 360 degrees but is reported as ϕ - 360.

A unique three-detector separation arrangement originally invented by Bachalo (US Patent 4,540,283) and first reported in 1982 (NASA Technical Report) is shown in figure A5. The phase versus diameter curves that correspond to these detector separations are also shown. With this configuration, the phase shift between the signals from the closely spaced detectors, D1 and D2 follow the smaller slope on the phase-diameter plot indicated by the dotted lines. The phase between the signals for the detectors with the larger spacing, D1 and D3, follow the curves with the greater slope. With this arrangement, the phase may be measured for detector separations that extend over several fringes (1 fringe corresponds to a measured phase shift of 360°) when placed in the field of the scattered light. More recently (patent pending), Bachalo has reported the use of three pairs of detectors (ϕ_{12},ϕ_{13},and ϕ_{23}) to be used in the measurement as shown in the updated diagram of phase versus diameter

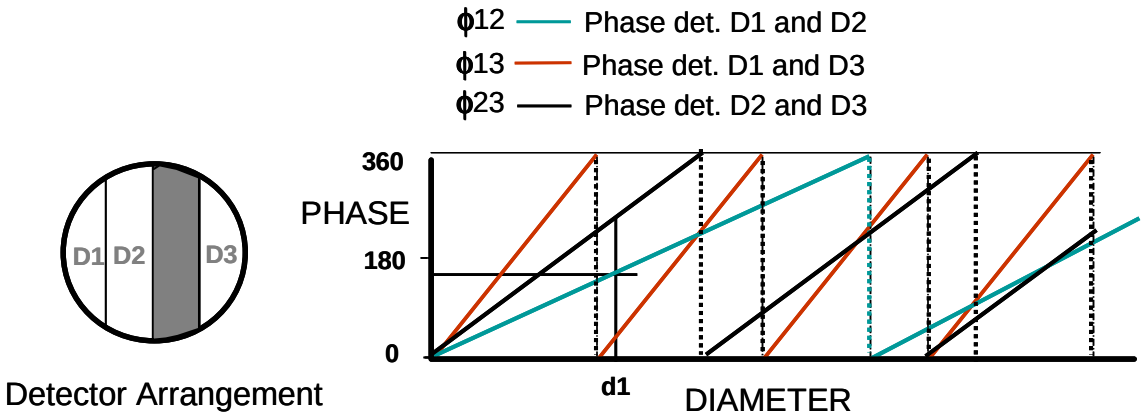

Figure A5: Three-detector configuration and the resulting phase diagram used to avoid ambiguity and extend the measurement range with high resolution (Patent Pending).

It is relatively easy to see that the interference fringe pattern produced by reflection will appear to move in the opposite direction to that produced by refraction. With the three detectors set to detect the phase shift for refraction, as shown in figure A6, the correct phase shifts for ϕ12, ϕ13 and ϕ23 will be detected. However, when the dominant light scatter is by reflection, the wave will travel in the opposite direction. For this case, the relationship between ϕ12, ϕ13, and ϕ23 will no longer pass the phase comparison criteria so these samples will be rejected.

Unfortunately, spray droplets will also pass on trajectories through the Gaussian beam, which will result in a significant superposition of scattered light intensity by reflection and refraction. In this case, the resultant interference fringe pattern is no longer a pure sinusoidal wave but a superposition of several interference patterns. Additional means are required to reject particles passing on these trajectories to avoid or minimize measurement errors. Bachalo (1980) recognized this problem, and it was the primary reason for selecting the 30^{o} light scatter detection angle wherein refraction is approximately 80 times the reflection (assuming a uniformly illuminated sphere). Bachalo and Houser (1984) addressed this problem experimentally by traversing monodisperse drops along controlled trajectories within the measurement probe volume for a range of drop-size-to-beam-diameter ratios. Fortunately, the redundant phase information coupled with other information has been proven successful in mitigating or eliminating this source of measurement error.

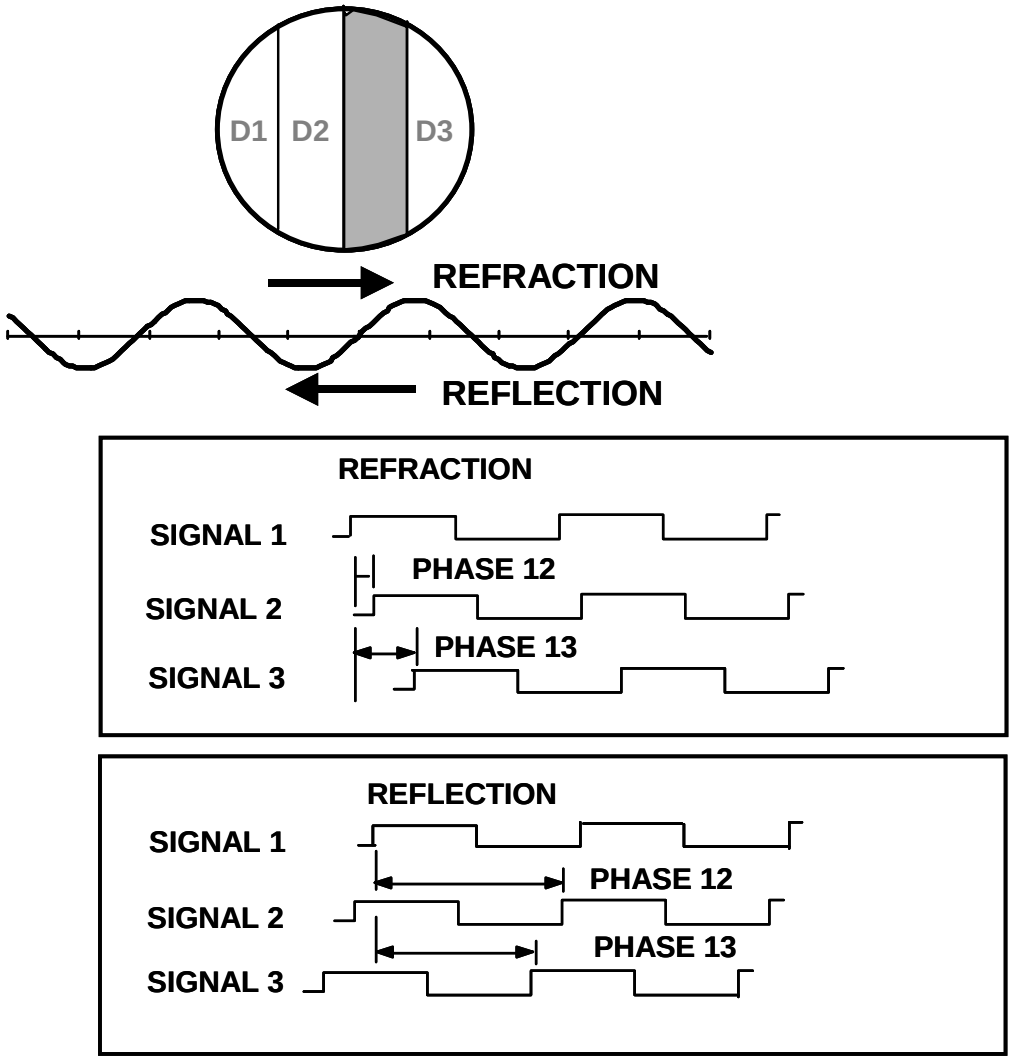

Figure A6: Three-detector configuration used by Bachalo, 1982 to resolve the phase ambiguity and to extend the measurement range and resolution.

The key parameter in the analysis of this problem is the drop diameter-to-beam diameter ratio, $\Gamma = d / D_o$ where d is the drop diameter and D_o is the diameter of the focused beams at the sample volume, figure A7. At this point, it is useful to consider the problem in three regimes: particles smaller than the focused beam diameter, ($\Gamma << 1$) particles similar in size ($\Gamma \sim 1$), and particles larger than the beam diameter ($\Gamma >> 1$). In the first case, the particles can be assumed to be approximately uniformly illuminated so the trajectory error is not a problem. In the case of the particles being of similar diameter to the focused beam diameter, the trajectory problem is most difficult since the scattering intensities from reflection and refraction can be of similar order producing a complex interference fringe pattern with a progressively increasing magnitude of error. If the particles are larger than

the focused beam diameter, then either reflection or refraction will dominate the scattering. For this case, the phase ratio will be effective in rejecting signals produced by the wrong scattering component.

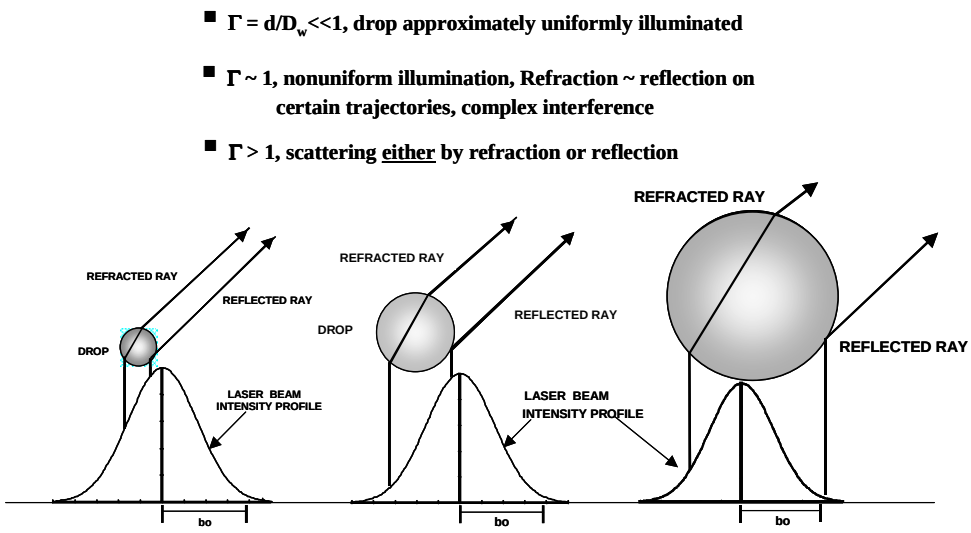

Figure A7: Schematic illustrating the three drop size cases passing a Gaussian beam; Γ<<1, Γ~1, and Γ>1.

Sankar et al. (1992) have shown that the trajectory-dependent sizing errors can be minimized by the proper selection of the optical parameters, namely, the beam intersection angle and using the two-detector-pair arrangement of the PDI. This work represented the first recognition of the importance of the relative phase difference between the reflected and the refracted light in resolving the trajectory-dependent error problem. Increasing the beam intersection angle serves to increase the difference between the phase of light scattered by refraction and reflection, allowing a more effective discrimination using the phase ratio from the two pairs of detectors. In a later paper by Sankar et al. (1995), it was shown that with the proper selection of the optical parameters, the phase Doppler response for particles passing along the error-prone trajectories could be forced to always result in a size over-prediction, if at all, and never an under prediction. This information can then be used in conjunction with the scattered light intensity level for each particle to eliminate the erroneous measurements (Bachalo, US Patent 4,986,659).

The intensity validation method is based on the observation that when particles pass on the “bad” trajectories near the edge of the beam, the incident intensity and hence, the

scattered light is at least an order of magnitude lower than for particles passing on a trajectory through the center of the beam. In addition, if the light scattering by reflection is detected, the signal will be approximately two orders of magnitude lower than for the light scattered by refraction because of the lower light scattering efficiency. Thus, calculating a minimum acceptable light intensity level for each size class and measuring the signal amplitudes along with the drop size can provide information for eliminating the particles passing on the trajectories susceptible to errors from consideration. Using this approach, the definition of the edges of the sample volume are better defined at higher levels than is possible on the wings of the Gaussian wherein a small uncertainty in amplitude corresponds to a large change in the size of the sample volume. Detailed experimental studies and theoretical simulations have been conducted to evaluate the reliability of the intensity validation method. Sankar et al. (1995) and Strakey et al. (2000) have shown that the method is effective in controlling trajectory errors.

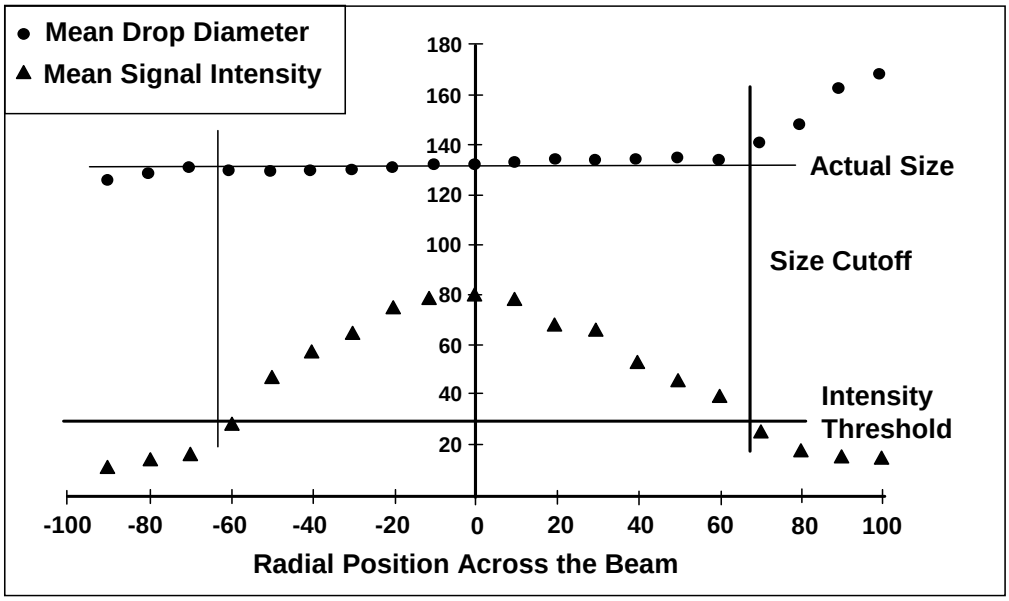

Figure A8: Plot showing the light scattering intensity and the measured drop size for a monodisperse drop stream traversed through the sample volume from one side to the other.

Numerous experimental evaluations of the method have been conducted. Figure A8 shows the results of traversing a monodisperse stream of droplets through the probe volume. The drops had a nominal size of 132 μm. The plot shows the resulting light scattering intensity which is nearly Gaussian and the measured size as the stream is traversed from one side of the beam to the other (-100 μm to +100 μm). The scattered light intensity profile will not be completely Gaussian in shape since the light scattering

mechanisms change from one side of the beam to the other (more reflection detected on one side as a result of the location of the receiver). If a threshold intensity level is set (as shown in figure A8) for each drop size class, the error in the measured size at the side with the reflective light scattering may be eliminated. For the "bad" trajectories, the measured size begins to deviate from the true value but setting a threshold signal amplitude level serves to exclude these readings. In principle, the adaptive threshold validation method limits the region of detection over the sample volume for each particle size class.

Examples of PDI Applications

Numerous examples are available in the literature wherein the PDPA has been used to investigate spray characteristics in highly complex environments. This includes study of sprays injected into turbulent flow fields, reactive fuel sprays in swirl-stabilized combustors, characterization of rocket injectors in a high pressure environment using cryogenic liquids, and the study of transient fuel sprays such as in spark ignition (SI) and diesel engines. The usefulness of the PDPA (now referred to as PDI instrument) in understanding various complex spray and combustion processes becomes apparent through the following brief description of some of the results that have been obtained to-date by various researchers.

SPRAY COMBUSTION MEASUREMENTS

The development of the Phase Doppler Interferometer (PDI) has enabled the detailed measurement of drop size, velocity, number density and volume flux in realistic spray combustion environments [Bachalo et al. (1990); Edwards and Rudoff (1990)]. Chehroudi and Ghaffarpour (1991) investigated the effects of swirl and dilution air flow rates on the shape and stability of a kerosene flame on a model combustor with comparisons made of the non-combusting and combusting cases. The gas temperature was also measured within the flame using a thermocouple. Flow visualization showed nonuniformly-distributed separated finger-like regions of visible flames wrapped around the spray sheath. These structures were possibly due to large-scale eddies formed by the swirling flow. At the center of the spray, drops with a reversed flow velocity were measured indicating a region of recirculation, figure A9. In the burning case, no drops were detected in this region indicating that only vitiated air is recirculated toward the injector. At the uppermost end of the flame brush, a significant number of large drops were measured with velocities of approximately 10 m/s indicating that unburned drops were exiting the flame.

TRANSIENT FUEL SPRAYS

Transient spray injection such as that used in Diesel and spark ignition engines shows some unique atomization characteristics. Diesel injection may take place into a relatively quiescent environment at pressures of approximately 15 atmospheres and at injection pressures of between 50 and 180 MPa. The important combustion parameters are the fuel penetration, mixing, and vaporization. These parameters depend upon the spray drop velocity and trajectory, the drop size distribution, and the turbulent gaseous flow field. The characterization of sprays having droplets of high velocity, small diameter, and high number density, which are typical of Diesel engines, is a challenging task, Harrington (1995). This is particularly true for smaller bore, light-duty, and medium-duty Diesel engines that utilize relatively short distances from the injector tip to the piston-bowl impact point. The combination of the above factors with high beam extinction in the spray core, and the need for a high pressure optical chamber, leads to difficulties in all laser diagnostic methods. In spite of these challenges, the advanced frequency domain signal processors that are available for the PDPA has allowed for the reliable characterization of Diesel sprays.

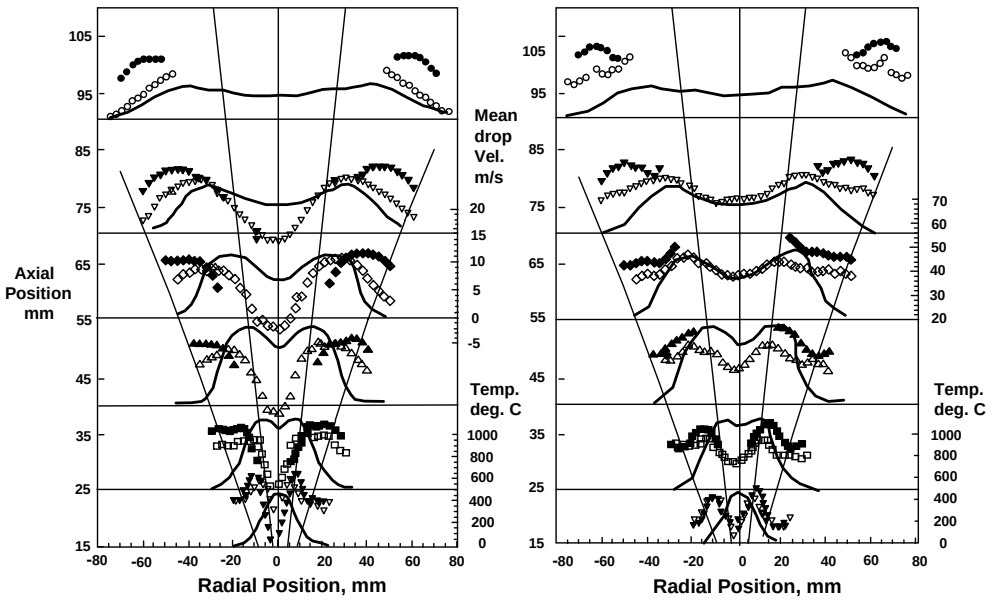

Figure A9: Drop size and velocity data obtained in a swirl-stabilized combustor comparing the results with and without combustion. The solid symbols are for the reacting case. Also shown is the gas temperature (solid line) obtained with a thermocouple (Courtesy of Chehroudi and Ghaffarpour [1991]).

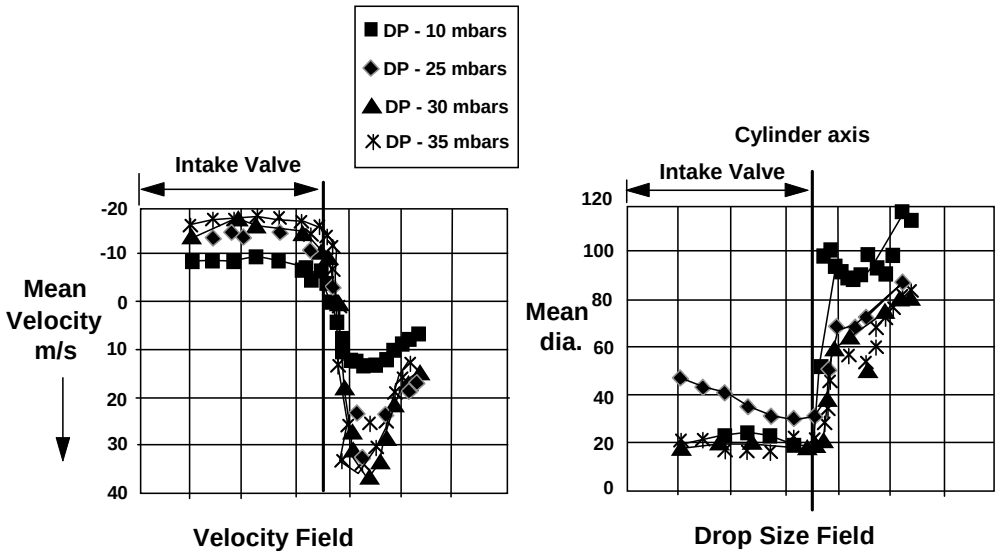

Figure A10: Air flow rate effect on drop size and velocity fields inside a SI engine cylinder.

As with Diesel engines, the atomization for spark ignition (SI) engines is highly transient and must be accomplished over a wide range of operating parameters. Vannobel et al. (1992) have used the PDPA to perform measurements in a gasoline spray inside the inlet port and downstream of the induction valve of a SI engine. Their interest was in studying quality of the air/fuel mixture and its dependence upon injection timing, injector position, and orientation within the manifold. The PDPA measurements were made inside the engine cylinder. The various curves in figure A10 representing the different air pressures, illustrate the trajectories followed by the drops.

Bibliography

W. D. Bachalo, "Method for Measuring the Size and Velocity of Spheres by Dual-beam Light-Scatter Interferometry," Applied Optics, Vol. 19, No. 3, pp. 363-370, February 1, 1980.

W. D. Bachalo and M. J. Houser, "Phase Doppler Spray Analyzer for Simultaneous Measurements of Drop Size and Velocity Distributions," Optical Engineering, Vol. 23, pp. 583-590, 1984.

W. D. Bachalo and M. J. Houser, “Analysis and Testing of a New Method for Drop Size Measurement Using laser Light Scatter Interferometry,” NASA Contractor Report 174636, August, 1984a.

W. D. Bachalo, A. Brena de la Rosa, and R. C. Rudoff, “Diagnostics Development for Spray Characterization in Complex Turbulent Flows,” 33rd ASME Gas Turbine and Aeroengine Congress and Exposition, Amsterdam, The Netherlands, June 6-9, 1988.

W. D. Bachalo and S. V. Sankar, “Analysis of the Light Scattering Interferometry for Spheres Larger than the Light Wavelength,” Proc. 4th Intl. Symp. on the Applications of Laser Anemometry to Fluid Mechanics, Lisbon, Portugal, July 11-14, 1988.

W. D. Bachalo, R. C. Rudoff, and S. V. Sankar, “Time-Resolved Measurements of Spray Drop Size and Velocity,” Liquid Particle Size Measurement Techniques: 2nd Volume, STP 1083, pp. 209-224, 1990.

W. D. Bachalo, E. J. Bachalo, J. M. Hanscom, and S. V. Sankar, “An Investigation of Spray Interaction with Large-Scale Eddies,” AIAA 93-0697, 31st Aerospace Sciences Meeting and Exhibit, Reno, NV, January 11-14, 1993.

B. Chehroudi and M. Ghaffarpour, “Spray Drop size and Velocity Measurements in a Swirl-Stabilized Combustor,” 35th International Gas Turbine and Aeroengine Congress and Exposition, Orlando, FL, June 3-6, 1991.

L. G. Dodge, “Comparison of Performance of Drop-Sizing Instruments,” Applied Optics, Vol. 26, No. 7, April, 1987.

C. F. Edwards and R. C. Rudoff, Structure of a Swirl-Stabilized Spray Flame by Imaging, Laser Doppler Velocimetry, and Phase Doppler Anemometry, Proc. Twenty-Third Symp. (Intl.) on Combustion, Orleans, France, The Combustion Institute, pp. 1353-1359, 1990.

D. L. Harrington, PDA Measurement Considerations for Pulsed Air Assist and Diesel Fuel Sprays,î Proc. 26th Annual Meeting of the Fine Particle Society, Chicago, IL, August 22-25, 1995.

K. M. Ibrahim, G. D. Werthimer, and W. D. Bachalo, Signal Processing Considerations for Laser Doppler Applications, Proc. 5th Intl. Symp. on the Application of Laser Techniques to Fluid Mechanics, Lisbon, Portugal, July 9-12, 1990.

K. M. Ibrahim, G. D. Werthimer, and W. D. Bachalo, Signal Processing Considerations for Low Signal to Noise Ratio Laser Doppler and Phase Doppler Signals, Proc. 4th Intl. Conf. on Laser Anemometry, Advances and Applications, Cleveland, OH, August 5-9, 1991.

K. M. Ibrahim and W. D. Bachalo, ìThe Significance of the Fourier Analysis in Signal Detection and Processing in Laser Doppler and Phase Doppler Applications, Proc. 6th Intl. Symp. on the Application of Laser Techniques to Fluid Mechanics, Lisbon, Portugal, July 20-24, 1992.

K. M. Ibrahim, M. J. Fidrich, and W. D. Bachalo, Evaluations of an Advanced Real-Time Signal Processor System Using the Fourier Transform, Proc. 2nd Intl. Conf. on Fluid Dynamics Measurement and its Application, Beijing, China, October 1994.

S. V. Sankar and W.D. Bachalo, Response Characteristics of the Phase Doppler Particle Analyzer for Sizing Spherical Particles Larger than the Light Wavelength, Applied Optics, Vol. 30, No. 12, pp. 1487-1496, 1991.

S. V. Sankar, B. J. Weber, D. Y. Kamemoto, and W. D. Bachalo, Sizing Fine Particles with the Phase Doppler Interferometric Technique, Applied Optics, Vol. 30, No. 33, pp. 4914-4920, 1991.

S. V. Sankar, A. S. Inenaga, and W. D. Bachalo, Trajectory Dependent Scattering in Phase Doppler Interferometry: Minimizing and Eliminating Sizing Errors, Proc. 6th Intl. Symp. on the Application of Laser Techniques to Fluid Mechanics, Lisbon, Portugal, July 20-23, 1992.

S. V. Sankar and W. D. Bachalo, Performance Analysis of Various Phase Doppler Systems, Proc. 4th Intl. Congress on Optical Particle Sizing, Nuremberg, Germany, March 21-23, 1995.

S. V. Sankar, W. D. Bachalo, and D. A. Robart, An Adaptive Intensity Validation Technique for Minimizing Trajectory Dependent Scattering Errors in Phase Doppler Interferometry, Proc. 4th Intl. Congress on Optical Particle Sizing, Nuremberg, Germany, March 21-23, 1995.

Peter A.,, Strakey, Douglas G., Talley, Subra, V. Sankar, and W.D. Bachalo, “Phase-Doppler Interferometry With Probe-to-Droplet Size Ratios Less Than Unity. Trajectory Errors I.”, Applied Optics, Vol. 39, No. 22, August 2000.

Peter A.,, Strakey, Douglas G., Talley, Subra, V. Sankar, and W.D. Bachalo, “Phase-Doppler Interferometry With Probe-to-Droplet Size Ratios Less Than Unity. Application of the Technique II.”, Applied Optics, Vol. 39, No. 22, August 2000.

H. van de Hulst, Light Scattering by Small Particles, New York: Wiley, 1957.

Vannobel (1992), Private communications.